Research Programme of the Research Fund for Coal and Steel

Steel RTD

Project carried out with a financial grant of the

Research Programme of the Research Fund for Coal and Steel

Draft Final Report

Technical Report No: 7

Period of Reference: 01/07/2008 – 31/12/2011

Technical Group: TGS8 "Steel products and applications for buildings, construction and industry"

PERFORMANCE-BASED APPROACHES FOR HIGH STRENGTH TUBULAR COLUMNS AND CONNECTIONS UNDER EARTHQUAKE AND FIRE LOADINGS

Project Acronym: ATTEL

Grant Agreement Number: Contract N° RFSR-CT-2008-00037

Beneficiaries: University of Liège - ULGG (Belgium)
Centro Sviluppo Materiall – CSM (Italy)
Stahlbau Pichler - STBPI (Italy)
University of Thessaly - UTHESSA (Greece)
University of Trento – UTRE (Italy)

Location: ULGG, Place du 20 août, 7 4000 Liège Belgium
CSM, Via di Castel Romano, 100/102, 00128, Italy
STBPI, Via Edison, 15, 39100 Bolzano, Italy
UTHESSA, Argonafton & Filellinon, 38221 Volos, Greece
UTRE, Via Belenzani, 12, 38100 Trento, Italy

Co-ordinator: Jean-Pierre Jaspart, University of Liège

Authors: Jean-François Demonceau (ULGG)
Long Van Hoang (ULGG)
Jean-Pierre Jaspart (ULGG)
Manuel Sommariva (STBPI)
Daniele Maio (STBPI)
Giuliana Zilli (CSM)
Giuseppe Demofonti (CSM)
Jan Ferino (CSM)
Aglaia-Eugenia Pournara (UTHESSA)
George E. Varelis (UTHESSA)
Charis Papatheocharis (UTHESSA)

Philip Perdikaris (UTHESSA)
Patricia Pappa (UTHESSA)
Spyros A. Karamanos (UTHESSA)
Fabio Ferrario (UTRE)
Oreste S. Bursi (UTRE)
Gabriele Zanon (UTRE)

Commencement Date: 01/07/2008

Completion Date: 31/12/2011

I. Distribution list

TGS8 members:

- CHAIRMAN: **Louis–Guy CAJOT**, Arcelormittal Belval & Differdange S.A.
  lg.cajot@arcelormittal.com
- **Nancy BADDOO**, The Steel Construction Institute
  n.baddoo@steel-sci.com
- **Darko BEG**, Univerza V Ljudljana
  dbeg@fgg.uni-lj.si
- **Anthony KARAMANOS**, A.S. Karamanos & Associates
  karama@otenet.gr
- **Andrzej KLIMPEL**, Silesian University of Technology – Politechnika Slaska
  andrzej.klimpel@polsl.pl
- **Mr Jouko KOUHI**, Finnish Constructional Steelwork Association
  jouko.kouhi@fcsa.fi
- **Joaquín ORDIERES MERE**, Universidad De La Rioja
  joaquin.ordieres@unirioja.es
- **Walter SALVATORE**, Universita Di Pisa – Dipartemento Di Ingegneria Strutturale
  walter@ing.unipi.it
- **Adam BANNISTER**, Corus UK LTD – Swinden Technology Centre
  adam.bannister@corusgroup.com
- **Thierry BRAINE-BONNAIRE**, Arcelor France S.A.
  thierry.brainebonnaire@arcelormittal.com
- **Giuseppe DEMOFONTI**, Centro Sviluppo Materiali SPA
  g.demofonti@c-s-m.it
- **Gerhard KNAUF**, Salzgitter Mannesmann Forschung GmbH
  g.knauf@du.szmf.de
- **Antonio Augusto FERNANDES**, Faculdade De Engenharia Da Universidade Do Porto
  aaf@fe.up.pt

II. Table of contents

III. Notations/Abbreviations

σ_b	is the bending component of residual stress;
σ_m	is the membrane component of residual stress;
$\sigma_{res,ext}$	is the residual stress measured on the external surface;
Φ_u	in a combined load test the end column rotation at maximum bending moment
A	permanent elongation after fracture expressed as a percentage of the original gauge length
A_g	percentage plastic extension at maximum force (percentage of the extensometer length)
CFT	concrete fillet tube
CHS	circular hollow section
CSM	Centro Sviluppo Materiall
D	diameter
D_0	original cross sectional diameter
d_u	in an axial load tests the column shortening at maximum compressive axial
E	is the Young modulus of the material;
e	dimples or wrinkling imperfections
EC3	Eurocode 3
EC4	Eurocode 4
EC8	Eurocode 8
ECCS	European Convention for Constructional Steelwork
f	in the application of sectioning method is the flexural deformation of a strip
FE	Finite elements
HSS	high strength steel
ID	specimen identification
l	in the application of sectioning method is the strip length;
L_0	original gauge length
LVDT	linear displacement transducer
M_{max}	in a combined load test the maximum bending moment reached
N_{apply}	in a combined load test the applied compressive axial load
N_{max}	in an axial load tests the maximum compressive axial load reached
O	ovality imperfections $(D_{max}-D_{min})/D_{nominal}$
R_m	tensile strength
$Rp_{0,2}$	stress at 0.2% of plastic extension
S_0	original cross sectional area
STBPI	Stahlbau Pichler
t	thickness
T0	time corresponding to the beginning of the fire test
ULGG	University of Liège
UTHESSA	University of Thessaly
UTRE	University of Trento
WP	Work Package
Z	percentage reduction of area
ε_y	the total strain (elastic + plastic) corresponding to $R_{p0.2}$ of the material
σ_{max}	maximum stress of a stress controlled cyclic tests
σ_{min}	minimum stress of a stress controlled cyclic tests

IV. Abstract

The use of high strength steel (HSS) circular hollow sections (CHS) is still limited in the construction industry despite their excellent structural and architectural properties and the fast development of end-preparation machines. Moreover, although EC3-1-12 extends its scope to steel grades up to S690/S700MC, limitations exist at the material, structural and design levels.

The project ATTEL intended to develop both analytical and experimental know-how in order to support new design criteria for the exploitation of HSS and steel-concrete composite circular hollow sections for columns and connections subjected to exceptional loads, like earthquakes and fire.

Experimental (through testing of tubular members and connections), analytical and numerical (through the use of the component method and advanced finite element simulations) investigations have been achieved in ATTEL so as to allow practitioners to make full use of high strength steels ranging from S500Q/ S500MC to S690Q/S700MC which represents nowadays an upper limit for structural applications.

The different planned works have been successfully conducted and the different objectives of the ATTEL project have been met. The main achievement of the project is the proposal of design rules and design recommendations for structures using HSS tubular columns and for structural elements made of HSS such as steel/composite columns, beam-to-column joints and column bases in fire conditions and/or under moderate/strong seismic actions.

Besides that, the field of economical application of HSS CHS solutions has also been identified for the various above-mentioned loading situations.

V. Project overview

CATEGORY OF RESEARCH:	STEEL
TECHNICAL GROUP:	TGS 8
REFERENCE PERIOD:	01/07/2008 – 31/12/2011
GRANT AGREEMENT N°:	Contract N° RFSR-CT-2008-00037
PROJECT N°:	
TITLE:	ATTEL – Performance-based approaches for high strength tubular columns and connections under earthquake and fire loadings
BENEFICIARIES:	• University of Liège (Belgium) • Centro Sviluppo Materiall (Italy) • Stahlbau Pichler (Italy) • University of Thessaly (Greece) • University of Trento (Italy)
COMMENCEMENT DATE:	01/07/2008
COMPLETION DATE:	31/12/2011
NEW COMPLETION DATE:	NO
WORK UNDERTAKEN:	• State-of-the-art • Design of three reference buildings from which the tested specimens have been extracted • Realisation of experimental tests at room and elevated temperature • Analytical and numerical investigations (parametrical studies) • Derivation of design recommendations
MAIN RESULTS:	• State-of-the-art available • Definition of three reference "actual" buildings using HSS tubular columns • Experimental test results available • Validation of numerical tools • Results of numerical and analytical investigations (parametrical studies) • Design recommendations available for structures and structural elements in low and high seismicity regions • Economical considerations on the use of HSS and CHS seamless tudes
FUTURE WORK TO BE UNDERTAKEN:	-

ON SCHEDULE (*YES /NO)*:	YES
PROBLEMS ENCOUNTERED:	Delivery of the testing material by the tube producer delayed because of production planning. Accordingly, the publication of the deliverables for WP3 had to be delayed to the end of the project.
CORRECTION – ACTIONS *(USE OF A TABLE IS RECOMMENDED)*:	The planning of the project has been adapted but the problem did not affect globally the project as all the promised project objectives have been achieved in the three and a half years project duration
BUDGET INFORMATION PER PARTNER:	See the table here below
TOTAL BUDGET (EURO) :	1148828,64 euro

PUBLICATIONS – PATENTS :

Published

Aglaia-Eugenia Pournara and Spyros A. Karamanos, *Strength and Stability of High-Strength Steel Tubular Beam-Columns*, 7th National Conference of Steel Structures, Volos, Greece, September 2011.

George E. Varelis, Aglaia-Eugenia Pournara and Spyros A. Karamanos, *High-strength Steel Tubular Beam- Columns -Strength and Stability under Static and Cyclic Loading*, 6th European Conference on Steel and Composite Structures, Budapest, Hungary, September 2011.

Hoang Van Long, Demonceau Jean-François, Ly Dong Phuong Lam, Rossi Barbara. *Field of application of high strength steel circular tubes for steel and composite columns from an economic point of view*. Journal of Constructional Steel Research 67(2011) 1001-1021.

G. Zanon, A. Kumar, O.S. Bursi, F. Ferrario and A. Giacobbe, *High strength tubular columns and connections under earthquake, fire loading and fatigue*, in METALLURGIA ITALIANA, v. 3 , p. 25-31, March 2011.

G. Zanon, O.S. Bursi & R. Zandonini and R. Pucinotti. *Seismic behaviour of beam-to-column joints with high strength steel tubular columns*, in Proceedings of the 4th International Conference on Advances in Experimental Structural Engineering, Ispra (Italy), June 29-30, 2011.

O.S. Bursi, R. Pucinotti, N.Tondini and G. Zanon. *Seismic behaviour of high strength steel column joints*, in EUROSTEEL 2011 , Bruxelles, Belgium: ECCS(European Convention for Constructional Steelwork), 2011, p. 573-578. Proceedings of the: Eurosteel 2011, Budapest,2011, August 31-September 2

O.S. Bursi, G. Zanon and R. Pucinotti. *Performance of beam-to-column joints made of high strength steel tubular columns subject to earthquake loadings*, XXIII GIORNATE ITALIANE DELLA COSTRUZIONE IN ACCIAIO - XXIII ITALIAN STEEL CONFERENCE, Napoli, 2011, p. 29-36. Proceedings of the: XXIII Congresso C.T.A., Ischia (NA), October 9 - 12, 2011.

O.S. Bursi, G. Zanon and R. Pucinotti. *Performance of column bases made with high strength steel tubular columns subject to earthquake loading*, XXIII GIORNATE ITALIANE DELLA COSTRUZIONE IN ACCIAIO - XXIII ITALIAN STEEL CONFERENCE, Napoli, 2011, p. 37-44. Proceedings of the: XXIII Congresso C.T.A., Ischia (NA), October 9 - 12, 2011.

Under review

N. Tondini, V.L. Hoang, J.-F. Demonceau and J.-M. Franssen *Experimental and numerical investigation of high-strength steel circular columns subjected to fire loading.* Under review by Journal of Constructional Steel Research.

In preparation

Aglaia-Eugenia Pournara and Spyros A. Karamanos, Jan Ferino and Antonio Lucci, "*Strength and stability of high-strength steel tubular beam-columns under compressive loading*," 14th International Symposium on Tubular Structures, (ISTS 14), Paper No. 103, London, UK, September 2012.

Hoang Van Long, Demonceau Jean-François, Jaspart Jean-Pierre. *Design guidelines for a type of seat-connection used in buildings with steel circular tubular columns. Part I: at normal temperature*. To be submitted to Journal of Constructional Steel Research.

Hoang Van Long, Demonceau Jean-François, Jaspart Jean-Pierre. *Design guidelines for a type of seat-connection used in buildings with steel circular tubular columns. Part II: at high temperature*. To be submitted to Journal of Constructional Steel Research.

Hoang Van Long, Demonceau Jean-François, Jaspart Jean-Pierre. *Application of component method for column-bases using rectangular end plate with four anchor bolts*. To be submitted to Journal of Constructional Steel Research.

Hoang Van Long, Demonceau Jean-François, Jaspart Jean-Pierre. *Beam-to-tubular column joints subjected to fire action – Experimental and numerical investigations*. To be submitted to Fire Safety Journal.

Hoang Van Long, Demonceau Jean-François, Jaspart Jean-Pierre. Column-base joints subjected to fire action – *Experimental and numerical investigations*. To be submitted to Fire Safety Journal.

Pappa, P. and Karamanos, S. A., "*Buckling of High-Strength Steel CHS Tubular Members Under Axial Compression and Bending*.", 14th International Symposium on Tubular Structures (ISTS 14), Paper No. 104, London, UK, September 2012.

Bursi O.S., Pucinotti R., Tondini N., Zanon G. *Test and analysis of beam-to-column joints and column bases for steel-concrete moment-resisting frames with high strength steel tubular columns*. To be submitted to Journal of Constructional Steel Research.

Hoang Van Long, Demonceau J.F. , Pucinotti R., Tondini N., Zanon G. Analysis and behaviour of beam-to-column joints and column bases made with high strength steel tubular columns subjected to fire loading. To be submitted to Fire Safety Journal

BUDGET INFORMATION PER BENEFICIARY		
BENEFICIARY	TOTAL AMOUNT SPENT TO DATE (€)	TOTAL ALLOWABLE COST AS FORESEEN IN GRANT AGREEMENT (€)
University of Liège (Belgium)	247.487,03	241.111,30
Centro Sviluppo Materiall (Italy)	234.490,96	217.193,20
Stahlbau Pichler (Italy)	296.489,13	282.378,75
University of Thessaly (Greece)	166.310,33	170.444,70
University of Trento (Italy)	264.180,24	237.700,69

VI. Final summary

Circular hollow sections (CHS) are mainly used for columns and lattice girders or space frames for roofs in buildings and halls. Moreover, accidental actions, like earthquake and fire, should be considered in the design of structures; and particularly for those hosting large crowds of users (airport, station, stadium, office building), often made of CHS profiles.

As a direct result of the CHS shapes (symmetry about all cross-sectional axis passing through the gravity centre, CHS profiles are commonly used in welded steel frames where members experience loading in multiple directions. The similarity of the resistance properties of CHS about any axis makes them also good choices for columns. Finally CHS have excellent resistance to torsion.

The use of concrete filled section is often adopted for low cost fire protection and earthquake-prone zones where member fire protections can be damaged. Under earthquake loading, steel-concrete composite CFT (Concrete Filled Tube) columns offer different advantages: i) the steel tube provides efficient confinement to the concrete core, developing full composite capacity of the column; ii) the concrete core limits the appearance of local buckling and (iii) the concrete spalling is prevented by the confined steel tube, contributing to the strength and ductility and improving the seismic energy dissipation.

Detailed criteria for design checks both at the Ultimate and Serviceability Limit States are required in order to allow the designer to profit from the advantages offered by CHS and to evaluate the adequacy of his own design. Moreover, CHS column bases and bolted and/or welded connections for H beam-to-CHS column joints always lead to difficulties in detailing when earthquakes and fires have to be faced to. In the highlighted field of application (HSS and seismic/fire conditions), the lack of knowledge, data, experimental evidences and design code provisions is even larger. For these reasons, the ATTEL project intended to develop both analytical and experimental know-how in order to support new design criteria for the exploitation of HSS and steel-concrete composite circular hollow sections for columns and connections subjected to exceptional loads, like earthquakes and fire.

The conducted investigations have been both experimental, through testing of tubular members and connections, analytical and numerical, through the use and the extension of EC3 design approaches and advanced finite element simulations, in order to make full use of high strength steel ranging from S500Q/ S500MC to S690Q/S700MC according to the new Eurocode 3 Part 1-12, for structural seamless circular tube with diameters ranging from 2 to 24 inches, with $D/t > 30$ (which represents nowadays an upper limit for structural applications). The ambitious targets were to increase structural performance of steel structures and so to reduce weight and construction costs for buildings subjected to exceptional loadings; in a greater detail, investigations have been conducted on some key structural elements:

1. Steel and composite CFT (concrete filled tubes) columns made of HSS;

2. Welded and bolted composite beam-to-steel and CFT column joints made of HSS;

3. Steel and composite CFT column base-joints made of HSS.

The results of these investigations are summarised below. In particular, it is be demonstrated how the different objectives of the project have been achieved, work package per work package.

VI.1. WP1 – Collection and evaluation of test data and design procedures on HSS tubular members and connections subjected to earthquake and fire loadings

In the project proposal, the objectives of this work package were described as follows:

- evaluation of existing methodologies for low-cycle fatigue design of members and joints;
- collection and evaluation of experimental test data on steel and composite steel-concrete tubular members and connections under earthquake and fire loadings;
- collection and evaluation of experimental test data on HSS, HSS-concrete composite joints and HSS tubular elements subjects to earthquake and fire loadings;
- collection and evaluation of design procedures on over-design approach, capacity design and displacement based design applicable on HSS-concrete composite joints.

The above-mentioned collection and evaluation of tests and design procedures were categorized in three categories:

(a) connections and elements under static loading;
(b) connections and elements under seismic loading;
(c) connections and elements under fire loading.

This work package resulted in the production of a state-of-the-art document, i.e. Deliverable 1.1 (see also § VIII.3 for more information), which constituted the basements for the performed developments within the ATTEL project.

Through this work, the lack of information identified in the initial project proposal has been confirmed; in particular: the limited data on the use of HSS in beam-to-column joints and column bases, whatever is the loading type, the classification of HSS circular cross-sections, the fire response of HSS, … But on the other hand, the conclusions of this intensive bibliographical work led the partnership to re-discuss the experimental campaign to be carried out within the project. As a result, it was finally decided to amend the initially planned testing program, in close collaboration and agreement with the TGS8 technical experts.

VI.2. WP2 – Design of specimens

The objectives of this work package were expressed as follows:

- choice and optimization of the specimens to be tested (Task 2.1);
- design and numerical modelling of HSS steel and composite columns to be tested under earthquake and fire loading (Task 2.3);
- selection and design of HSS-concrete composite beam-to-column joints to be tested under earthquake and fire loading (Task 2.4);
- selection and design of base joints to be tested (Task 2.2).

During the kick-off meeting held in Liège, the need to work on integrated structural solutions and to test actual geometrical and loading situations has been highlighted. As a result, three different situations have been identified:

(a) structures under static and fire loading;
(b) structures under moderate seismic and fire loading;
(c) structures under strong seismic and fire loading;

For these three situations, the best economical use of HSS CHS elements has been first identified; details about this work may be found in Deliverables 6.

In a next step, three reference building frames have been designed in three partner universities and further selected as realistic study cases (see Table 1).

Table 1. Structural designs proposed for each university

	ULG – Building I	**UNITN – Building II**	**UNITH – Building III**
Loading conditions	Static + Fire	"Medium" earthquake (<0,25g) + Fire	"Strong" earthquake (>0,25g) + Fire
Structural elements extracted from the designed buildings	Beam-to-column joints	Beam-to-column joints	Beam-to-column joints
	Columns	Columns	Columns
	Column bases	Column bases	Column bases

Then the tested joint specimens have been "extracted" from the reference buildings cases. As a result, well adapted elements and critical loading situations have been so selected, therefore leading to the

definition of reality-representative testing procedures. Finally, appropriate beam-to-column joint configurations for testing have been similarly defined for the three reference situations.

The structural elements/joints selected through this procedure are the following ones (the interested reader will find more detailed justifications for the selection of the test specimens – as a result of WP1 conclusions and here-above expressed considerations – in Appendix XIII-1 of the present document):

- Two different tubular HSS columns (S590 CHS 355x12 and S590 CHS 324x10)
- Two different types of beam-to-column joints (see Figure 5 and Figure 10):
    - "Static joint" extracted from Building I
    - "Seismic joint" extracted from Building II (and III)
- Three different types of column bases (see Figure 5, Figure 11 and Figure 12):
    - "Static base joint" extracted from Building I
    - "Seismic base joint 1" extracted from Building II (and III)
    - "Seismic base joint 2" extracted from Building II (and III)

More details about the tested specimens are available in § VIII.5 and §VIII.6 related to WP3 and WP4 respectively. Also, all the conducted investigations are reported in Deliverable 2.1 and 2.2.

VI.3. WP3 – Cyclic testing

The objectives of this work package may be summarized as follows:

- experimental investigations on the mechanical behaviour of designed HSS-CHS columns and HSS-CFT columns (Task 3.3);
- experimental investigations on the mechanical behaviour of HSS-concrete composite beam-to-column joints (Task 3.4);
- experimental investigations on the mechanical behaviour of base joints (Task 3.2).

These experimental tests have been conducted in three different laboratories (i.e. CSM, University of Trento and University of Thessaly) on columns, beam-to-column joints, beam-to-column joint components, column bases and column base components:

- 6 tests on base joints with three different types of connections, as defined in WP2, subjected to cyclic and ground acceleration time-history loadings (Trento);
- 3 tests on components extracted from the column bases subjected to monotonic loading (Thessaly);
- 18 tests on short and slender steel columns with 2 different cross-sections subjected to monotonic loading (CSM);
- 3 tests on beam-to-column joints with the "seismic" joint configuration subjected to cyclic and ground acceleration time-histories loadings (Trento);
- 8 tests on "single-components" extracted from the beam-to-column "static" joint configuration subjected to monotonic loading (Thessaly).

Besides that, tests for the mechanical characterization of materials were conducted by CSM.

All the tests were successfully performed and the obtained results are reported in Deliverables 3.1 to 3.4. Some more details are also available in § VIII.5 of the present report. The so-obtained results were used for the model calibration of WP 5 and for the derivation of design guidelines within WP 6.

VI.4. WP4 – Fire testing

Following experimental investigations were planned:

- fire response of designed HSS-CHS columns and HSS-CFT columns (Task 4.2);
- fire response of HSS-concrete composite beam-to-column joints (Task 4.3);
- fire response of base-joints (Task 4.4).

Accordingly, different fire tests have been conducted at the University of Liège:

- Four fire tests on columns:
  - 3 HSS-CHS columns (2 on 323,9x10 tubes and 1 on 355,6x12 tube) and;
  - 1 HSS-CFT column (355,6x12 filled tube).
- Four fire tests on beam-to-column joints:
  - 2 on the "static" joint and;
  - 2 on the "seismic" joint.
- Three tests on column bases:
  - 1 on "static" column base;
  - 1 on "seismic" column base 1 and;
  - 1 on "seismic column base 2 (innovative solution).

Also, in parallel to these tests, a significant amount of coupon tests for mechanical characterisation at room and elevated temperatures have been performed on the tested HSS.

All these tests were successfully performed. Some of the obtained results are summarised in § VIII.6 ; more details can be found in Deliverables 4.1 to 4.4.

VI.5. WP5 – Model calibration

In this WP, it was intended to:

- provide stability curves to be applied with HSS according to test results of WP3 (task 5.1);
- provide mathematical formulation and calibration by means of the results obtained experimentally in WP3 and WP4 (Task 5.2);
- provide prequalification data and design procedures for HSS columns and joint tested (Task 5.3).

Within task 5.1, the applicability of existing design recommendations to tubular columns made of HSS was investigated in details.

The tests conducted both on elements and joints within WP 3 and WP 4, as beam-to-column and column-base joints, were fundamental to calibrate the 2D-3D numerical models in Task 5.2. In detail, modelling and calibration activities concentrated on:

- columns under both axial and bending actions;
- joint components under both high and room temperatures;
- hysteretic behaviour of beam-to-column and column base joints;
- mechanisms in the plinth of an innovative seismic column base joint.

More details are available in § VIII.7.2.

Finally, on the basis of the calibrated 2D-3D numerical models, parametric numerical analyses were conducted, as a contribution to Task 5.3, in order to investigate the response of the columns, joints and reference structures (see § VIII.7.3 for more details). The analysis took into account different input data and/or loading conditions. In particular, parametric numerical analyses were conducted on:

- columns at room temperature;
- columns at high temperature;
- joint components at room temperature;
- structures under seismic loading.

The results obtained within WP 5 were extensively used for the derivation of design guidelines in WP6. The outcomes of WP 5 are gathered in Deliverables 5.1 to 5.3.

VI.6. WP6 – Design guidelines

The tasks planned in this WP relate to:

- the development of design guidelines and recommendations endowed with HSS and HSS-CFT columns under earthquake and fire loading (Task 6.2);

- the development of design guidelines and recommendations endowed with HSS tested beam-to-column joints under earthquake and fire loading (Task 6.3);
- the development of design guidelines and recommendations endowed with HSS tested base-joints (Task 6.1).

Within this work package, design guidelines for buildings for which HSS CHS elements can give an economical solution have been derived. For the reference buildings I and II introduced in Table 1 (see WP 2 in § VIII.4), static, seismic and fire actions are considered; design guidelines from global structural analysis to the verification of structural elements (e.g. column bases, tubular columns and beam-to-column joints) are proposed. The extension to reference building III is immediate.

It should be noted that the presented guidelines (i) are in-line with the current EN 1993 design practice and (ii) propose possible improvements for HSS tubular CHS members. The proposed improvements are based on the experimental, numerical and analytical works achieved in the present research project. The guidelines developed within ATTEL are listed below and further described in § VIII.8; more details may be obtained in Deliverables 6.1 to 6.3.

- Structural solution
  - Building structures in low-seismicity areas
  - Building structures in areas of significant seismicity
- Global analysis of frames
  - Building structures in areas of low seismicity
  - Building structures in areas of significant seismicity
- Design of high-strength steel CHS columns
  - Design of HSS CHS columns at normal temperature
  - Design of HSS CHS columns at elevated temperature
- Design of column bases subjected to combined bending moment and axial force
  - "Static" column-base joints under static loading (at normal and elevated temperature)
  - "seismic" column-base joints (at normal and elevated temperature)
- Design of beam-to-column joints
  - "Static" beam-to-column joints (at normal and elevated temperature)
  - "seismic" beam-to-column joints

It can be observed that the different objectives of this work package have been achieved and the results of this work package constitute, with the experimental results, one of the main and valuable outcomes of the project.

VI.7. WP7 – Project coordination

Four tasks were planned within this work package:

- Task 7.1: Definition of standard protocols
- Task 7.2: Monitoring of the activities of each research unit
- Task 7.3: Global evaluation of the research project
- Task 7.4: Final report of the research activities

Meetings for the ATTEL project were organised in Liège, Moena, Volos, Bolzano, Pula, Asturias and Roma during the project. Minutes for these meetings are available.

At the beginning of the project, an FTP server for the ATTEL project was created. In agreement with the partners of another RFCS project entitled HITUBES (RFSR-CT-00035) in which all the ATTEL partners are involved, it was agreed to merge the two FTP servers initially created separately for the two projects in one FTP server. The requested information to be connected to this server is given here below:

- Address: ftp://msmsr05.gciv.ulg.ac.be
- Username: HITEL

- Password: HSS590

In particular, directories for the collection of interesting articles, reports and documents have been created on the FTP server according to different domains identified during the kick-off meeting in Liège and updated during the second meeting in Moena.

VI.8. Conclusions

The use of high strength steel (HSS) circular hollow sections (CHS) is still limited in the construction industry despite their excellent structural and architectural properties and the fast development of end-preparation machines. Moreover, although EC3-1-12 extends its scope to steel grades up to S690/S700MC, limitations exist at the material, structural and design levels.

The project ATTEL intended to develop both analytical and experimental know-how in order to support new design criteria for the exploitation of HSS and steel-concrete composite circular hollow sections for columns and connections subjected to exceptional loads, like earthquakes and fire.

The investigations have been experimental (through testing of tubular members and connections), analytical and numerical (through the use of the component method and advanced finite element simulations).

Globally, but also looking to details, it can be concluded that the different investigations were successfully conducted and the different objectives of the ATTEL project were met. The main achievement of the project is obviously the proposal of design recommendations for structures using HSS tubular columns and for structural elements made of HSS such as columns, beam-to-column joints and column bases in fire conditions and/or under seismic actions.

Through the proposed recommendations, it is now possible to perform an optimized and economical design of the structural elements considered within the present project, taking full advantage of the properties of HSS. Most of these recommendations have been developed respecting the Eurocode philosophies and principles. Accordingly, the implementation of proposed rules within the Eurocodes could be contemplated.

Beyond that, the project provides also to designers key information related to the economical fields of application of HSS in structures subjected to fire and static or seismic loading.

VII. List of deliverables

Deliverables	Planned delivery date	Actual delivery date	Location of the report	Name of the file
WP1: D1.1	December 2008	30/03/2010 (delivered with the mid-term report)	On CIRCA server	ATTEL-WP1-D1
WP2: D2.1 to D2.2	June 2009	30/03/2010 (delivered with the mid-term report)	On CIRCA server	ATTEL-WP2-D2
WP3: D3.1 to D3.4	October 2010	April 2012	On CIRCA server	ATTEL-WP3-D3
WP4: D4.1 to D4.4	October 2010	13/10/2011	On CIRCA server	ATTEL-WP4-D4
WP5: D5.1 to D5.3	October 2011	March 2012	On CIRCA server	ATTEL-WP5-D5
WP6: D6.1 to D6.4	December 2011	March 2012	On CIRCA server	ATTEL-WP6-D6
WP7: D7.1 to D7.3	December 2011	December 2011	Paper copies sent to the commission	These deliverables are in fact the sum of the six-monthly reports, the mid-term report and the final report

VIII. Scientific description of the results

VIII.1. Objectives of the project

Circular hollow sections (CHS) are mainly used for columns and lattice girders or space frames for roofs in buildings and halls. Moreover, accidental actions, like seismic and fire loads, should be considered in the design of structures subjected to possible exceptional crowd condition (airport, station, office building), often realized by means of CHS.

CHS are commonly used in welded steel frames where members experience loading in multiple directions and are then endowed with very efficient shapes for this multiple-axis loading as they have uniform geometry and thus uniform strength characteristics along all cross-sectional axes; this makes them good choices for columns. They also have excellent resistance to torsion.

The use of concrete filled section is customarily adopted for low cost fire protection and earthquake-prone zones where member fire protections can be damaged. Under earthquake loading, steel-concrete composite CFT (Concrete Filled Tube) columns offer different advantages: i) the steel tube provides efficient confinement to the concrete core, developing full composite capacity of the column; ii) concrete core delays steel tube from local buckling and concrete spalling is prevented by the confined steel tube, contributing to the strength and ductility and improving the seismic energy dissipation.

Detailed criteria for checks both at the Ultimate and Serviceability Limit States are required in order to allow the designer to evaluate the adequacy of his own design; and advanced analysis methods need to be developed to assess the actual structural behaviour. Moreover, bolted or welded connections both for circular columns and H beam-to-CHS column joints still exhibit difficulties in detailing when earthquakes and fires have to be faced to. Nonetheless, in the highlighted application fields there is a lack of knowledge, data, experimental evidences and design code provisions that are not able to cover some important aspects in the use of high strength steel (HSS) for CHS. For these reasons, the present project ATTEL intended to develop both analytical and experimental know-how in order to support new design criteria for the exploitation of HSS and steel-concrete composite circular hollow sections for columns and connections subjected to exceptional loads, like earthquakes and fire.

The conducted investigations have been both experimental, through testing of tubular members and connections, analytical and numerical, through the use of the component method and advanced finite element simulations, in order to make full use of high strength steel ranging from S500Q/ S500MC to S690Q/S700MC according to the new Eurocode 3 Part 1-12, for structural tubes diameter ranging from 2 in to 24 in, with $D/t > 30$ which represents nowadays an upper limit for structural applications. The ambitious targets were to increase structural performance of steel structures, reduce weights and construction costs for buildings subjected to exceptional loadings; in a greater detail, investigations have been conducted on some key structural elements:

1. Steel and composite CFT columns made of HSS;

2. Welded or bolted composite beam-to-steel and CFT column joints made of HSS;

3. Steel and CFT column base-joints made of HSS.

The results of these investigations are summarised within the present section. All the details are made available in the different deliverables of the project.

VIII.2. Comparison of initially planned activities and work accomplished

In the early course of the project, the partnership converges on the need to amend the experimental program initially planned within WP 3.

Indeed, proposals for changes in Tasks 3.2, 3.3 and 3.4 – resulting from technical discussions amongst the partners during the first partner meetings - have been suggested (these ones were already detailed and duly justified in the ATTEL mid-term technical report) and approved by the TGS8 committee at the occasion of its 2010 meeting in Aachen on 17-19 May and then further by the Commission. The modifications brought to the WP3 test campaign are reported in the appendices (see § XIII.1).

Besides that, because of production planning, a late delivery of the testing material by the tube producer had to be faced by the partners. This explains why the publication of the deliverables for WP3 had to be delayed to the end of the project.

Nevertheless, the work actually achieved in ATTEL is fully in line with the initially planned activities. All the objectives of the project have been met; in particular, valuable results in terms of scientific outcomes and design recommendations for the use of HSS tubular column in steel and composite constructions have been obtained.

VIII.3. WP1 – Collection and evaluation of test data and design procedures on HSS tubular members and connections subjected to earthquake and fire loadings

This work package consists of two tasks:
• Task 1.1 Collection and evaluation of experimental test on High Strength Steel
• Task 1.2 Collection and evaluation of design procedures on over-design approach, capacity design and displacement based design usable on HSS concrete composite joints.
The above collection and evaluation of tests and design procedures are categorized in (a) static, (b) earthquake and (c) fire loading summarized in the following. More details in this collection and evaluation are offered in Deliverable 1.

VIII.3.1. Static loading

VIII.3.1.1. High Strength Steel

The use of Circular Hollow Section (CHS) and steel-concrete Composite Filled Tube (CFT) section has recently had a significant development both for their excellent structural and architectural properties. Conversely, the use of high strength steel (HSS) circular hollow sections (CHS) is still very limited in the construction industry. The high-strength steels have specific chemical compositions which depend primarily on rolling and tempering techniques, element thickness and producers. It can be said that the ductility of material and section for HSS elements can be considered lower than that of ordinary steel and hence need to pay particular attention to use plastic analysis, particularly in seismic conditions. EN 1993-1-12 was recently developed in order to give rules (additions and changes) to make EN 1993-1-1 applicable to high strength steel. Concerning the weldability, it is more difficult to weld quenched and tempered HSS and thermo-mechanically rolled HSS than mild steel.

VIII.3.1.2. Local and global buckling

There are numerous studies on the effect of buckling on structures of HSS. In general those studies show that HSS performs better than ordinary steel or at least not worse. This means that the normal design rules can be used as a conservative approach (Richter et al, 2002, Sivakumaran, 1998 and Rasmussen & Hancock, 1995). The reason for the better behaviour of HSS is a smaller influence of imperfections and lower influence of residual stresses because the value of the ratio between residual stresses and yield strength is small. Studies and tests on long box and I-section columns fabricated from HSS have shown that the buckling behaviour of these sections is better than that described in Eurocode (EN1993-1-1, 2005). In fact the Eurocode 3 design curves are conservative compared with the tests and with Australian (Standards Association of Australia, 1990), American (American Institute of Steel Construction, 2005) and British specifications (British Standard, 2000). Therefore a more rational way towards the enhancement of the current specifications for HSS steel, would be to give a gradual increase of the buckling curves by modifying the imperfection parameter (British Standard, 2000).

VIII.3.1.3. Classification of cross sections for CHS made of HSS

The classification of cross sections is closely related to the ductility of the material, the ductility of the element section and the local buckling phenomena. An important problem of HSS section, owing to the high yield strength, consists of respecting the classification limits imposed by Eurocode 3-1-1. Several studies and tests have shown that the slenderness limits in EC3-1-1 are probably too conservative both for mild steel up to grade S460 and for HSS, in particular for circular hollow section (Beg & Hladnik, 1996). It is therefore necessary to perform experiments and tests with regard to these issues, mainly investigating the behaviour of circular sections in HSS.

VIII.3.2. Earthquake loading

VIII.3.2.1. Tubular CHS and CFT structural members under cyclic bending loading

Experimental research has been conducted on CHS and CFT beams under various types of seismic loading in order to investigate the structural behaviour, the degradation (Elchalakani et al, 2004), and the influence of the D/t ratio[10], under cyclic loading. The CHS beams exhibited stable hysteresis behaviour up to local buckling and then showed considerable degradation in strength and ductility depending upon the *D*/*t* ratio. The CFT beams exhibited stable hysteresis behaviour up to the formation of plastic ripples and then showed considerable degradation in stiffness, strength, and ductility depending on the D/t ratio. Furthermore, empirical formulations are proposed by several studies (Kyriakides & Shaw, 1987) in order to simulate the relationship between the prescribed curvature and the number of cycles necessary to produce buckling.

VIII.3.2.2. Tubular CHS and CFT beam-columns under static (monotonic) loading

Extensive experimental and numerical research has been conducted, in the past, in order to investigate and compare the CHS and CFT tubular and square beam-columns under compressive loads (Furlong, 1967). The test results indicate that the column capacity was significantly improved due to the concrete strength gained from the confinement provided by the steel tube. Analytical models were also developed (Schneider & Alostaz, 1998) to predict the capacity of circular CFT beam–columns accounting for the interaction between the steel and concrete, which were in good agreement with the test results.

VIII.3.2.3. Tests on structural joints between tubular columns and I-beams

Experimental and analytical research have been conducted in previous works (Cheng & Chung, 2003) in order to estimate the structural behaviour of various bolted steel/composite beam-to-column joints under cyclic loading. In particular, the sufficiency of bending strength and the appropriate activation of the shear transfer or force distribution mechanisms through the joints are investigated. Moreover, in a recent publication, (Bursi et al., 2008) proposed a multi-objective advanced design methodology for steel-concrete composite moment-resisting frames.

VIII.3.3. Fire loading

VIII.3.3.1. Material properties for concrete and steel at elevated temperature

The “high-temperature properties” of concrete and steel are defined by the temperature dependent changes in their characteristic thermal values (density, specific heat capacity, thermal conductivity) and their characteristic mechanical values (strength, Young’s modulus, stress-strain diagram, thermal strain).“Material laws” for concrete and steel material can be found in Eurocode models and several proposed analytical material models. These material models are validated and employed on both numerical heat transfer analysis and nonlinear thermal stress analysis of Concrete Filled Hollow Section (CFHS) columns at elevated temperatures. Furthermore, the behaviour of HSS at elevated temperatures has been studied in a research program conducted by Chen and Young (Young, 2008).

VIII.3.3.2. Concrete filled hollow section columns

In Concrete Filled Hollow Section (CFHS) columns, concrete filling has been shown to improve the fire resistance. One reason is that the concrete increases the heat capacity of the column. More important however is that, when exposed to fire, a redistribution of load will occur in the column from the hot steel section to the relatively cold concrete core. Furthermore, as the behaviour of CFHS columns under fire conditions has been studied since the1980s, it is proven that at higher temperatures, the steel section gradually yields as its strength decreases, and the column rapidly contracts at some point between 20 and 30 minute after exposed to fire (Kodur, 2007).

VIII.4. WP2 – Design of specimens

The objectives of WP2 are defined as follows:

- choice and optimization of the specimens to be tested;
- design and numerical modelling of HSS column and HSS-CFT column to be tested under earthquake and fire loadings;

- selection and design of HSS-concrete composite beam-to-column joints to be tested under earthquake and fire loadings;
- selection and design of base joints to be tested;
- estimation of specimens characteristics by means of F.E. models and calibration of models.

To define the specimens to be tested, it was agreed at the kick-off meeting held in Liège to extract these specimens from "actual" study cases in order to test realistic elements. Accordingly, it was proposed to design three different reference buildings corresponding to different loading conditions as described in Table 2. The objectives through the design of these reference buildings is i) as mentioned before to propose realistic configurations for the structural elements to be tested in laboratory (i.e. columns, beam-to-column joints and column bases) and ii) to show the benefit of the use of HSS, compared to the use of the "normal" steel.

Table 2. Structural designs proposed for each university

	ULG – Building I	**UNITN – Building II**	**UNITH – Building III**
Loading conditions	Static + Fire	"Medium" earthquake (<0,25g) + Fire	"Strong" earthquake (>0,25g) + Fire
Structural elements extracted from the designed buildings	Beam-to-column joints	Beam-to-column joints	Beam-to-column joints
	Columns	Columns	Columns
	Column bases	Column bases	Column bases

VIII.4.1. Design of Building I

Before entering in the design of the building for such loading conditions, a preliminary economical study was performed to identify the situations when the use of HSS tubular columns is cost-effective The conducted study is a parametrical investigation performed on tubular columns. An optimization of the design has been performed on columns for different loading conditions (reflecting what can be met in practice in actual braced and unbraced buildings), different column heights and different steel grades (from S235 to S690); the obtained solutions for the different considered steel grades have been compared in term of cost. Through this study, it has been demonstrated that the use of HSS columns is interesting for braced frames in which the columns support significant axial loads and low bending moments.

From the remarks of the economical study, a building configuration is proposed and designed. The design of a shopping centre with a braced composite structural system and HSS tubular columns was contemplated to define the reference building. The general layout of the designed building can be seen in the Figure 1 and Figure 2. The loads which were considered are the loads recommended in the EN 1991-1-1 (2004) for such a building.

The main beams and the secondary beams have been designed as composite ones as illustrated in Figure 3. For the design of the secondary beams, two spans have been contemplated: 8 m and 12 m (length B on Figure 1). Three different column configurations have been considered as illustrated in Figure 4.

Through the design, different profiles for the beams and the columns were proposed for the different spans of secondary beams and the different column configurations. Through the performed investigations, it was illustrated that only the pure steel solution for the HSS columns can be economically interesting. So, for the definition of the specimens to be tested, only this configuration will be considered. In case of fire, it is recommended to protect these pure HSS columns appropriately (as it would have been the case with "normal" steel). Also, for this building, configurations for the beam-to-column joints and the column bases are proposed as illustrated in Figure 5.

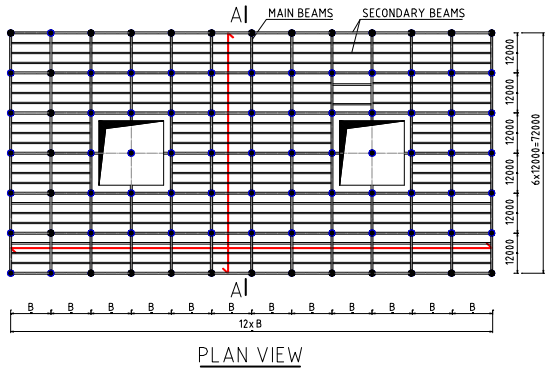

Figure 1. Plan view of the design building

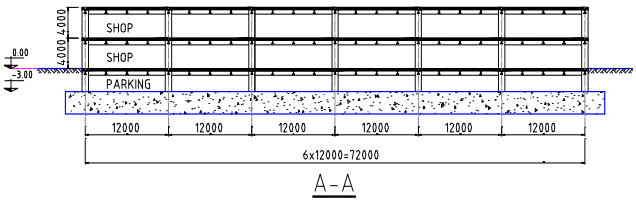

Figure 2. Main frame of the designed building

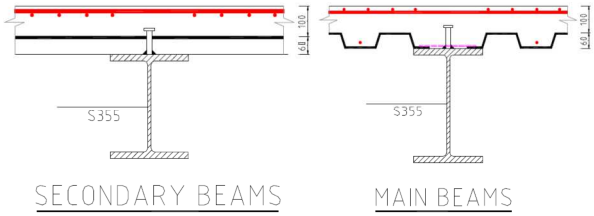

Figure 3. Designed composite beams

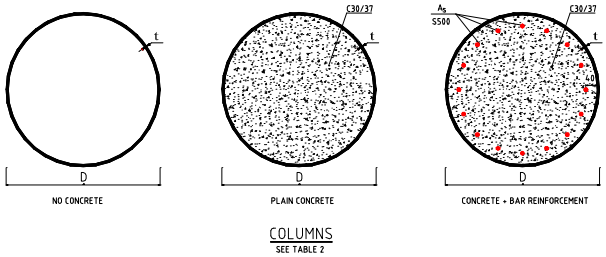

Figure 4. Contemplated column configurations

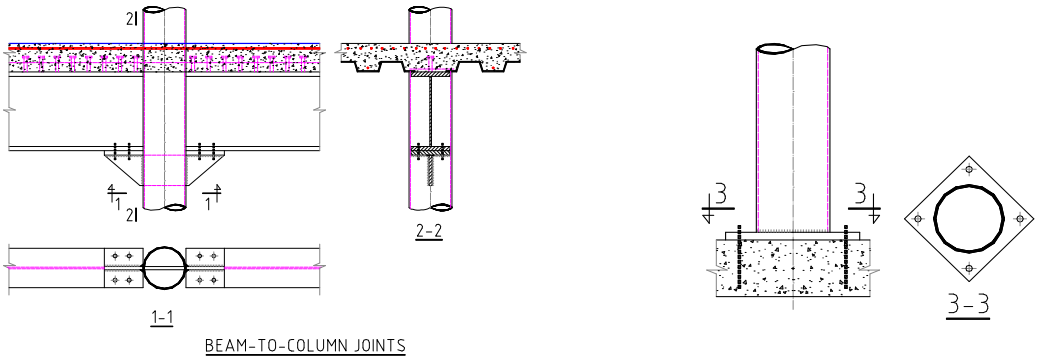

Figure 5. Proposed beam-to-column joint and base joint configuration

VIII.4.2. Design of Building II

The proposed second solution of structure is a composite steel-concrete structure with tubular columns and composite beams with a composite concrete slab. In order to better satisfy design criteria for static, seismic and fire situations, a moment resisting frame along the main direction was designed, whereas concrete walls along the secondary direction are inserted, obtaining in this direction a pinned system. This choice permits to realize a well performing structure, because the seismic action for a moment resisting frame in both directions could be too severe for columns and joints design.

The structure is characterized by the following geometrical dimensions: i) building category: office area (B); ii) 5 storeys and inter-storey height equal to 3,5 m; iii) plan dimensions equal to 32 x 32 m, with square meshes 8 x 8 m; iv) frame structure in main direction Y (moment resisting frame); v) pendulum frame in secondary direction (X); vi) open space in the first three storeys inside the building. Its plan dimension is 16 x 16 m.

This choice has been made in order to realize a bigger compartment and make an interesting study of the structural behaviour under fire and earthquake loads. Two staircases are localised between the concrete walls. These are necessary to evacuate building during fire or earthquake. In order to achieve the objective of the ATTEL project, the work focused on analysis and design of four types of columns:

- Circular hollow columns made with mild steel (*Normal Steel = NS*);
- Circular hollow columns made with high strength steel, (*High Strength Steel = HSS*);
- Mild composite columns CFT (*Composite Section with Normal Steel = CSNS*);
- High strength composite columns CFT (*Composite Section with High Strength Steel = (CSHSS)*.

The target consists to study and to compare performances of different tubular columns types under the seismic (a_g<0.25g) and fire actions, in order to investigate the actual possibility of using steel and steel-concrete composite HSS columns in order to satisfy the criteria of capacity design and fire resistance.

A static design of the building was first performed. Then, a verification of the building subjected to seismic loading was performed with the objective to determine if the use of HSS is useful both to respect capacity design criteria and to increase the column resistance under seismic loads. Through the performed studies, it was illustrated that the use of HSS columns satisfies the capacity design requirements given in EN 1998-1 (2005), without changing the diameter or the thickness of the column. Different is the case of the normal mild steel, where the designed steel or composite steel-concrete sections for the static design situation are not able to satisfy the seismic requirements or actions in the seismic design situation.

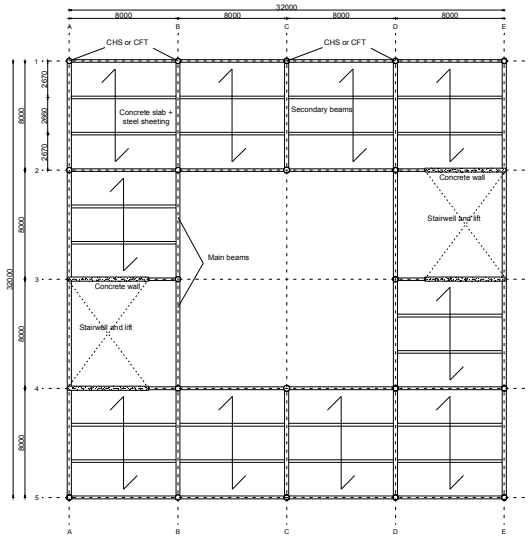

Figure 6. Plan view of a typical storey

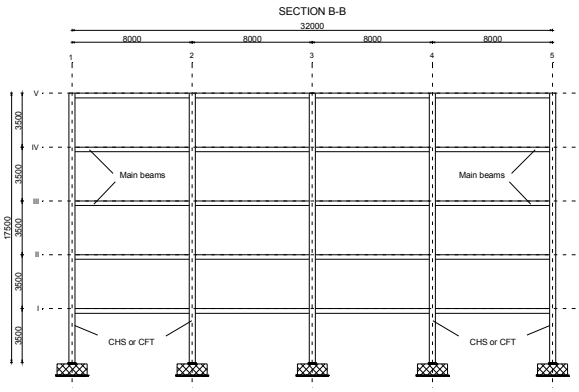

Figure 7. Building elevation view for section B-B

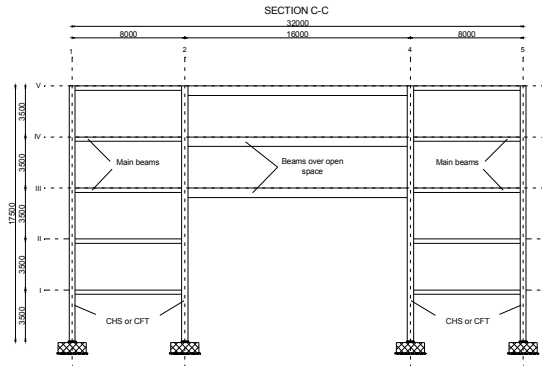

Figure 8. Building elevation view for section C-C

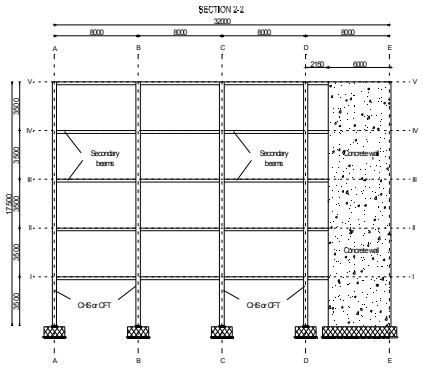

Figure 9. Building elevation view for section 2-2

The beam connection to circular steel tubes presents more difficulties if compared to the I shape. Analytical results suggested that connections which transfer load from the girder to the concrete core potentially offer better seismic performance than connections to the steel tube alone. In fact, connections to the steel tube alone may exhibit large distortion of the tube wall around the connection region. Besides, components transferring girder forces into the concrete core exhibit better strength and stiffness characteristics than a simple connection to the tube face. However, the improvement in behaviour depends also on the type of component penetrating the concrete core. Moreover, the choice to

obtain a collapse mechanism involving the formation of plastic hinges at the beams' ends required the realization of a beam-to-column joint possessing enough overstrength with respect to adjacent beams. Besides, by taking into account the difficulties related to the erection of this joint typology, it was decided to realize a rigid full strength connection. The configurations for beam-to-column joints and column bases are showed in following figures. The proposed welded/bolted solution was conceived to guarantee easiness of assembly and limited problems related to on site welding. The joint was made by two horizontal diaphragm plates and a vertical through-column plate attached on the pipe by groove welds. Flanges and web of each beam were connected to the horizontal plates and the vertical plate respectively by cover joint plates and two and three rows of bolts M27 and M20 10.9 as illustrated in Figure 10.

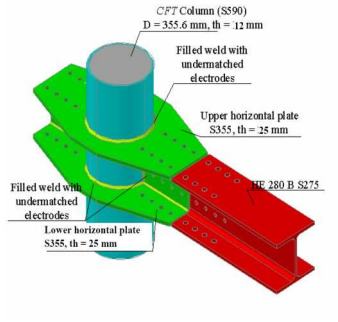

Figure 10 View of the beam-to-column moment resisting joint

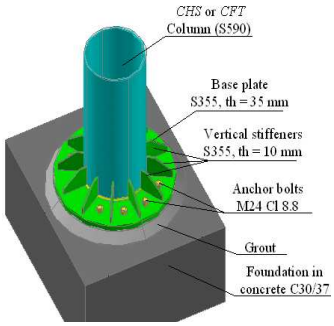

Figure 11. Base joint: Solution 1

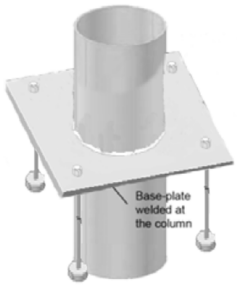

Figure 12. Base joint: Solution 2

For the column bases, two different solutions are proposed:

1. standard solution with a base plate, anchor bolts and vertical stiffeners. The base plate is welded around the perimeter of the column, the stiffeners are welded on column and base plate, the anchor bolts are inside the concrete foundation;
2. advanced solution with column embedded in the foundation. The idea is to satisfy the capacity design criteria by embedding the column inside the foundation. This solution is surely more performing for CFT columns. In other European projects (Bursi et al, 2004), it was noted that the first joint can result semi-rigid under cyclic loads. The reason of this behaviour is the elongation of the anchor bolts in tension when the grout will be damaged owing to the cyclic action of the earthquake. For this reason this second solution is proposed because it should perform better as rigid and full-strength base-joint.

The four types of columns previously designed under static loads are subjected to fire action with the help of the finite element program for non-linear analysis, SAFIR (2005) , developed by University of Liège. According to the design procedure contained in EN 1991-1-2, 2D numerical model was performed considering different fire scenario (fire in the small compartment, fire in the open-space, fire in the full ground floor) and the implementing of the ISO curve (perspective approach) and natural fire curve (performance-based approach) depending on: the design fire load; the presence of active prevention system; the dimension of the compartment; the dimension and location of the safety exit doors; the components of the partitions. Through the performed investigations, it was demonstrated that it is possible to reach the fire resistance requirements imposed by EN 1994-1-2 (2005), EN 1993-1-2 (2005) and National Standards (R60) by the use of HSS CHS columns without protection. Moreover, it is possible to reach exposure time greater than R60 with CFT columns and with or without HSS sections.

VIII.4.3. Design of Building III

On the basis of the results obtained from the previous study case it evidenced that, for tall moment resisting frames (with four or five stories) under high seismic actions, the design is governed by the satisfaction of the damage limit states instead of the ultimate limit states. This means that for this type of structures, in very high seismic regions, the use of the HSS in not useful being important the dimension of the columns in order to satisfy the limitation of the interstorey drift for the DLS and the interstorey drift sensitivity coefficient in order to consider the second order effects. For this reason, in

order to better identify a possible structural solution for the high seismic region, a five storey-composite building with braced and moment resisting framing system was proposed to be designed with high-strength steel CHS tubular columns and regular-strength steel I-beams with composite structural behaviour. This configuration corresponds to a typical office building, used in Greece, as showed in the following figures.

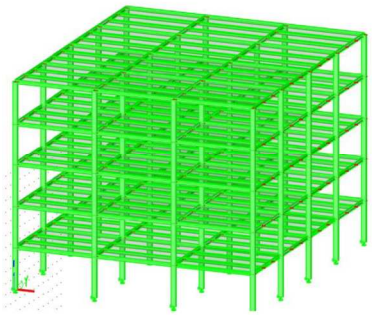

Figure 13 3D elevation view of the moment resisting building.

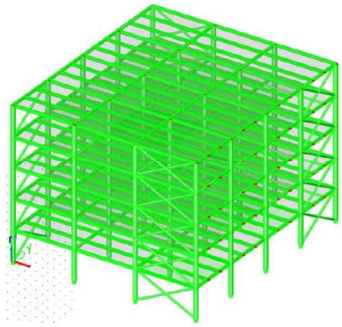

Figure 14 3D view of the "Type 1" braced frame building

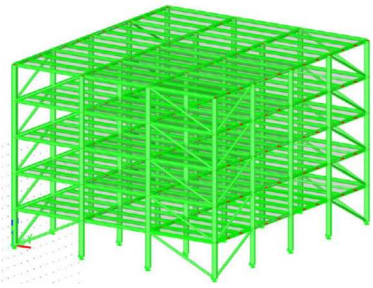

Figure 15 3D view of the "Type 2" braced frame building

The aim of this study is to compare performances of different tubular columns types mainly under strong seismic actions (ag>0.36g). The main interest is to investigate the actual possibility of using steel and steel-concrete composite HSS columns that will satisfy all the EN 1998-1 (2005) imposed criteria and will be competitive in terms of cost at the same time. For the design of this reference structure all the prescribed loading actions and the corresponding loading combinations will be considered. The earthquake loading is the major design parameter and it is expected to govern the total design of the building for some of the selected structural typologies. Following standard design practice in Greece, fire loading will be consider through appropriate paint or fibercoating protection of the steel elements.

VIII.4.4. Conclusions

From the previously designed structures, the following structural elements to be tested were extracted:

- Two different tubular HSS columns (S590 CHS 355x12 and S590 CHS 324x10);
- Two different types of beam-to-column joints (see Figure 5 and Figure 10);
  - "Static joint" extracted from Building I
  - "Seismic joint" extracted from Building II (and III)
- Three different types of column bases (see Figure 5, Figure 11 and Figure 12):
  - "Static base joint" extracted from Building I
  - "Seismic base joint 1" extracted from Building II (and III)
  - "Seismic base joint 2" extracted from Building II (and III)

More details about the tested specimens are available in § VIII.5 and §VIII.6 related to WP3 and WP4 respectively.

VIII.5. WP3 – Cyclic testing

VIII.5.1. Task 3.1: Mechanical characterization of materials

Two (2) different CHS made of HSS nominal strength grade S590 from seamless quenched and tempered products were studied:

Cross-section A	diameter (D) = 355 mm	thickness (t) = 12 mm
Cross-section B	diameter (D) = 323.9mm	thickness (t) = 10 mm

Material testing programme performed is summarized in Table 3.

Table 3. Material characterization testing program.

Test	**Nr. of test**
Tensile test at room temperature	4
Cyclic test at room temperature	10
Hole drilling	8
Chemical composition	4
Microstructural analysis and hardness	8
Material thoughness	4
Sectioning method	2

VIII.5.1.1. Tensile tests

Two (2) tensile tests each cross-section were performed at room temperature in accordance with (EN ISO 6892-1, 2009). Specimens were cylindrical (7 mm in diameter) machined in longitudinal direction. Results are reported in Table 4 and in the appendix given in § XIII.1.

Table 4. Results of tensile test at room temperature.

Cross section	**ID**	**S_0 mm²**	**D_0 mm**	**L_0 mm**	**$Rp_{0,2}$ MPa**	**R_m MPa**	**A_g %**	**A %**	**Z %**
A	A-1	37.72	6.93	50	746	821	7.2	16	72
	A-2	37.72	6.93	50	733	811	6.8	15	72
B	B-1	38.16	6.97	50	723	805	7.3	16	72
	B-2	37.61	6.92	50	735	813	6.9	15	70

VIII.5.1.2. Cyclic tests

Five (5) cyclic tests each cross-section were performed on cylindrical specimens (6 mm in diameter) machined in longitudinal direction. Testing programme and loading specifications are reported in Table 5.

Table 5. Testing programme and loading conditions for material cyclic tests.

Cyclic test	**Strain/stress range**	**specimen ID**	
		Cross section A	**Cross section B**
Strain controlled cyclic tests	$\pm 2\ \varepsilon_y$	A-1	B-1
	$\pm 1.5\ \varepsilon_y$	A-2	B-2
Stress controlled cyclic tests	$\sigma_{max} = \sigma\ (2\ \varepsilon_y)$; $\sigma_{min} = 0$	A-3	B-3
	$\sigma_{max} = \sigma\ (2\ \varepsilon_y)$; $\sigma_{min} = -\ 0.4\ \sigma_{max}$	A-4	B-4
	$\sigma_{max} = \sigma\ (2\ \varepsilon_y)$; $\sigma_{min} = -\ 0.8\ \sigma_{max}$	A-5	B-5

Each cyclic test was continued up to 100 cycle were completed, no premature failure was recorded. Whole test data are available up to 30^{th} cycle, after the 30^{th} cycle 1 each 5 cycle performed was recorded. Results are summarized in the appendix given in § XIII.1 where stress softening and strain stabilization are evaluable for strain and stress controlled tests respectively.

VIII.5.1.3. Residual stresses

Longitudinal residual stresses have been measured so as to characterize material imperfections. After some preliminary measurements giving not consistent results (see the appendix given in § XIII.1 for more details) it was decided to apply the "sectioning method" (Zieman, 2010).

Cross sectional distribution of longitudinal residual stress has been obtained in accordance with (Zieman, 2010). After sectioning the longitudinal residual stress measured on the external surface ranged between (-20 MPa ; + 63 MPa). Through thickness variation of residual stresses were evaluated by the application of Anderson-Fahlman method (Treuting et al, 1952) and bending component of longitudinal residual stress was evaluated to be (+ 15MPa on the external surface and – 15MPa on the internal surface).

More details on geometrical and material imperfections measurements are reported in the appendix given in § XIII.1

VIII.5.1.4. Discussion and conclusions

Products under study are HSS seamless quenched and tempered tubes. Several different material tests have been performed and main results are listed below:

- Material strength is well above the S590 nominal strength class, in fact its actual resistance can be classified as S690 steel grade.
- Material cyclic tests were performed with the scope of defining material behaviour for finite element modelling (task 5.1): stress softening and strain cyclic stabilization were well detected with constant strain and constant stress cyclic tests respectively.
- Residual stresses were measured via the application of the method of sectioning: very low values of residual stress (about 10% of yield stress) were measured in accordance with the heat treatment experienced by these products.

VIII.5.2. Task 3.2 and Task 3.4: Tests on base-joint specimens and on beam-to-column joint specimens

The present task concerns experimental activities performed on the following structural components:

- Beam-to-column joint
- Column-base joint
- Base plate component of column bases
- Slab reinforcement components of beam-to-column composite joints
- Through-plate components of beam-to-column composite joints

VIII.5.2.1. Beam-to-column and Column-base joint

With the scope of characterize the structural behaviour under seismic loadings of beam-to-column and column-base joints monotonic, cyclic and random tests were realized. The experimental programme covered 9 seismic tests on full-scale substructures, as reported in Table 6. In greater detail, the table collects:

- 3 beam-to-column joint specimens; 1specimen subjected to monotonic loading, 1 to cyclic loading and 1 to random loading. The specimens were sub-assemblages of interior beam-to-column joints connected by means of bolted connections.
- 6 column-base joint specimens; 3 specimens subject to cyclic loading; 3 specimens subject to random loading.

Table 6. Specimen nomenclature and test protocol.

Number	Label	Test Protocol	Type of Specimen
1	BTCJE	ECCS-SAC	Beam-to-column Joint
2	BTCJR	RANDOM	Beam-to-column Joint
3	BTCJM	MONOTONIC	Beam-to-column Joint
4	CBJSTE	ECCS-SAC	Column-base joint designed for static loads
5	CBJSTR	RANDOM	Column-base joint designed for static loads
6	CBJSEE	ECCS-SAC	Column-base joint designed for seismic loads
7	CBJSER	RANDOM	Column-base joint designed for seismic loads
8	CBJINE	ECCS-SAC	Column-base joint with an improved s. design
9	CBJINR	RANDOM	Column-base joint with an improved s. design

a. Beam-to-column joints

The geometry of the beam-to-column joint tested is depicted in Figure 16. In all specimens, a vertical load of 1000 kN was imposed on the top of the column in order to be consistent with the gravity loads applied to the reference frame.

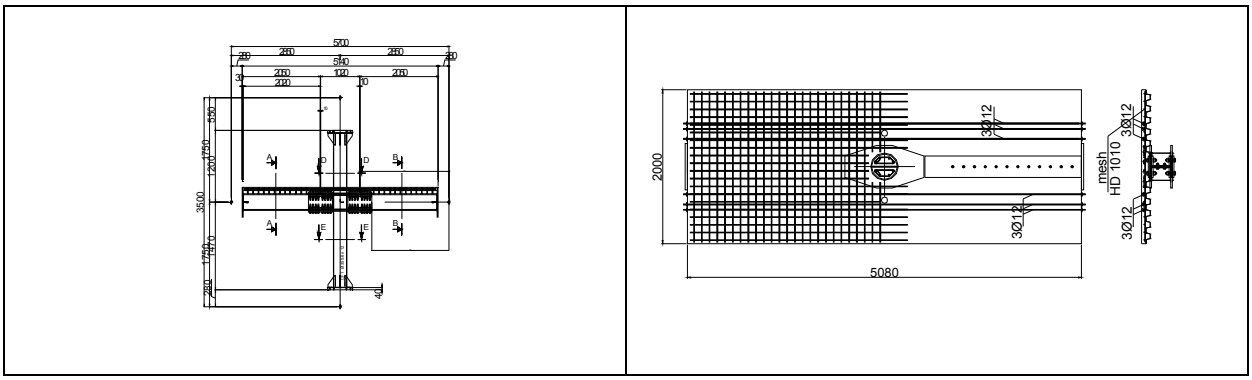

Figure 16. Geometry of tested beam-to-column joint specimens

The specimens were subjected to monotonic, cyclic and random loadings up to collapse. The cyclic test was realized according to the ECCS stepwise increasing amplitude loading protocol (ECCS, 1986), modified with the SACprocedure (Karl et al., 1997). Conversely, the random test was performed using as input the interstorey drift provided by the non-linear structural analysis on the companion 2D frame. Figure 17 shows the loading protocols.

Tested beam-to-column joints showed a ductile behaviour characterized by large rotations and values of strength without significant degradation. The only evident damage was spalling of concrete in compression near the column for high value of displacements. Plastic hinges were developed in the weaker sections between the plates welded to the column and the beam ends. The formation of plastic hinges was associated with slip, for high value of displacement, both between the butt strap plates and the plates welded at the column and between the butt straps plates and the beam. The slip was due to clearances in the holes.

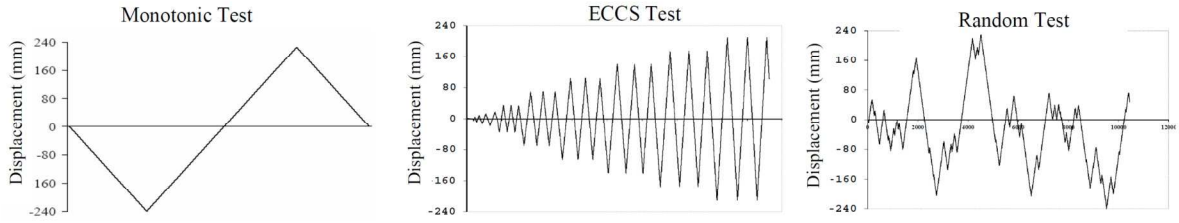

Figure 17. Loading protocols relevant to tested beam-to-column joints.

On the basis of mechanical and economic considerations, beam-to-column joints were realized without the connectors on the upper cover plate. Respect to similar joints tested in the past, these joints exhibit very limited stiffness and strength degradation to hogging moment. This is due to absence of instability phenomena in the bottom flange of beams. The relationship Force-Displacement on the top of the column and Moment-Rotation of plastic hinges recorded during testing are showed in following figures.

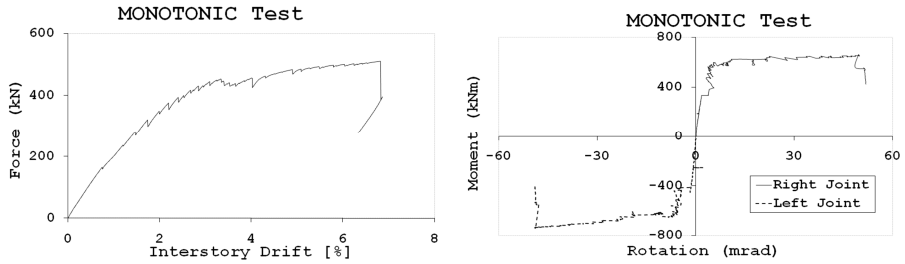

Figure 18. BTCJMbeam -to-column joint; Force-interstorey drift curves and Moment-rotation relationships.

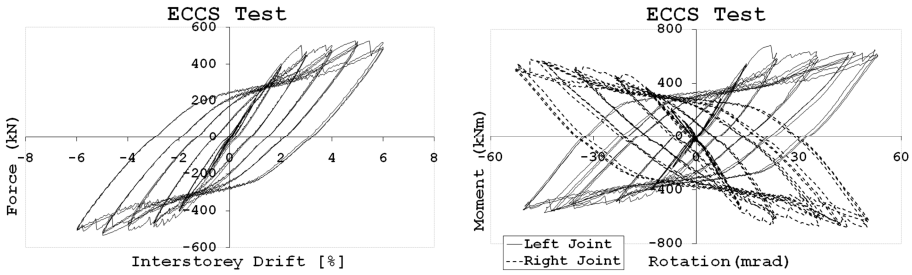

Figure 19. BTCJE beam -to-column joint; Force-interstorey drift curves and Moment-rotation relationships.

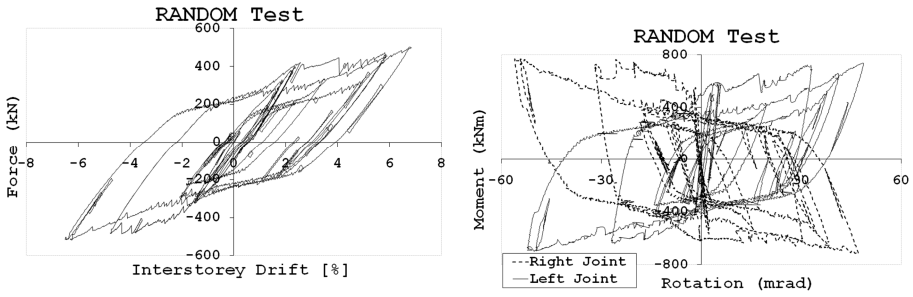

Figure 20. BTCJR beam -to-column joint; Force-interstorey drift curves and Moment-rotation relationships.

b. Column-base joints

Likewise beam-to-column joints, 3 different types of column-base specimens were subjected to cyclic tests, according with the ECCS procedure and with random loadings up to collapse. The first typology of column-base joint realized by CHS column was designed for gravity loads; the other two types of column-base joints devoted to medium-high seismicity were realized by means of CFT columns.

Column-base joint designed for static loads: the collapse of the joint was associated with plastic deformation of the thin base plate, as shown in Figure 21.

Figure 21. Column-base joint for static loads: Geometry and Failure.

Relevant hysteretic behaviour was characterized by high values of rotation without significant strength degradation, as showed in the following figures.

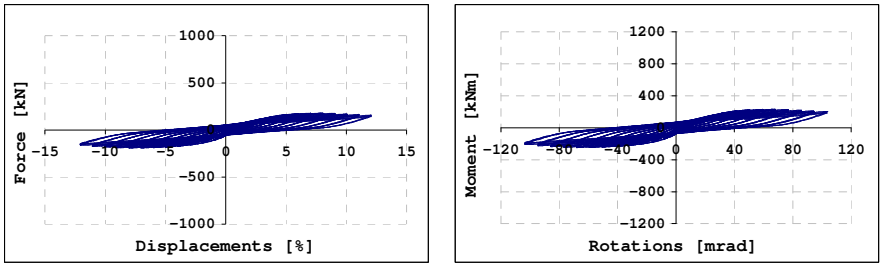

Figure 22. CBJSTEcolumn-base joint; Force-interstorey drift curves and Moment-rotation relationships.

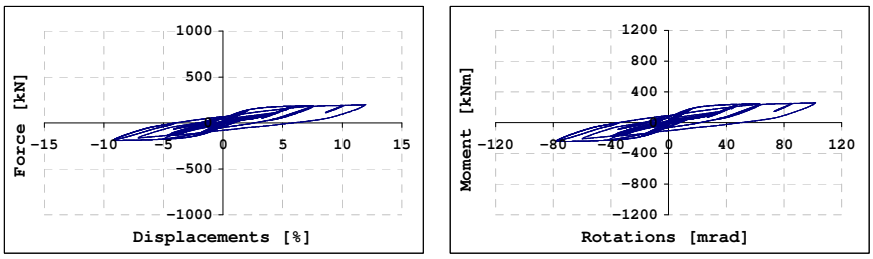

Figure 23. CBJSTRcolumn-base joint; Force-interstorey drift curves and Moment-rotation relationships.

Standard column-base joint designed for seismic loads: the stiffeners welded on the thick base plate permitted to obtain enough strength to the joint, see Figure 24. The ductile behaviour exhibited from the standard joint was correlated to the development of the plastic hinge at the base of the column. The collapse of the joint was due to failure of anchor bolts for high value of the plastic rotation of about 45 mrad. Until failure, the stiffness and strength degradation was negligible. The behaviour recorded during the test is showed in Figure 25and in Figure 26, respectively.

Figure 24. Standard column-base joint for seismic loads: Geometry and Failure.

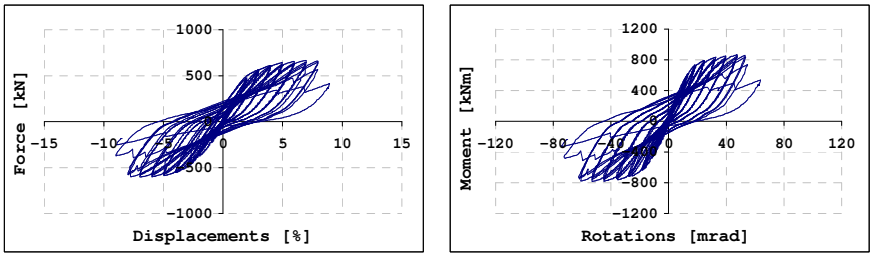

Figure 25. CBJSEEcolumn-base joint; Force-interstorey drift curves and Moment-rotation relationships.

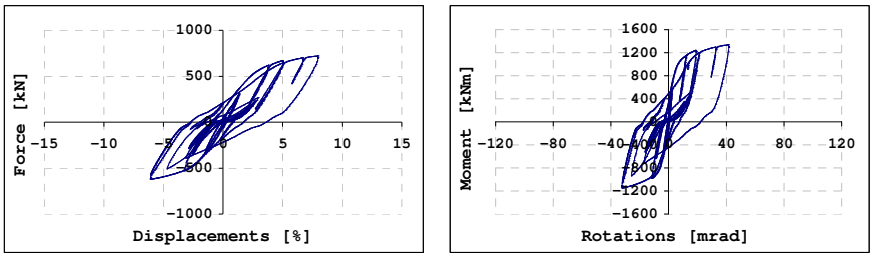

Figure 26. CBJSERcolumn-base joint; Force-interstorey drift curves and Moment-rotation relationships.

Innovative column-base joint designed for seismic loads: the aims of tests on the innovative seismic base joint, realized by means of a column embedded in the foundation, were two: i) the evaluation of the hysteretic behaviour of joint under seismic actions; ii) the study of the mechanism of transfer of force between the column and the foundation, similar to the Strut & Tie mechanism proposed in (EN 1992-1-1, 2005). The base joint exhibited stiffness and strength higher than the ones provided by the standard solution. This joint showed ductile behaviour characterized by large plastic rotation of about 45 mrad with brittle failure on weld between the column and the base plate, due to phenomena of local instability in the wall of the column. The hysteretic behaviour exhibited two plastic hinges on the column: i) one plastic hinge was located in the plinth due to compression of the concrete filling consequent to the rotation of the column; ii) a second plastic hinge located on the column outside of the plinth. To study the internal mechanism in plinths due to interaction between the column and the foundation strain gauges on the rebars in the plinths were welded. The tension recorded during the test permitted to check the validity of the numerical model set by the Abaqus program, to study the mechanical behaviour in the plinth.

Figure 27. Innovative column-base joint for seismic loads: Geometry and Failure.

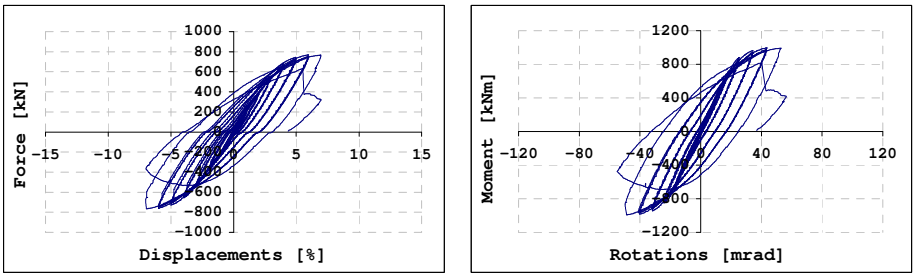

Figure 28. CBJINEcolumn-base joint; Force-interstorey drift curves and Moment-rotation relationships.

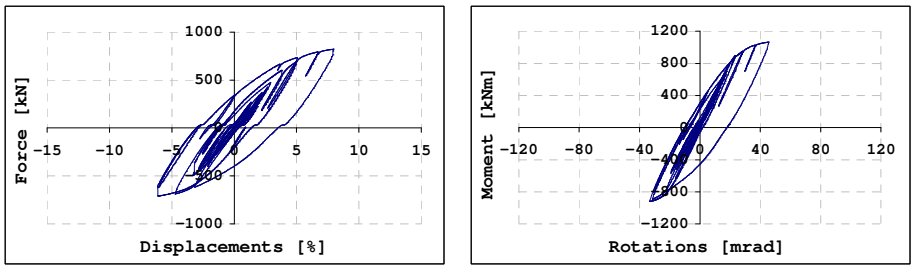

Figure 29. CBJINRcolumn-base joint; Force-interstorey drift curves and Moment-rotation relationships.

VIII.5.2.2. Base plate component

This experimental investigation consists of three (3) base plate tests (denoted as Component 3) to determine the flexural response of the rectangular base steel plate of a tubular column. The specimens

have been subjected to a monotonic pure bending moment. Three (3) plate thicknesses were examined, that is t_{pl}=14, 16 and 18 mm.

The steel tubes are made of high-strength steel (TS590) with a nominal yield stress of 735 MPa and the base plates of S355 steel. The nominal cross-section for the tubes is CHS 193.7x10. The dimensions of the steel plates are 400x400 mm and they are connected with four (4) M30 bolts, as shown in Figure 30. The high-strength tubes have been produced by Tenaris Dalmine, and the specimens segments were manufactured by Stahlbau Pichler. For the Component 3 tests, 4-point bending was applied to the tubular section of the specimens through a steel cross-beam with two special ball-joint hinges and appropriate wooden grip assemblies. Both ends of the specimens were supported by a double-hinge 'roller' system.

Strain gages were attached to the specimen to measure uniaxial and transverse strains on specific locations on the base plate (see appendix in § XIII.1). Wire position transducers and DCDT's were used for load-point and support displacement measurements. In addition, inclinometers were placed to measure the rotation of the base plates relative to the tube.

Three representative load-point displacements values of 90, 100 and 120 mm and corresponding base rotation values of 4, 5 and 6 deg. from the experimental results were chosen to describe flexural behavior of the specimens in the yielding region. The measured experimental results are presented in Table 7.

Table 7. Test results for Component 3 specimens.

type of specimen	**base plate thickness, t_{pl} (mm)**	**applied moment, M_{max} (kNm) at load-point deflection of**			**applied moment, M_{max} (kNm) at base rotation**		
		δ=90 mm	**δ=100 mm**	**δ=120 mm**	**r=4°**	**r=5°**	**r=6°**
Component 3	14	67.3	69.4	73.5	64.8	68.7	72.2
	16	89.8	92.7	96.6	87.5	92.7	97.3
	18	115.4	118.2	122.9	116.5	120.9	125.4

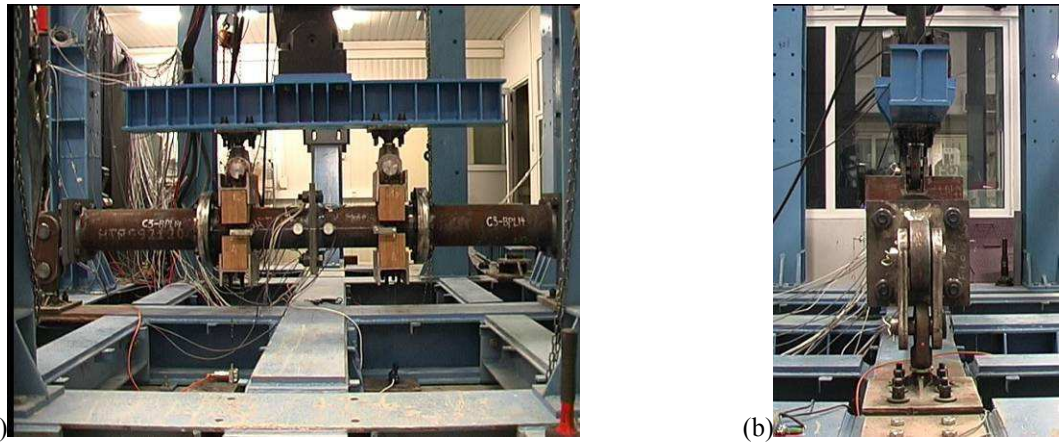

(a) (b)

Figure 30. Test setup for the Component 3 tests: (a) front view and (b) side view with double-hinge 'roller' system.

The specimens were subjected to monotonic 4-point bending loading with a stroke rate of 0.1 mm/sec. The specimen with a plate thickness of t_{pl}=14 mm resisted a bending moment of 67.3 kNm at a load-point displacement of δ =90 mm, a bending moment of 69.4 kNm at a load-point displacement of δ=100mm and a bending moment of 73.5 kNm at a load-point displacement of δ =120 mm. At the same load-point displacement values, the specimen with t_{pl}=16 mm resisted a bending moment of 89.8, 92.7 and 96.6 kNm, respectively, and that with t_{pl}=18 mm a bending moment of 115.4, 118.2 and 122.9kNm,

respectively. The applied bending moment vs. displacement and vs. base plate rotation diagrams for the Component 3 specimens under monotonic loading are shown in Figure 31. The flexural stiffness of the specimens, which is the same initially at about 3÷4 kNm/mm as expected, is approximately constant in the yielding region of the plate at about 0.25 kNm/mm due to the same steel grade used, independently of the thickness of the base plate . However, the level of the resisted bending moment for each plate increased by about 25 kNm for every 2 mm increase in plate thickness from 14 to16mm and 16 to18 mm. All specimens failed due to large deformations of the base plates, as shown in Figure 32 (see Appendix in § XIII.1).

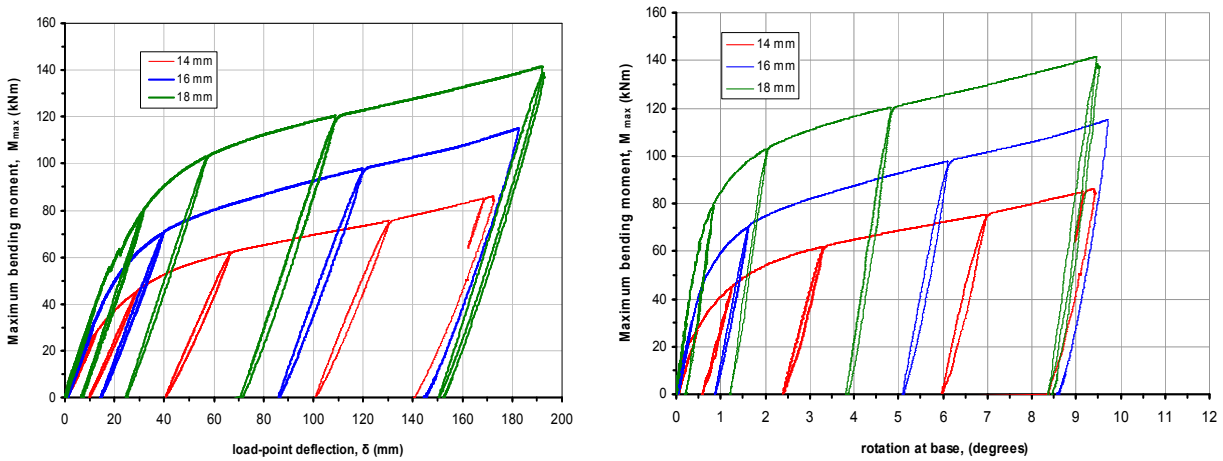

(a) (b)

Figure 31. Experimental results for the Component 3 specimens under monotonic loading: (a) applied bending moment vs. load-point displacement, (b) bending moment vs. base rotation.

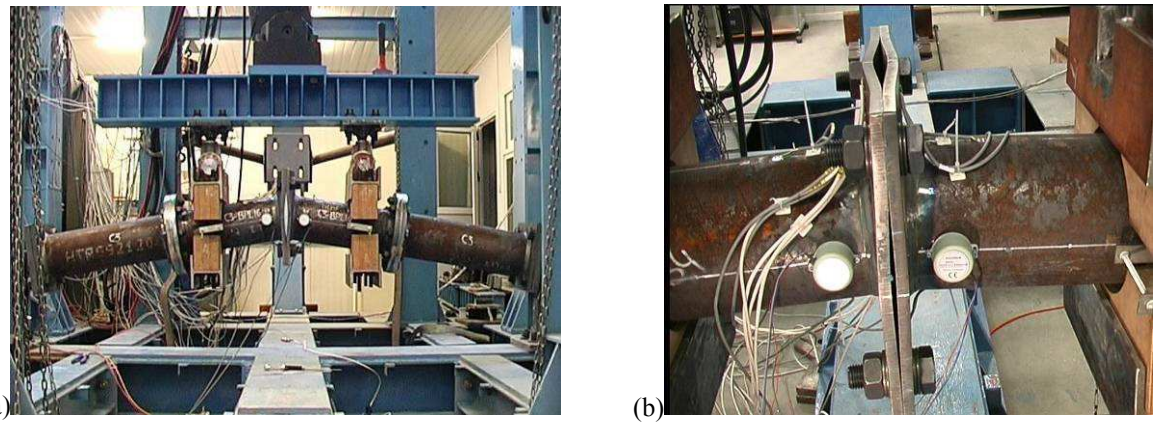

(a) (b)

Figure 32. (a) Deformed Component 3 specimen and (b) failure mode of base plate.

VIII.5.2.3. Slab reinforcement components of beam-to-column composite joints

This experimental investigation consists of four (4) tests on composite concrete slabs to study the tensile flexural behavior of the slabs. Three (3) specimens (1.1, 1.2 and 1.3a) have been subjected to monotonic bending loading, whereas the forth specimen 1.3b has been subjected to cyclic bending loading, according to ECCS loading protocol. Specimens 1.1 and 1.2 are similar to those used in the structural joints tested at the University of Liege, and specimens 1.3a and 1.3b are similar to those used in the structural joints tested at the University of Trento.

Each of the specimens consists of a concrete slab on a thin steel sheeting and supported by a heavy steel beam HEM 280 from S355 material, as shown in Figure 33a. Each specimen also contains a steel tube, made of high-strength steel (TS590), with nominal yield stress of 735 MPa, located in the middle of the slab. Before casting the concrete slabs, appropriate instrumentation with strain gages has been done in specific rebars. The 28-day cube compressive strength of the concrete has been measured as 40.4 MPa.

The test results are tabulated in the table of Figure 33b and the failure modes of all specimens are shown in Figure 34.

(a)

Specimen	*Type of loading*	*Maximum bending moment (kNm)*
1.1	monotonic	329.7
1.2	monotonic	331.8
1.3a	monotonic	264.0
1.3b	cyclic	290.0

(b)

Figure 33. (a) concrete slab specimens (b) test results.

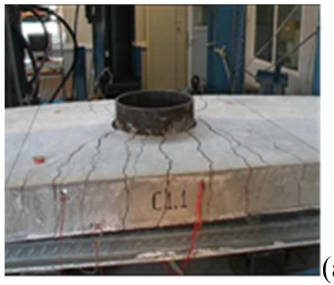

(a)

(b)

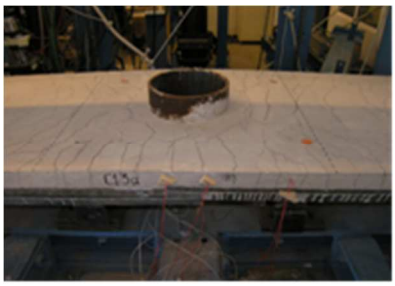

(c)

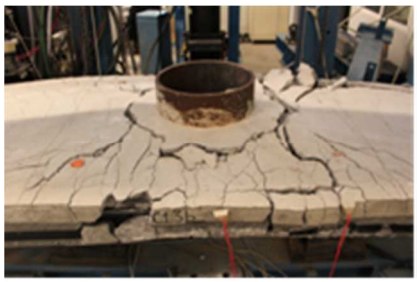

(d)

Figure 34. Failure modes of specimens: (a) 1.1; (b) 1.2; (c) 1.3a; (d) 1.3b.

In the case of specimens 1.1 and 1.2, the cracks started from the tube perimeter and propagated along the tube's radial direction. At a later stage, the cracks opened progressively through the slab thickness. For both specimens 1.1 and 1.2 the major cracks developed and propagated from the region around the tube circumference up to the stud closer to the tube. The cracks developed normal to the plane of bending near the studs closer to the tube, at both sides. In the case of specimens 1.3a and 1.3b, the developed cracks formed a crown around the tube perimeter at a distance equal to the length of the studs placed radially around the tube. Furthermore, in specimens 1.3 cracking was not localized as in specimens 1.1 and 1.2 in the constant bending moment region, and cracking developed throughout the entire slab, indicating a more ductile behaviour and more distributed damage in the concrete slabs.

VIII.5.2.4. Through-plate components of beam-to-column joints

For this component, four (4) geometries of steel through-plates were studied, as shown in Table 8. The CHS 323.9x10 steel tubes (produced by Tenaris Dalmine) are made of high-strength steel (TS590-fy=735 MPa) and the HEM280 beams and through-plates of S355 steel. The parts of the specimens were manufactured by Stahlbau Pichler. For the Component 2 tests, 3-point bending was applied to the simply supported specimens through a midspan concentrated load at the top of the column tube, as shown in Figure 35a. Wire transducers and DCDT's were used to measure load-point and support displacements and strain gages to study the deformations in the through-plates. The specimens were subjected to monotonic 3-point bending (stroke rate=0.1 mm/sec). While the specimen with the 100x15-mm through-plate failed due to lateral buckling of the plate outside the column tube at a bending moment of 221.2 kNm, the remaining three specimens failed due to buckling of the through-plate inside the tube, as shown in Figure 36b. The specimen with the 120x10-mm steel plate resisted a bending moment of 189.7 kNm, that with 120x12-mm plate a bending moment of 185.4 kNm and the specimen with a 100x12-mm plate a bending moment of 191.2 kNm (see Figure 35b). There is a kink in

all load-deflection curves due to slipping of the bolted connections along the span of the beam, so the true estimated load-point displacement at failure is about 10÷12 mm.

Table 8. Experimental results for Component 2 tests.

specimen type	height of through-plate, h_{pl} (mm)	thickness of through-plate, t_{pl} (mm)	bending moment at plate failure, M_{max} (kNm)
Component 2	120	10	189.7
	120	12	185.4
	100	12	191.2
	100	15	221.2

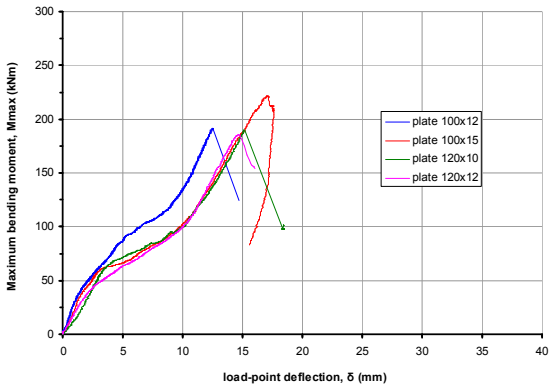

(a) (b)

Figure 35. (a) Test setup for Component 2 specimens and (b) applied bending moment vs. LP displacement diagram for Component 2 specimens under monotonic loading.

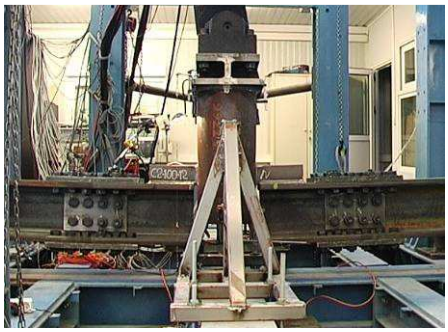

(a) (b)

Figure 36. .(a) Deformed Component 2 specimen and (b) buckling of through-plate inside the tube.

VIII.5.3. Task 3.3: Tests on column specimens

Eighteen (18) full scale monotonic tests were performed on HSS CHS columns made from seamless quenched and tempered products. Cross section dimensions and classification in accordance with (EN 1993-1-1, 2005) and (EN1993-1-12, 2007) are reported in the following table.

Table 9. Cross sectional dimensions of specimens.

ID	diameter D [mm]	thickness t [mm]	D/t	Nominal S590 Class	Actual S690 Class
A	355	12	29.6	3	3
B	323.9	10	32.4	3	4

As cross sectional classification depends also on yield strength of materials, both actual and nominal values of yield stress are considered in Table 9. In the following of this task only actual value of yield stress is considered.

The full scale testing arrangement is shown in Figure 37 where a Bs specimen is ready to be tested. Bending moment is applied at column ends leading to uniform bending along the column. Columns are connected to the machine hinges via two symmetric extensions (1.5 m long for long specimens and 2.0 m for short specimens), the second order moment generated by is taken into account in the elaboration of experimental data performed in Task 6.2.

Figure 37. Column Bs arranged in the testing machine before testing.

With the scope of reducing time needed for the testing arrangement, dedicated testing grips have been designed and fabricated. Hence full scale column specimens have been delivered with base column flanges to be bolted on the dedicated frame grips (Figure 38).

Each cross section was tested in two different column lengths:

- Short column (1850mm) relevant for cross sectional behaviour
- Long column (4850 mm) relevant for member behaviour

Loading conditions applied are several different combinations of axial compressive load (N) and bending moment (M) as detailed in Table 10. In this way main points of M-N interaction diagrams can be checked.

Figure 38. Full-scale column test: one of the testing grips dedicated to column test of the project and column specimens delivered with stiffened flanges.

Table 10. Testing program for monotonic full scale tests

Cross section	Class EN 1993-1-12	Short column			Long column		
		slenderness		Nr. of tests	slenderness		Nr. of tests
		Pin ends	Fixed ends		Pin ends	Fixed ends	
A	3	15	7.6	Nr. 5 tests: - 1 N - 4 N+M	40	20	Nr. 4 tests: - 1 N - 3 N+M
B	4	17	8.3	Nr. 5 tests: - 1 N - 4 N+M	44	22	Nr. 4 tests: - 1 N - 3 N+M

VIII.5.3.1. Geometrical measurements before testing

The actual dimensions of columns (thickness, diameters and outer profile) were measured before testing so as to characterize geometrical imperfections relevant for cross sectional and/or member stability.

The geometrical survey of the outer profile was performed employing a measuring equipment, developed and realized for the scope. It is composed by an aluminium stiff reference frame able to rotate around a reference axis of the column and equipped with a sliding guide supporting an LVDT which is always in contact with the column outer profile (Figure 39). It allow to obtain actual diameters (D), ovality imperfections ($O = (D_{max}-D_{min})/D_{nominal}$) and dimples (wrinkling) imperfections (e).

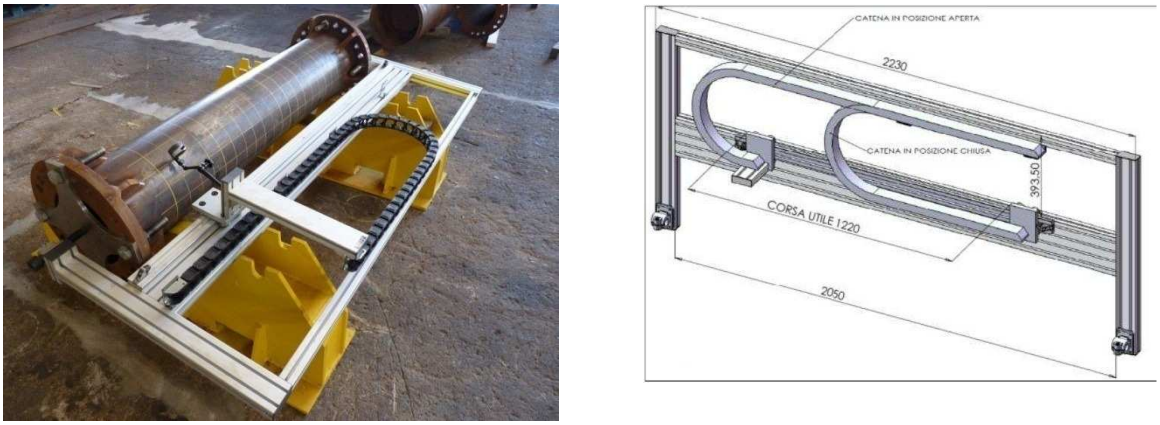

Figure 39. Actual geometry measurements: measuring device arranged on short specimen.

Thickness (t) distribution has been measured on the short column to be tested under combined loading. Three cross sections have been measured each column, using ultrasonic device for thickness for the diameters.

Maximum deviations of the above dimensions (D, O, t and e) from the nominal values are summarized in Figure 40 while complete set of measurements are available on the relevant Deliverable.

A comparison with tolerances reported in the relevant standard of products (EN 12010-2, 2006) was also performed. It can be noted that columns actual dimensions are in accordance with and satisfy the admissible tolerances reported in Table 11.

Table 11. Dimension tolerances reported in (EN 12010-2, 2006).

dimension	ID	tolerance
Diameter	D	± 1 %
Thickness	t	- 10 % (the positive deviation of thickness is implicitly limited by the tolerance on the mass: ± 6 % on each delivered member length)
Ovality	O	2 %
Out-of-straightness	e	± 0.2 % of the total length

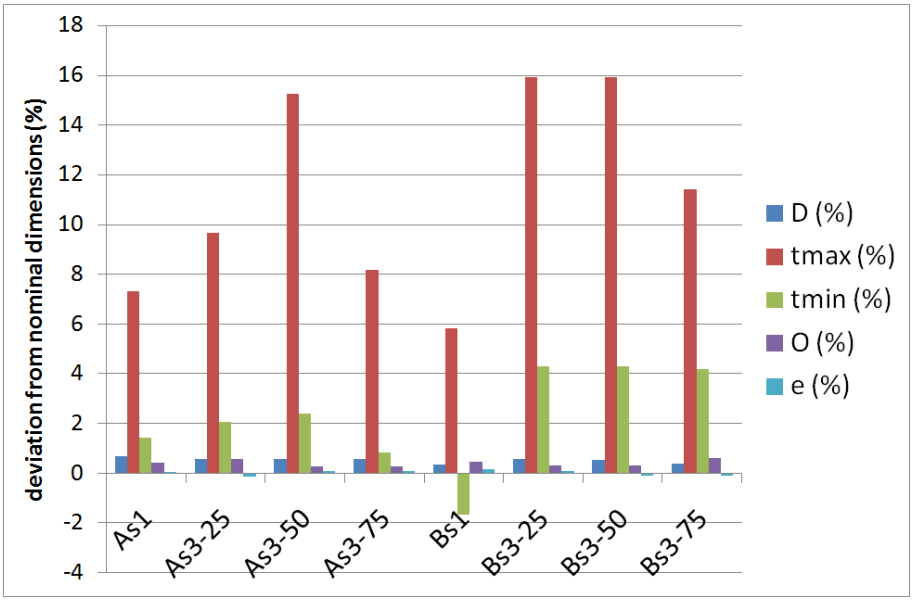

Figure 40. Measurement of geometrical imperfections: deviations from nominal dimensions of column specimens.

VIII.5.3.2. Axial compression tests

Four (4) tests were conducted in pure axial compression and fixed ends conditions. The load was applied at a constant displacement rate of 1.7mm/min.

Columns instrumentation is listed below:

- nr. 12 strain gauges on circumferential positions through 3 different cross sections;
- nr. 4 LVDT in axial direction on circumferential positions ;
- specimens were grid marked with a 50mm edge square grid;
- evolution of global deformation process by video-recording.

The test results are summarized in Table 12.

Table 12. Axial compressive test results.

specimen	ID	slenderness	N_{max} [kN]			d_u [mm]
			nominal	actual	delta	
Short column	As1	7.6	9556	10254	+ 7.30%	10.4
	Bs1	8.3	6449	7961	+ 23.4%	8.79
Long column	Al1	20	9307	10857	+ 16.7%	18.7
	Bl1	22	6171	7812	+ 26.6%	17.0

In the figures below the load-displacement curves obtained from short column tests and long column tests are reported together with photographs of the columns after testing.

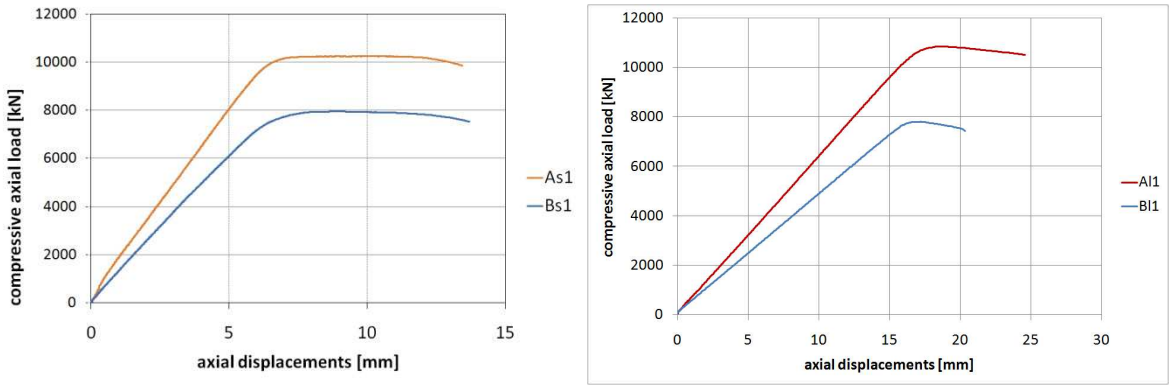

Figure 41. Axial compression tests: load vs. shortening diagram

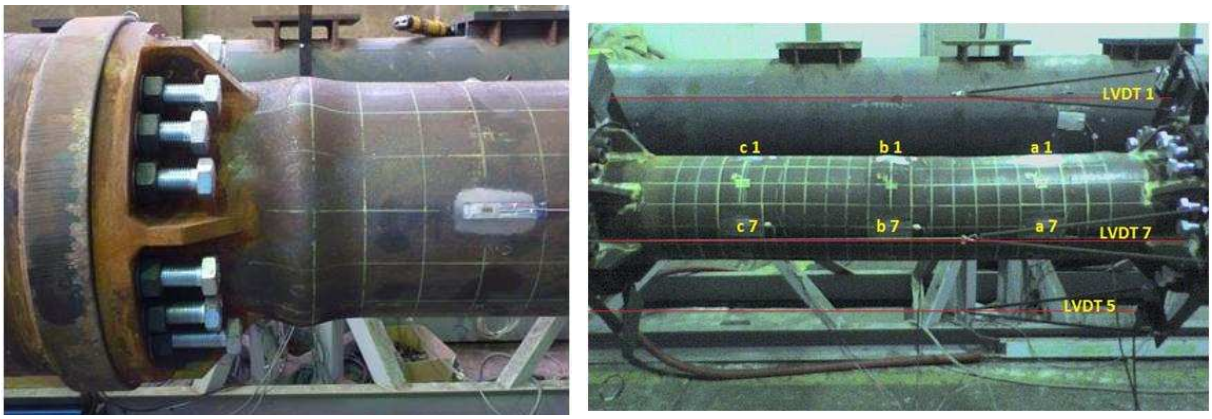

Figure 42. Axial compression tests: short column after testing As1 (left) and Bs1 (right).

Figure 43. Axial compression tests: long column Al1 after testing.

The geometry of bulge developed during the test was measured and is available in the relevant Deliverable.

VIII.5.3.3. Combined axial and bending tests

Fourteen (14) full scale tests have been performed under combined loading condition and free end rotations. Testing procedure consists of axial load increase at a constant rate up to the desired value then while axial load is hold fixed, slowly increase of the bending moment.

The columns were instrumented as listed below:

- nr. 4 strain gauges on 4 circumferential positions at mid span cross section;
- nr. 2 LVDT in axial direction (positions 90° and 180°);
- nr. 2 LVDT to measure column transversal displacement;
- hinges rotation;
- evolution of global deformation process by video-recording.

Some photographs of the specimen after testing are reported in Figure 44. In Table 13 results obtained on short columns are summarized.

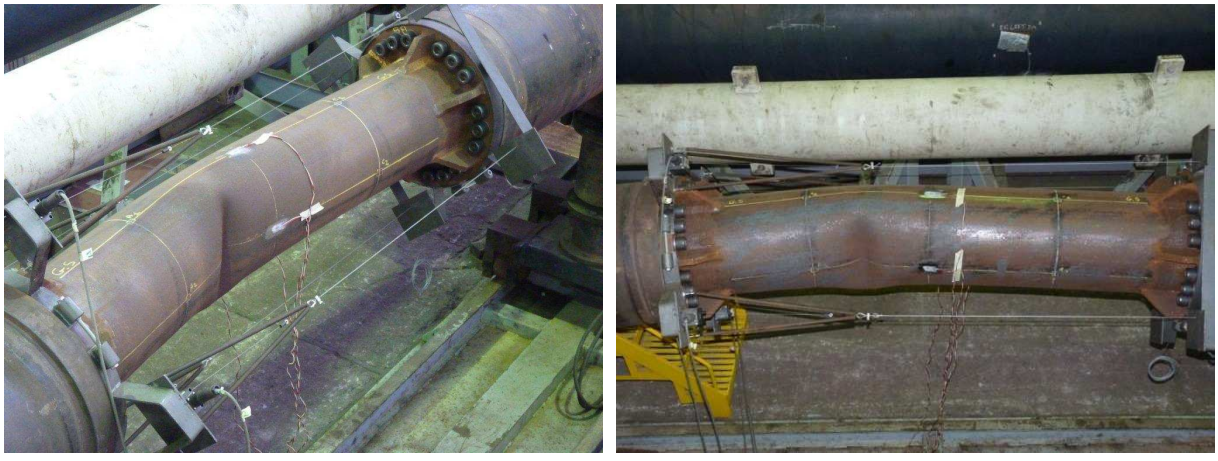

Figure 44. Column Bs3-13 and column As3- 13 after testing.

Table 13. Combined loading tests: short column results.

ID	N_{apply} [kN]	M_{max} [kN m]	Φ_u [degrees]
As3-13	1340	891	2.6
As3-25	2500	732	1.9
As3-50	5000	377	1.1
As3-75	7600	102	0.4
Bs3-13	1000	575	2.4
Bs3-25	1865	492	1.8
Bs3-50	3980	209	1.0
Bs3-75	5822	76	0.5

Complete moment vs. rotation diagrams are shown in Figure 45.

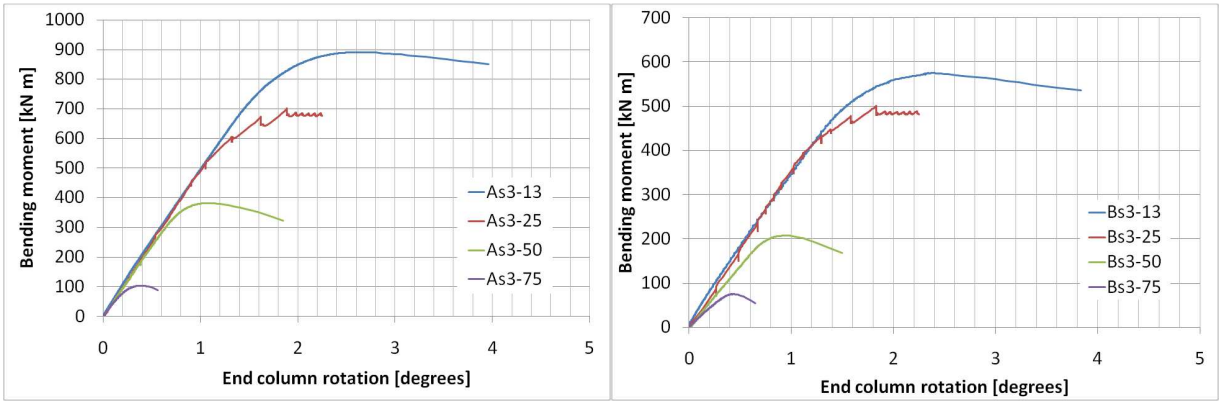

Figure 45. Combined loading tests: short column Moment vs. Rotation curves.

In Table 14 results obtained on long columns are summarized.

Table 14. Combined loading tests: long column results.

ID	N_{apply} [kN]	M_{max} [kN m]	Φ_u [degrees]
Al3-25	1530	670	4.4°
Al3-50	2590	441	3.3°
Al3-75	4588	150	1.7°
Bl3-25	1000	450	4.2°
Bl3-50	2020	232	3.0°
Bl3-75	3298	79	1.5°

Complete moment vs rotation diagrams obtained for long columns are shown in Figure 46.

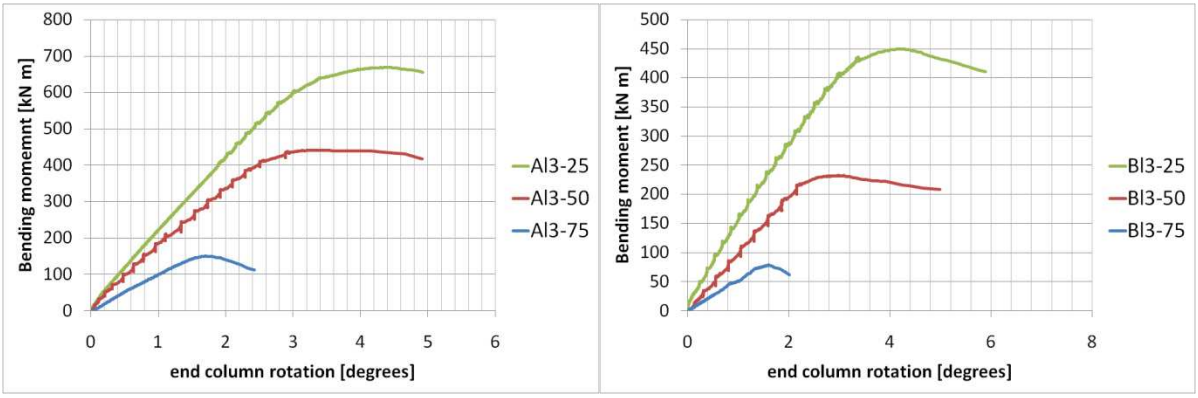

Figure 46. Combined loading tests: long column Moment vs. Rotation curves.

Some photographs of long specimens after testing are reported in Figure 47.

Figure 47. Columns (left to right) Al3-50 Bl3 – 25 Bl3-50 Bl3-75 after testing.

Extensive discussion of the so-obtained experimental data is reported in WP 6 (see § VIII.8).

VIII.6. WP4 – Fire testing

VIII.6.1. Introduction

The three main objectives of this work package are:

- Experimental investigation of the fire behaviour of HSS-CHS columns and HSSCFT columns;
- Experimental investigation of the fire behaviour of HSS-concrete composite beam-to-column joints;
- Experimental investigation of the fire behaviour of base-joints.

The activities were divided in 4 tasks:

- Task 4.1: Thermal characterization of materials;
- Task 4.2: Tests on column specimens;
- Task 4.3: Tests on beam-to-column joint specimens;

- Task 4.4: Tests on base joint specimens.

VIII.6.2. Main activities

Details on the performed tests can be found in Deliverable D4, only a summary of the latter is given here below.

VIII.6.2.1. Test campaign outline

As mentioned within the work package objectives, the following structural elements were chosen for the test campaign:

- Four (4) column specimens - three steel columns and one composite column (Task 4.2);
- Four (4) beam-to-column joints – two tests on the "static" joint configuration and two tests on the "seismic joint" configuration (Task 4.3);
- Three (3) column bases – one test on the "static" column base, one test on the "seismic" column base 1 and one test on the "seismic" column base 2 (Task 4.4).

The specimen descriptions are briefly presented in Table 15 and in Figure 48. The steel parts of the specimens were manufactured by STAHLBAU PICHLET (see WP2) while the concrete casting were executed in Liege. All tests were performed by Fire testing laboratory (Laboratoire d'Essai au Feu) at the University of Liège.

Table 15. Conducted test campaign on structural elements on fire (Tasks 4.2, 4.3 and 4.4)

N^0	Specimen name	Specimen description	Reference building
1	C1	Steel column: 323,9x10 tube, TS590 (Figure 48a)	Type 1
2	C2		
3	C3	Steel column: 355,6x12 tube, TS590 (Figure 48a)	Type 1
4	C4	Composite column (Figure 48a) - Steel tube: 355,6x12, TS 590 - Rebar: 8Φ18, B450C - Concrete : C30/37	Type 2
5	J1.1	Static joint (Figure 48b) - Bolts: 10.9, non-preloaded; - Steel Column: 323,9x10 tube, TS590; - Beam: IPE600, S355; - Concrete: C30/37; - Rebar: B450C.	Type 1
6	J1.2		
7	J2.1	Seismic joint (Figure 48c) - Bolts: 10.9, preloaded; - Composite column: 355,6x12 tube, TS590; - Beam: HEB 280, S355 ; - Concrete: C30/37 ; - Rebar: B450C.	Type 2
8	J2.2		
9	CB1	Static column base (Figure 48d) - Bolts: 10.9, non-preloaded ; - Steel Column: 323,9x10 tube, TS590 ; - Concrete: C30/37; - Rebar: B450C ;	Type 1

		- Grout: GROUTEX6.	
10	CB2	Seismic column base 1 (Figure 48e) - Bolts: 10.9, preloaded - Composite Column: 355,6x12 tube, TS590 - Concrete: C30/37 - Rebar: B450C - Grout: GROUTEX6	Type 2
11	CB3	Seismic column base 2 (Figure 48f) - Bolts: 10.9, preloaded - Composite embedded column: 355,6x12 tube, TS590 - Concrete: C30/37 - Rebar: B450C - Grout: GROUTEX6	Type 2

Figure 48. Specimens for the fire tests

VIII.6.2.2. Tests on base materials (Task 4.1)

The tests for the characterization of the thermal properties were only planned for the HSS, as the behaviour of normal steel (S355) at high temperature is well known from literature. Therefore, the characterization tests for materials within WP4 can be grouped as follows:

- Tests (1): Coupon tests at high temperature for HSS tubes: two HSS tubes (323.9x10 and 355.6x12) are used within the ATTEL project. The base materials of those tubes were tested at

six (6) different temperatures (from 2000C to 12000C) in order to obtain their mechanical characteristics (yield strength and Young modulus).

- Tests (2): Coupon tests at normal temperature for S355 steel and for the bolts: tensile tests giving the nominal σ-ε curves have been performed. With respect to the bolts, coupons were extracted from the bolt shanks.
- Tests (3): Compression tests on concrete cubes: tests on 15x15x15 cm concrete cubes were performed the same day as the fire test on the corresponding structural element (Table 16).
- Tests (4): Humidity tests on concrete: these tests were performed on similar specimens and at the same day as the tests (3).

For some elements, it was not required to perform coupon tests at room temperature as they were already tested within WP 3 (the tubes (323.9x10, 355.6x12) and the structural components of J2.1, J2.2, CB2, CB3 (seismic joint and seismic column bases), including the rebars).

Tests (1), (2) and (3) reported in Table 16 were performed at M&S laboratory (Laboratoire de Mécanique des matériaux et Structures), University of Liège, while Tests (4) were carried out by Fire testing laboratory (Laboratoire d'Essai au Feu), University of Liège.

Table 16. Summary of the coupon tests

N^0	Structural elements (see Table 15for the specimen names)	Number of specimens			
		Tests (1)	Tests (2)	Tests (3)	Tests (4)
1	323.9x10 HSS tubes*	6			
2	355.6x12 HSS tubes*	6			
1	End plate of column base CB1		5		
3	Vertical plate of joint J1.1 or J1.2		4		
4	Horizontal plate of joint J1.1 or J1.2		6		
5	Beam IPE 600 of joint J1.1 or J1.2		6		
6	Bolts M36 in joint J1.1 or J1.2		2		
7	Concrete of C4			2	1
8	Slap concrete of J1.1			2	1
9	Slap concrete of J1.2			2	1
10	Slap concrete of J2.1			2	-
11	Slap concrete of J2.2			2	1
12	Foundation concrete of CB1			2	1
13	Foundation concrete of CB2			2	1
14	Foundation concrete of CB3			2	-
Total number of specimens in each group		**12***	**23**	**16**	**6**

* As can be seen, 12 coupon tests at elevated temperatures were performed instead of 30 as announced within the project proposal. It is due to the fact that only two tubes made of HSS are met in the tested specimens and 6 coupon tests at elevated temperatures per tube were sufficient to characterise the HSS However, as can be seen in Table 16, a significant amount of other characterisation tests at normal temperature (not initially planned within the project) have been performed.

VIII.6.2.3. Furnace chambers and testing set-up

Two furnaces were used for the tests, a vertical one and a horizontal one (Figure 49). The fire is produced by burners with capacity of 2500 kW and the temperature in the furnaces is measured by thermoplates. The ISO 834 standard temperature-time curve was simulated during the tests.

The columns were tested in the vertical furnace, while the connections were tested in the horizontal furnace. The main schemes of the testing set-ups are presented in Figure 50. Hinges at the column extremities are placed for the column tests. With the adopted testing set-up for the beam-to-column joints, the two hand sides of the joints were under the same negative moments and the column was in traction. The columns in the column basis were subjected to a compression force and a bending moment.

Figure 49. Furnaces for the tests

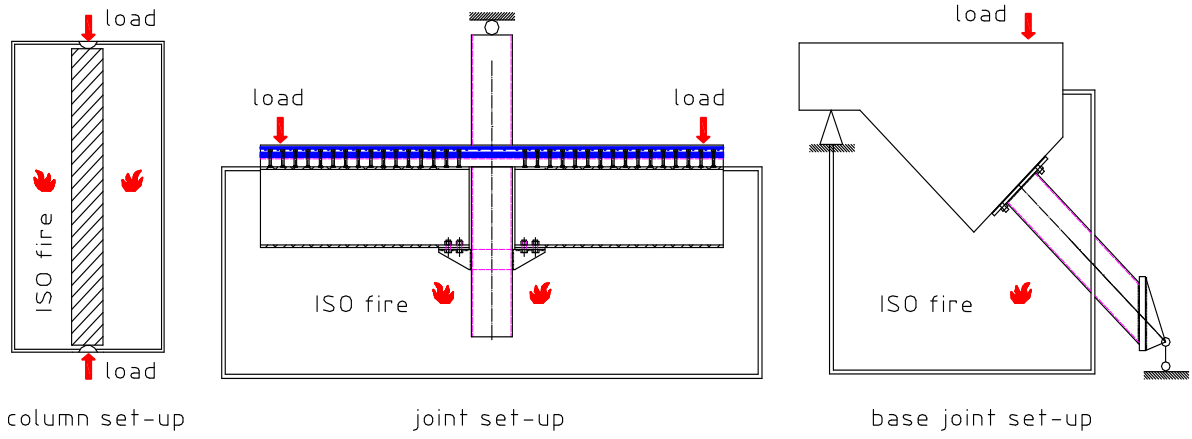

Figure 50. Principle schemes of the testing set-ups

VIII.6.2.4. Instrumentation

For the fire tests, the following measurement devices were used:

- Displacement transducers that allow controlling the movement of the specimens.
- Thermocouples which allow measuring the development of the temperature in important zones of the specimens.

For the joints and column bases, only the behaviour of the connections were under consideration; accordingly, the part of beams/columns which were not closed to the joints were protected so as to limit the zones directly affected by the fire; for the protection, intumescent paint was used.

Displacement transducers were used to control the cinematic behaviour of the specimens during the tests (i.e. during the loading stage at room temperature and during the fire stage). To measure the displacements in the heat-affected zones, ceramic wires in contact with the specimen and going outside the furnace were used. The displacements were measured at the cold end of the wires; the temperature

of the wire inside the furnace was measured so as to be able to extract the wire elongation from the measurements.

For the recording of the evolution of temperatures in the different zones of the specimens, a significant number of thermocouples were used. The thermocouples of type K (Nickel-Chrome/Nickel-Aluminium) were used to instrument the specimens.

VIII.6.2.5. Loading process

The loading process was as follows (Figure 51):

- First, the external load was applied on the tested specimen through hydraulic jack and was kept constant;
- then, a waiting time of 15 minutes was observed as recommended in the codes;
- finally, fire action was applied following the "ISO curve" until failure of the tested specimen.

The fire resistance observed during the test is defined as the time between the start of the application of the fire action and the failure of the specimen.

The values of the loads to be applied during the tests were predicted so as to reach a certain fire resistance depending of the type of specimens: about 20-25 minutes for the steel columns (C1, C2, C3); about 30 minutes for the static joints and the static column base (J1.1, J1.2, CB1); about 60 minutes for the composite column (C4), seismic joints (J2.1, J2.2) and the seismic column bases (CB2, CB3).

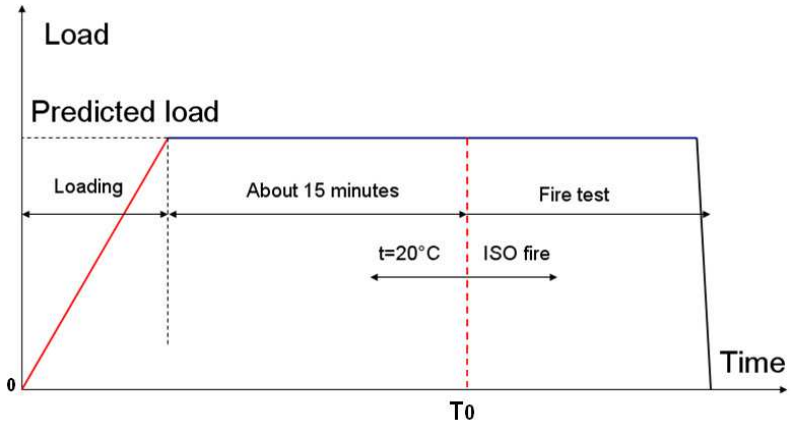

Figure 51. Loading process during the fire tests

VIII.6.2.6. Test results

The following data were collected from the tests:

- Data of the tests on base materials: tubes, plates, bolts, and concrete (see § XIII.3.2);
- Load-time curves (see § XIII.3.3);
- Temperature-time curves given by the thermoplates in the furnace (see Deliverable D4);
- Temperature-time curve given by the thermocouples located on/in the specimens (see Deliverable D4);
- Displacement-time curves recorded by the displacement transducers (see § XIII.3.3);
- Fire resistance of the specimens (see § XIII.3.3);
- Failure modes (see § XIII.3.3).

As an example, Figure 52 presents the curves obtained for the C1 column test (steel column). The time 0 in Figure 52b is corresponding with time T0 (=32) on Figure 52a, c, d, e, f and Figure 51, as the beginning of the fire test.

- Some remarks can be drawn:

- the axial fore in the column was completely kept constant (=700 KN) during the fire test (Figure 52a);
- the ISO fire curve is well simulated from 5 minutes (Figure 52b) until the end of the test;
- the temperature in the column reach 7000C after 20 minutes, but there are some differences between temperatures in different zones of the column (Figure 52c);
- global buckling of the column was observed at the end of the test (Figure 52f) with a significant lateral displacement at the middle-high of the column (Figure 52d);
- before failing, the column has much elongation due to the thermal dilatation (Figure 52e);
- the fire resistance of the column is equal to 22 minute, from T0 to the end of the test.

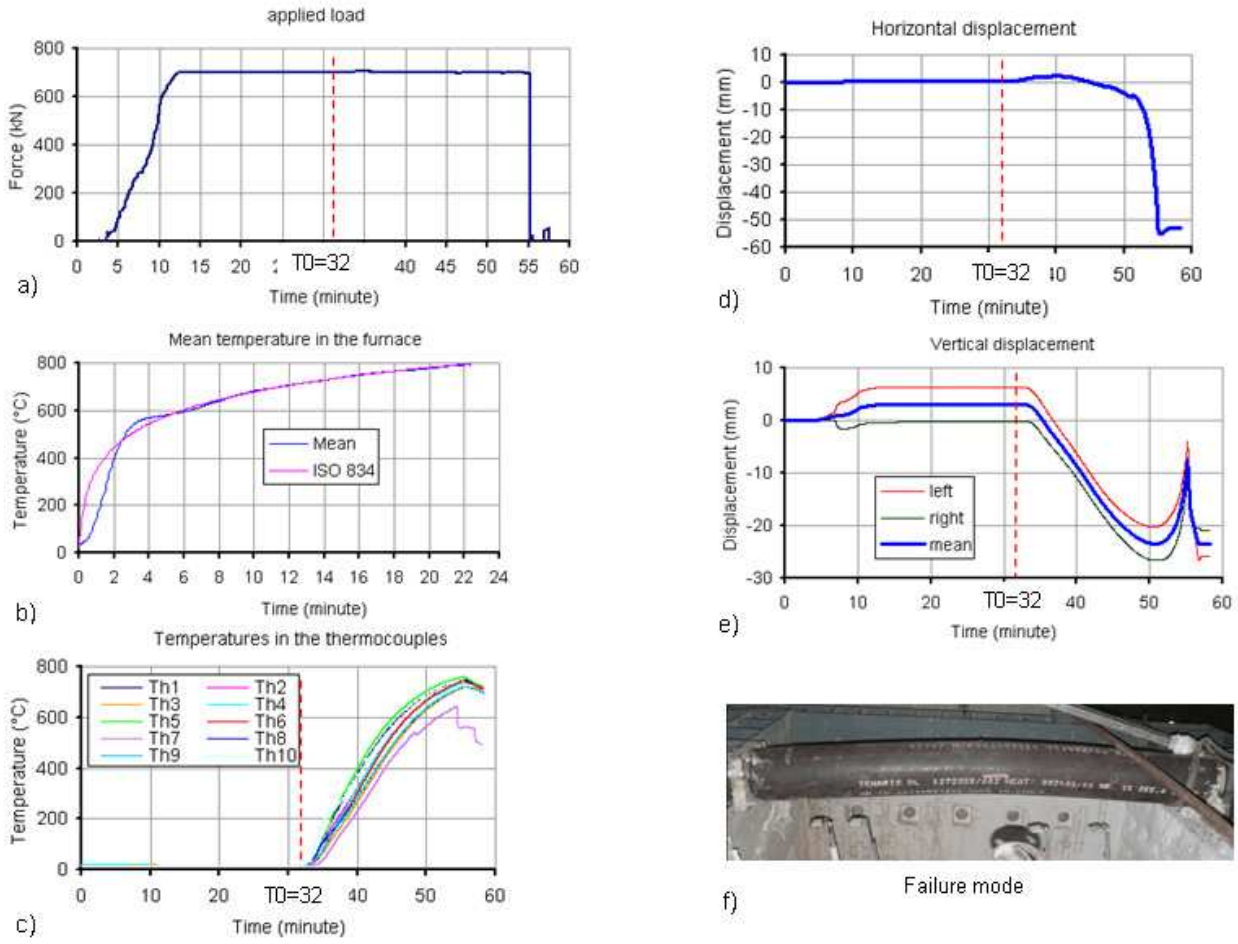

Figure 52. Example of results for C1 column test

VIII.6.3. Conclusions

All tests were well done, the obtained results were used for the numerical investigations (see WP5) and for the derivation of design guidelines for the investigated structural elements (see WP6).

VIII.7. WP5 – Model calibration

VIII.7.1. Task 5.1 Definition of stability curves

This task aims at investigating the validity of the current design curves proposed by Eurocode (EN 1993-1-1 & CIDECT No3) and American provisions (API, AISC) for stability curves of HSS tubular members.

The structural design of tubular members under axial compression, bending and combined loading conditions is covered by the current provisions of EN-1993-1-1 (EN 1993) [1], in section 5.5 For classification and in sections 6.2 and 6.3, officially applicable for steel grade up to 460 MPa for thin-walled tubes, referred to as “Class 4” sections, the designer should use EN-1993-1-6 [2]. EN 1993-1-12

[3] does not impose any restrictions on the use of those rules for higher grades. The AISC specification [4] for hollow sections (AISC 1999) contains rules for structural steel tube design. In addition, the API RP2A – LRFD rules [5], Chapter D, have been developed for the design of tubular for offshore steel platforms. Both specifications do not cover the case of high-strength steel. Finally, the CIDECT provisions [6] (CIDECT 1992) are based on the old provisions of ENV 1993-1-1 and, therefore, they are not considered in the present study.

VIII.7.2. Task 5.2 Calibration of 2D-3D numerical models

The tests conducted both on elements and parts of structure, as beam-to-column and column-base joints, were fundamental to calibrate the 2D-3D numerical models. In detail, we conducted the modelling and calibration of: i) columns under both axial and bending action; ii) joint's components both under high and room temperature; iii) hysteretic behaviour both of beam-to-column and column base joints; iii) mechanisms in plinth of the innovative seismic joint.

VIII.7.2.1. Columns under axial load and bending moment

The purpose of this Task is the calibration of the models by comparing with test results for short and long tubular members of high strength steel reported in Work Package 3, in order to validate the numerical model of the joints and elements.

The corresponding cross sectional dimensions are ∅355.6/12.5 (referred to as "section A"), and ∅323.9/10 (referred to as "section B") and the experimental results are shown in Table 17, together with the numerical predictions.

Table 17. Experimental results

Specimen	D_{nom} (mm)	t_{ave} (mm)	Length (mm)	N_{exp} (kN)	M_{exp} (kNm)	M_{Fea} (kNm)
A0	355.6	12.49	1490	10254	0	--
A1	355.6	--	1490	1345.0	891.5	917.8
A2	355.6	12.63	1490	2563.5	701.0	758.28
A3	355.6	12.74	1490	5127.0	382.4	389.99
A4	355.6	12.62	1490	7690.5	104.0	127.79
A5	355.6	12.75	4490	1538.4	668.97	699.57
A6	355.6	12.97	4490	2597.2	441.4	468.19
A7	355.6	12.85	4490	4591.7	150.5	156.28
B0	323.9	10.26	1490	7961	0	--
B1	323.9	--	1490	1003.0	575.8	615.86
B2	323.9	10.86	1490	1990.3	500.7	489.4
B3	323.9	10.86	1490	3980.5	208.5	232.19
B4	323.9	10.79	1490	5970.8	76.4	58.87
B5	323.9	10.61	4490	994.194	449.6	495.33
B6	323.9	10.83	4490	2035	232.31	272.7
B7	323.9	10.8	4490	3380.33	78.52	75.69

The finite element results are compared in Table 17 and Figure 53a&b, with the experimental data from the tubular members tested by CSM under combined axial load and bending (reported in WP3), in terms of thrust-bending interaction curves. The comparison shows that the numerical models provide very good predictions of the axial-bending combined capacity of the high strength steel short or long tubular columns. Furthermore, the buckled shapes of the specimens obtained numerically compare very well with the corresponding buckled shapes observed in the experiments, as shown in Figure 54.

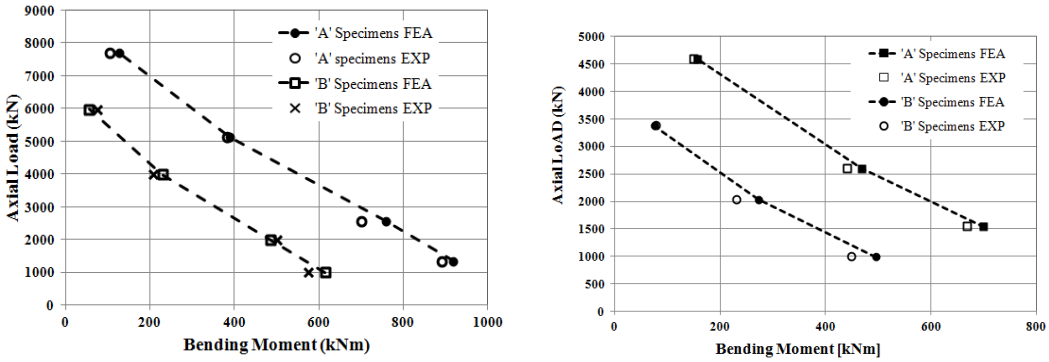

(a) (b)

Figure 53. Interaction diagrams; numerical results in comparison with the experimental data for (a) short (1.49m) and (b) long (4.49m) columns.

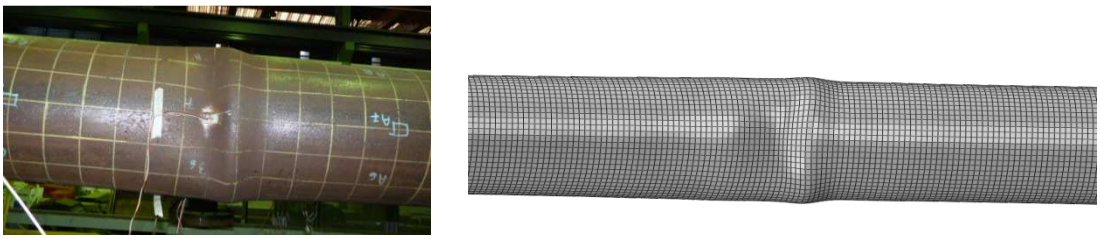

Figure 54. Buckled shape for A4 specimen and FE simulation

Additional FE models and simulations of the full scale tests were performed by CSM through the commercial software MSC.MARC. Experimental data and numerical predictions agree well with each other. Additional information can be found in Annex WP5.

VIII.7.2.2. Mechanical behaviour of elements and components at room and/or high temperature

In agreement with the WP objectives, the simulation campaign performed at Liege University is dedicated, on one hand, to the structural elements tested in fire (WP4), and, on other hand, to components of the static beam-to-column joints and of the static column-bases (tested at normal temperature in WP3). Therefore, the main activities can be summarized as follows:

- *Simulation of the columns* (Figure 55a): thermal and mechanical analyses in fire condition.
- *Simulation of the through plate component of the static beam- to- column joint* (Figure 55b): thermal analysis in fire condition and mechanical analysis at normal temperature.
- *Simulation of the end-plate component of the static column-bases* (Figure 55c): thermal analysis in fire condition and mechanical analysis at normal temperature.
- *Simulation of the seismic beam-to-column joint* (Figure 55d): thermal and mechanical analyses in fire condition.
- *Simulation of the seismic column-base (solution 1) in fire condition* (Figure 55e): thermal and mechanical analyses in fire condition.
- *Simulation of the seismic column-base (solution 2) in fire condition* (Figure 55f): thermal and mechanical analysis in fire condition.

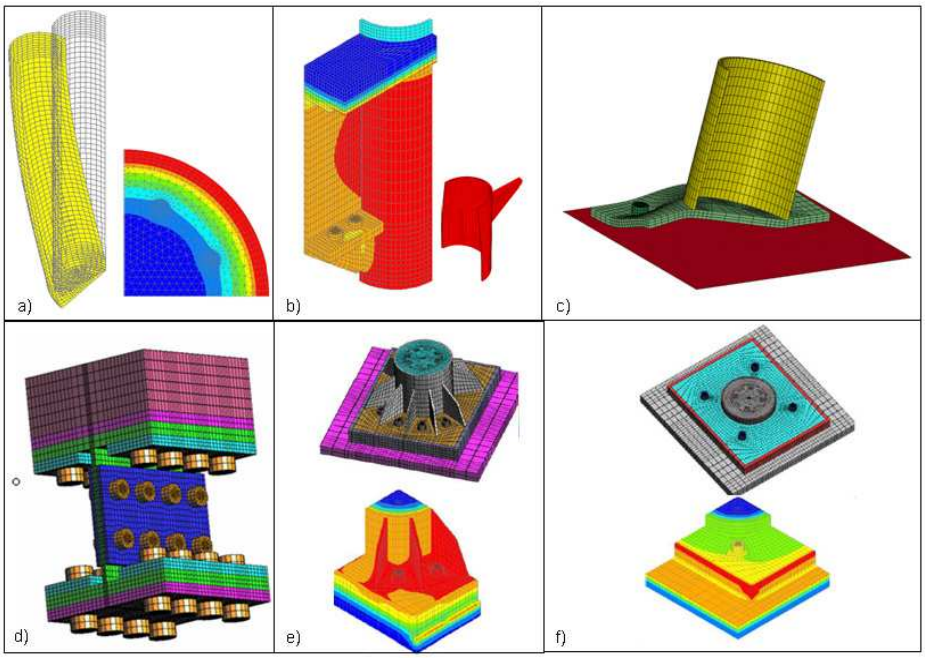

Figure 55. Finite element models developed at Liege University

For the numerical analyses in fire condition, SAFIR [3] – a computer program developed at Liege University – is used. For the latter, 2D and 3D solid elements have been used for the thermal analyses while beam and shell elements have been selected for the mechanical analyses at high temperature. Moreover, 3D solid models have been used for the mechanical simulations at normal temperature using LAGAMINE software – a nonlinear finite element code also developed at Liege University. More detail on the models can be found in Appendix C (WP5) and in Deliverable D5.2.

The numerical results obtained through the performed numerical studies have been validated through comparisons to the corresponding experimental results (WPs 3 & 4) and also through comparisons to available results in literature. The details can be found in Deliverable D5.2. In general, the numerical predictions are in good agreement with the test results, allowing us to realise parametric study on the basis of the so-validated numerical models (Task 5.3).

VIII.7.2.3. Hysteretic behaviour of both beam-to-column and column-base joints

In order to investigate the response of the prototype structure under seismic loading, it is fundamental the modelling of the hysteretic behaviour of both beam-to-column and column-base joints. The main steps were the following: i) analysis of test results to evaluate the position of plastic hinges; ii) choice of the model to take into account the behaviour, spread or concentrated plasticity; in those analyses concentrated plasticity was considered iii) choice of hysteretic models in order to schematize their actual behaviour iv) calibration of models parameters comparing numerical and experimental results. Both force-displacement of the actuator and moment rotation of plastic hinge were taken account. To calibrate the aforementioned models the whole structures tested were modelled, as showed in Figure 56 and inFigure 57, respectively.

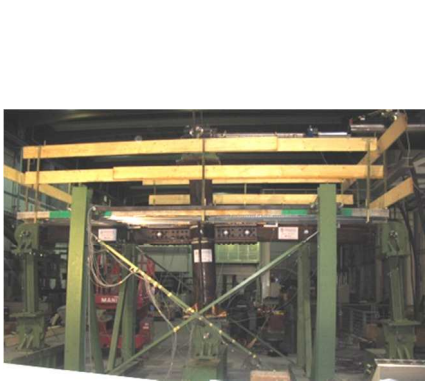

a)

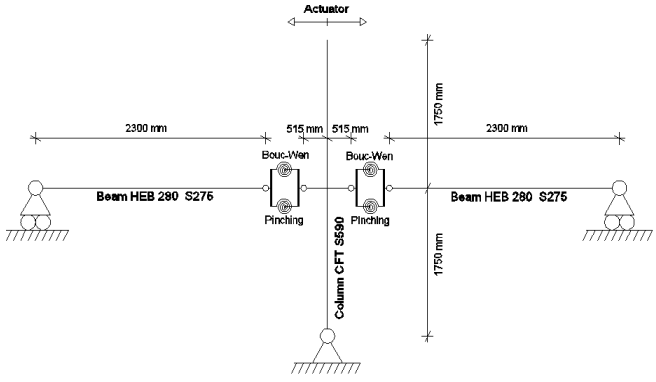

b)

Figure 56. Beam-to-column joint: a) specimen view; b) specimen model

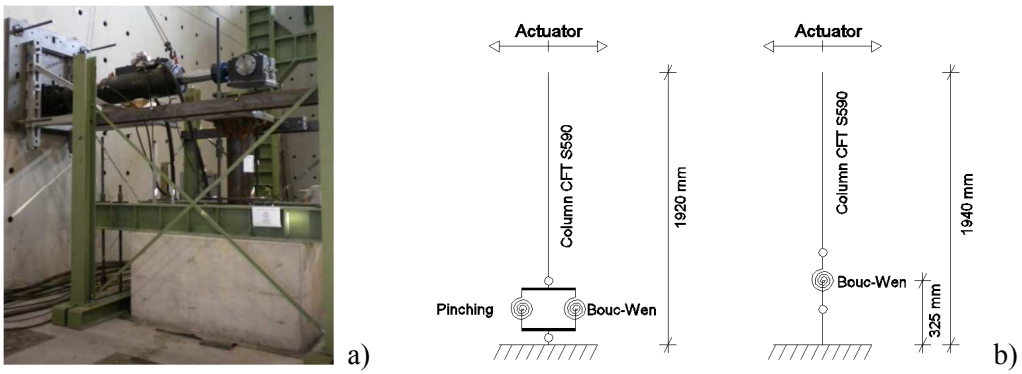

Figure 57. Column-base joints: a) specimen view; b) specimen model

Both beam-to-column and column-base joints were modeled using Bouc-Wen and Phincing hysteretic models provided by Opensees. The calibration of the parameters took into account a unique model for the plastic hinge, in order to simulate both the cyclic and the random test. For brevity, the comparison between numerical and experimental results in terms of force-displacement and moment rotation relationships are showed in the following figures.

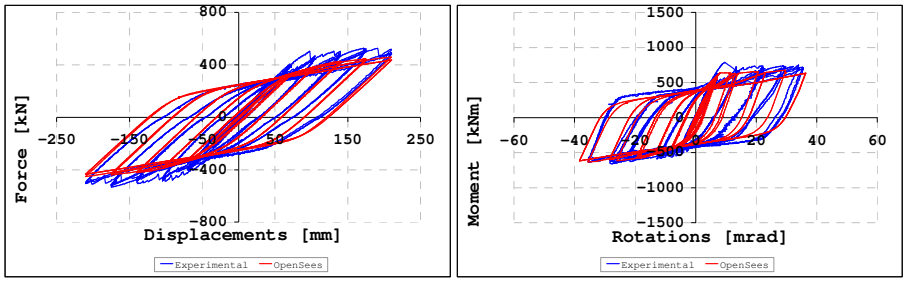

Figure 58. Cyclic test response of a beam-to-column joint

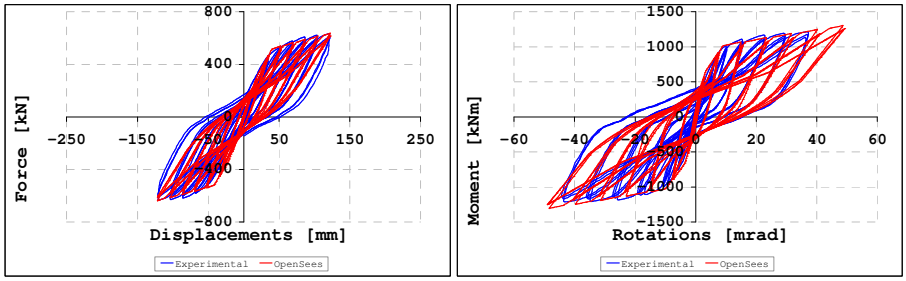

Figure 59. Cyclic test response of a standard seismic base-column joint

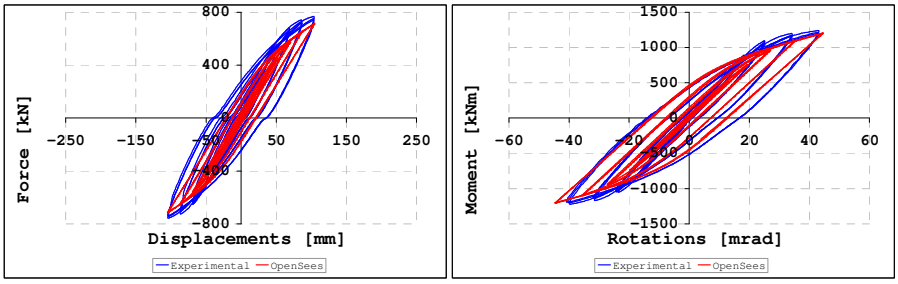

Figure 60. Cyclic test response on an innovative seismic base-column joint

VIII.7.2.4. Mechanical behaviour of a plinth relevant to an innovative seismic joint

Formulae proposed in EN 1992-1-1 (2005) for pocket foundations consider rectangular columns embedded in the plinth, as showed in Figure 61. The innovative solution realised by a circular column requires the investigation of the Strut & Tie mechanisms that transfer the force between the column and the foundation. The analysis of the mechanical behaviour of the innovative column-base joint requires a 3D numerical model set by the Abaqus program. The validity of the modelling was evaluated comparing: i) the horizontal force due to numerical analysis with one recorded by the actuator in order

to apply the same displacement during tests, as showed in Figure 62; ii) the forces recorded during the test by strain gauges welded on the rebars located in the plinth.

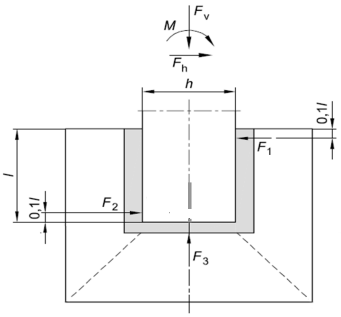

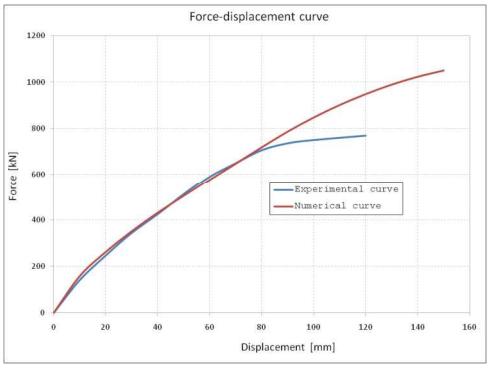

Figure 61. Plinth with a rectangular column Figure 62. Comparison between numerical and experimental results

The results obtained by a 3D numerical model were in agreement with experimental data till the onset of yielding. The resulting mechanism is endowed with: i) two frontal struts along the diagonal of the plinth with a rectangular section of about 400 x 360 mm; ii) a rear strut parallel to the face of the plinth with a rectangular section of about 500 x 400 mm. Figure 63 shows the geometry of the struts in the plinth obtained by means of a FE analysis.

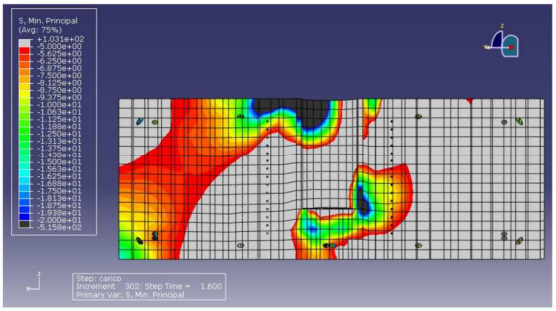

Figure 63. Strut & tie mechanism and distribution of compressive principal stresses for the plinth of the innovative column-base joint

VIII.7.3. Task 5.3 Parametric numerical analysis

On the basis of the calibration of 2D-3D numerical models, parametric numerical analyses were conducted in order to investigate the response both of columns and of joints and of the prototype structure. The analysis took into account different input and/or different bond conditions in order to evaluate the effects on the response.

VIII.7.3.1. Analysis of the behaviour of columns at room temperature

Extensive numerical investigation is being conducted throughout the present project in order to develop stability curves and interaction diagrams, considering the influence of the initial imperfections to the ultimate beam-column capacity. The analysis considers a combination of imperfection cases such as out-of straightness, wrinkling and residual stresses towards better understanding of the effects of initial imperfections on the structural behavior of the HSS tubes. The imperfection amplitudes are corresponding to the ones measured from actual specimens prior testing (WP3) in CSM laboratories. The geometrical characteristics of the tubular models (diameters and thicknesses) are also considered similar to the sections tested experimentally.

The finite element results are compared with the current standards as shown indicatively in Figure 64 and in Figure 65, in terms of stability curves and interaction diagrams. The axial load and bending moment values are normalized with the values $N_y = A\sigma_y$ and $M_y = W_{el}\sigma_y$, where σ_y is the nominal yield stress (considered equal to 590MPa) and W_{el} is the elastic modulus of the cross-section, representing the compressive and bending strength of the cross section respectively.

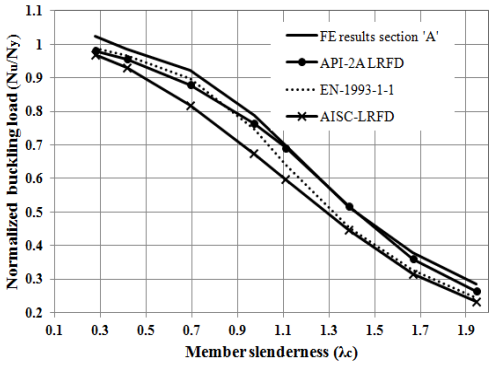

Figure 64. Finite element stability curve for section A (∅355.6/12.5) in comparison with EN and American provisions

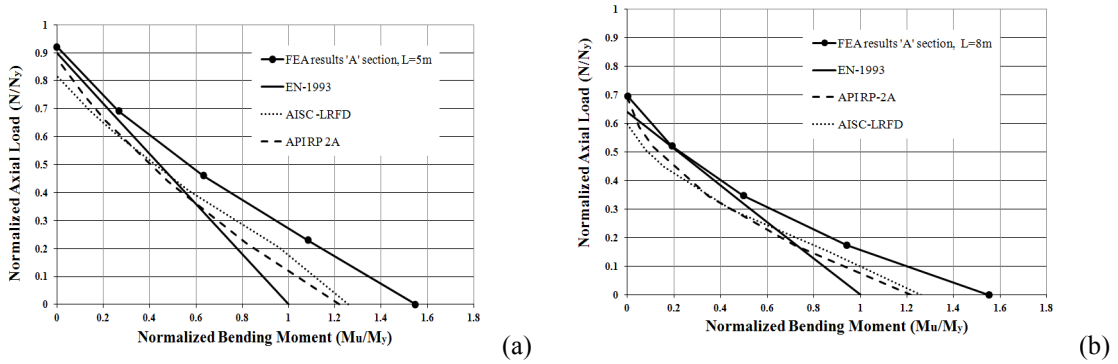

Figure 65. Interaction diagrams for A (a) 5m long and (b) 8m long tubular models in comparison with current provisions

As shown in Figure 64, the stability curve of A section compares reasonably well with the current EN 1993 and API provisions. For large values of member slenderness ($\lambda \geq 1$) EN 1993-1 underestimates by over 10% the buckling strength. On the other hand, for intermediate values of member slenderness, AISC seams to penalize the buckling strength significantly.

As shown in Figure 65, the current EN 1993 provisions (employed herein with beam-column method 1) significantly penalize the bending capacity of the tubular member so that the bending strength is underestimated by approximately 35%. The reason is that these CHS members are classified as class 3, respectively, but the finite element results indicate that the sections are capable of undergoing significant inelastic deformation before reaching an ultimate moment capacity. Moreover, AISC penalizes the bending strength by over 15%. Similarly, the bending capacity is underestimated by API by more than 18%.

It can be concluded from this parametric study that the current standards appear to be rather conservative, especially the EN 1993 predictions, mainly due to the "penalizing" classification of CHS cross sections in EN 1993-1-1.

VIII.7.3.2. Analysis of columns at high temperature and of joints components at room temperature

The parametric study has been carried out on the following structural joint components:

- *Parametric study on the column in fire condition*: two material models at high temperature for HSS are adopted: the first model is proposed in EN1993-1-1 (2005) for normal steel while second one is given by Chen et al (2008) for HSS steel. In the models, the degradation of the Young modulus and yield strength, according to the variation of the temperatures, for the steel are proposed. Moreover, parametric study on the initial imperfection of the columns, from L/500 to L/150, has been carried out (L being the column length).
- *Parametric study on the through plate component in the static beam- to- column joint at normal temperature* (Figure 66a): load direction (α - ratio between the vertical and the horizontal loads), column diameter (D) and plate dimensions (thickness (t), width (b), and height (h)) are varied, such that most of the practical cases are covered.

- *Parametric study on the end-plate component in the static column-bases* (Figure 662b): the following parameters have been parametrically studied, such that most practical cases are covered: tube (column) diameter (D), plate dimensions (width (b) and thickness (t)), and bolt positions (d).

The details of the conducted activities are reported in Deliverable D5.3.

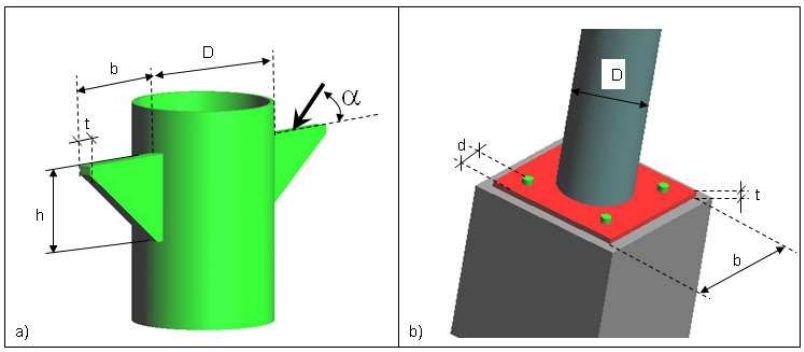

Figure 66. Parameters to be varied in the through plate and the end plate components

The performed parametric study using the calibrated models (Task 5.2) allows developing mathematical formulas for the characterisation of the investigated structural components. In particular, analytical formulas have been proposed for two crucial components (not yet well covered by the codes): the through plate component in the static beam- to-column joint and the end-plate component in the static column-bases. This has results in the proposition of design guidelines as reported in WP6.

VIII.7.3.3. Analysis of the prototype structure under seismic loading

In order to evaluate the response of the structure under seismic loading the 2D moment resisting frame was analysed by time history analysis, as showed in Figure 67 . Two different frames were considered using both beam-to-column and base-column joints through the model obtained in the previous calibration; see VIII.7.2.3 in this respect. The difference between the frames were the column-base joints, i.e. the standard and the innovative solution, respectively. The analyses were conducted using as input 3 artificial accelerograms matching the elastic response spectra in agreement with EN1998-1 (2005). To evaluate the response the following parameters were considered: i) the interstory drift; ii) the response of joints in term of stiffness and strength degradation; iii) the different level of peak ground acceleration, in order to estimate the q factor as shown in Figure 68 (Bursi et al, 2006).

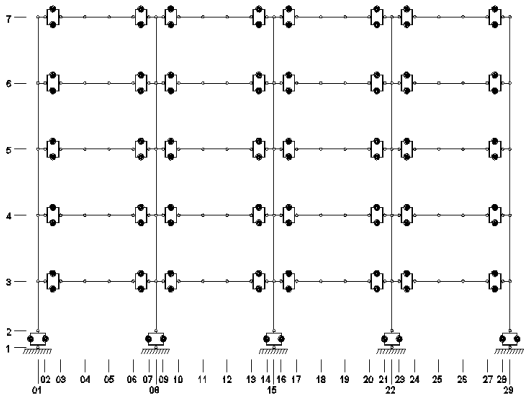

Figure 67. Modelling of 2D MRF

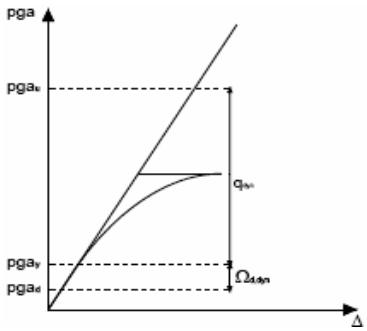

Figure 68. Behaviour and overstrength

Both joints and structure belong to the medium ductility class, characterized by: i) a plastic rotation of beam-to-column joints higher than 25mrad and with stiffness and strength degradation less than 20%; ii) a limited interstory drift (Id) of about 5% at failure; iii) a plastic rotation of both column-base joints higher than 41 mrad, in agreement with the request of ductility; iv) a q factor estimated higher than the 3.2 value considered in the relevant design. Table 18 summarizes relevant results.

Table 18. Response parameters of the 2D moment resisting frame of Fig. 15 under seismic loading

	Standard base-column joints			Innovative base-column joints		
Accelerogram	**1**	**2**	**3**	**1**	**2**	**3**
ag_y (g)	0.29	0.16	0.26	0.25	0.15	0.25
ag_u(g)	0.92	0.60	0.84	0.95	0.84	1.00
Id (%)	5.68	4.82	5.00	6.08	7.68	5.93
q	3.23	3.87	3.23	3.86	5.57	4.00
Ω_{dyn}	3.38	1.84	3.08	2.90	1.78	2.96

VIII.8. WP6 – Design guidelines

In this section, design guidelines for buildings for which HSS can give an economical solution are presented; the reference buildings 1 and 2 (see WP2) in the present project are examples of buildings for areas of low and high seismicity respectively. For these building, static, seismic and fire actions are considered; design guidelines from global structural analysis to the verification of structural elements (e.g. column bases, tubular columns and beam-to-column joints) are proposed.

It should be noted that the present guidelines (a) are in-line with the current EN 1993 design practice and (b) propose some possible amendments for HSS tubular CHS members. The proposed amendments are based on the imperfection and residual stress measurements, the test data and the numerical results obtained within the present research project, for the seamless CHS tubes described in the previous sections of this report. A list of publications is offered, which support the proposed guidelines.

VIII.8.1. Structural solution

VIII.8.1.1. Building structures in low-seismicity areas

A cost-efficiency study has been carried out within the present project (Hoang et al, 2011); from the latter, the following conclusions can be drawn for the definition of a structural solution where HSS can have an economical interest.

a. Columns

(1) For isolated steel columns: stocky columns are recommended and the interest of using HSS decreases when the eccentricity of the axial load increases.

(2) For columns in frames: a global schematic view on the interest of using HSS in comparison with normal steel (NS)/S355 is presented in Table 19. Possibilities for using HSS are quite large when considering braced/non-sway frames using steel columns. On the other hand, there is no benefit in using HSS for steel columns in sway frames, if compared to frames using normal steel. Moreover, for frames using composite columns, very few possibilities for using HSS can be identified.

Table 19. Summary of the conclusions of the analysis

Frame type	Column type	
	Steel column	Composite column
Braced/non-sway frames	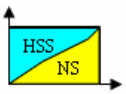 Many possibilities for HSS	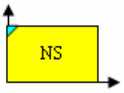 Very few possibilities for HSS
Un-braced/sway frames	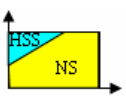 There are possibilities for HSS	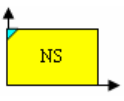 Very few possibilities for HSS

(3) In fire condition: almost no economic interest exists in using columns made of HSS without protection, in both steel and composite columns. If a protection is used, the use of HSS may lead to benefits as it is the case for normal temperature.

Accordingly, in the next section, mainly guidelines for braced/non-sway frames will be recommended/derived.

b. Slabs and joints

The following solutions for slabs and joints are suggested for a braced/non-sway frame using HSS tubes for the columns.

(1) Using composite floors with a concrete/composite slab connected to the steel beams through shear connectors in order to activate a composite action at the joint level

(2) Using configurations for column bases and beam-to-column joints as shown in Figure 69. The column bases are formed by one full end plate welded to the column and anchored in the concrete block by four anchor bolts. With respect to the beam-to-column joint configuration: one through plate is welded to the column, on this plate two horizontal plates (each side of the column) are attached by fillet welds. The lower flanges of steel beam are connected to the horizontal plates using bolts.

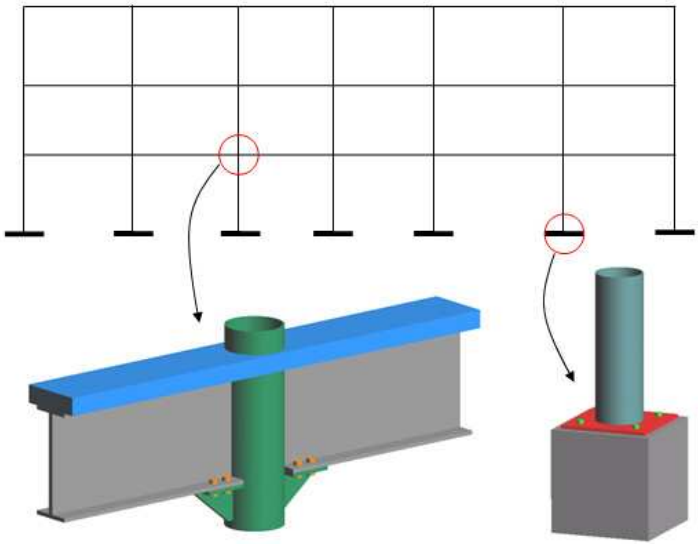

Fig.1

Figure 69. Suggested beam-to-column joint and column base for frames subjected to static loads

VIII.8.1.2. Building structures in areas of significant seismicity

Building structures subjected to medium-high seismic loadings are usually realized using moment resisting frames only along one direction. This is customarily done to contain the cost of joints designed satisfying capacity design rules. A cost-efficiency study was carried out considering the 2D moment resisting frame, see Figure 70, of the prototype structure. In detail both the design and the economic evaluation of the frame were realized considering four different solutions of circular columns: i) hollow columns with mild steel, NS S355; ii) composite columns with mild steel, NS S355; iii) hollow columns with high strength steel, HSS S590; iv) composite columns with high strength steel, HSS S590.

a. Columns

The analysis conducted on the different solutions showed the advantage of using HSS S590 with respect to the mild steel NS S355. In fact the use of columns endowed with HSS with the same geometry of the columns realized with mild steel complies with capacity design rules. This does not require the increase of the column scetions with economic savings of about 15%.

b. Beam- to- column and column-base joints

The solutions suggested for beam-to-column and base-column joints with columns with HSS follow:

(1) beam-to column joints designed as rigid and full strength joints and realized by bolted connection, as showed in Figure 69. A vertical through plate and two horizontal plates were welded to the column in order to bolt the beams by means of cover plates. The use of composite columns exhibits better strength and stiffness than simple connections to the tube face. In fact, this connection avoids all possible phenomena of large instability in the wall around the joint region.

(2) Two solutions for column-base joints: i) a standard solution with base plate, anchor bolts and vertical stiffeners; ii) an innovative solution with a column embedded in the concrete foundation. Both the plate welded around the column and the four anchor bolts are used for column erection purposes.

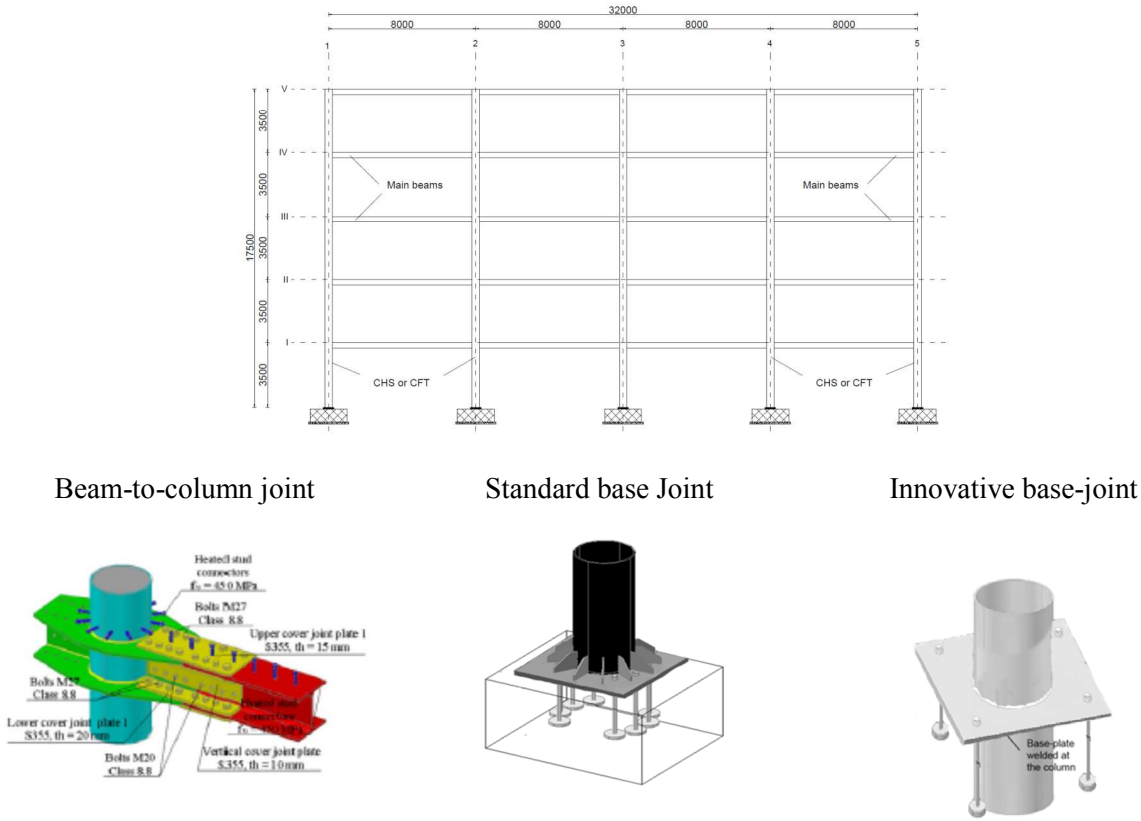

Figure 70. Suggested beam-to-column joint and column bases, standard and innovative, for MRF subjected to seismic loads

VIII.8.2. Global analysis of frames

VIII.8.2.1. Building structures in areas of low seismicity

(1) During the construction phase: the behaviour of beam-to-column joints as illustrated in Figure 69 must be considered as hinges. The column base behaviour may be considered as semi-rigid and partial strength. Globally, elastic analysis for simple steel frames should be adopted.

(2) During the exploitation phase: both beam-to-column joints and column base can be considered as semi-rigid and partial strength joints. Globally, elastic/plastic analyses for semi-continuous composite frames could be applied.

VIII.8.2.2. Building structures in areas of significant seismicity

The behaviour of both beam-to-column and column-base joints, showed in Figure 70, could be assumed as rigid and full strength both during the erection and exploitation phases. In particular, the configuration of column-base joints is the same in both phases; event though beam-to column joints lack the presence of the composite action during erection, they are rigid and full strength anyway. In this phase, in fact, the strength is assured by the slip resistance owing to preloaded bolts used in connections. Both the joints and the structures can be assumed to belong to a medium ductility class during structural analysis under seismic loading. These properties were confirmed by test results.

VIII.8.3. Design of high-strength steel CHS columns

VIII.8.3.1. Design of HSS CHS columns at normal temperature

The design procedure follows the general framework of EN 1993 parts 1-1 (EN1993-1-1, 2005) and 1-6 (EN1993-1-6, 2007). The rules in EN1993-1-1 (Sections 6.3.1-6.3.3) can be used, following the existing classification, shown in Table 20. This design procedure results in safe, yet conservative predictions. However, some amendments to these rules are proposed, to account for the above

conservativeness for high-strength steel CHS seamless members, similar to the tubes considered in the present work (Pappa & Karamanos, 2012 and Pournara et al, 2012), with wrinkling imperfection amplitudes not exceeding 2.6% of the tube thickness.

Table 20. CHS member classification according to EN 1993-1-1

Class	Class limits	Class limits in terms of shell slenderness $\bar{\lambda}$
1	$D/t \le 50\varepsilon^2$	$\bar{\lambda} \le \bar{\lambda}_1 = 0.278$
2	$50\varepsilon^2 \le D/t \le 70\varepsilon^2$	$\bar{\lambda}_1 = 0.278 < \bar{\lambda} \le \bar{\lambda}_2 = 0.328$
3	$70\varepsilon^2 \le D/t \le 90\varepsilon^2$	$\bar{\lambda}_2 = 0.328 < \bar{\lambda} \le \bar{\lambda}_3 = 0.372$
4	$D/t \ge 90\varepsilon^2$	$\bar{\lambda} > \bar{\lambda}_3 = 0.372$

a. Cross-sectional strength for axial loading

Shell slenderness is defined as follows [3]:

$$\bar{\lambda}=\sqrt{\frac{\sigma_y}{\sigma_e}} \tag{1}$$

where σ_y is the yield stress and

$$\sigma_e=0.605C_xE\frac{t}{r} \tag{2}$$

For member slenderness $\bar{\lambda} \le 0.60$, the axial compression load is calculated as follows:

$$N_{Rk}=\sigma_y A \quad \text{if} \quad \bar{\lambda} \le \bar{\lambda}_3=0.373 \tag{3}$$

$$N_{Rk} = \sigma_y A\left(1-\beta_\alpha \frac{\bar{\lambda}-\bar{\lambda}_3}{\bar{\lambda}_\alpha-\bar{\lambda}_3}\right) \quad \text{if} \quad \bar{\lambda} > \bar{\lambda}_3 \tag{4}$$

where $\beta_a=0.133$, $\bar{\lambda}_\alpha=0.6$ and $\bar{\lambda}_3=0.373$.

The above equations are valid for values of shell slenderness $\bar{\lambda}$ less than 0.60, and are shown in Fig.3a, together with test data and numerical results (Pappa & Karamanos, 2012).

b. Cross-sectional strength for bending loading

The value of shell slenderness $\bar{\lambda}$ is obtained from the equation (1). The bending strength of the cross section is calculated as follows:

$$M_{Rk}=M_p=\sigma_y W_{pl} \quad \text{if} \quad \bar{\lambda} \le \bar{\lambda}_2=0.329 \tag{5}$$

$$M_{Rk} = M_p\left(1-\beta_b \frac{\bar{\lambda}-\bar{\lambda}_2}{\bar{\lambda}_b-\bar{\lambda}_2}\right) \quad \text{if} \quad \bar{\lambda} > \bar{\lambda}_2 \tag{6}$$

where $\beta_b=0.22$, $\bar{\lambda}_b=0.5$ and $\bar{\lambda}_2=0.329$

The above equations are valid for values of shell slenderness $\bar{\lambda}$ less than 0.60, and are shown in Fig.3b, together with test data and numerical results (Pappa & Karamanos, 2012).

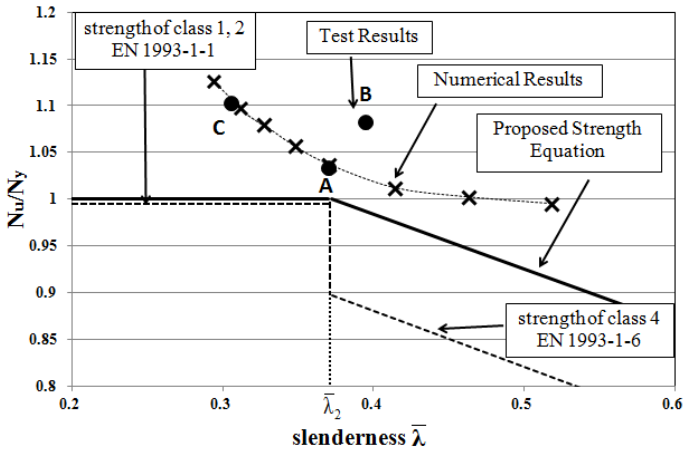

Fig.3a Bending capacity versus shell slenderness (Pappa & Karamanos, 2012).

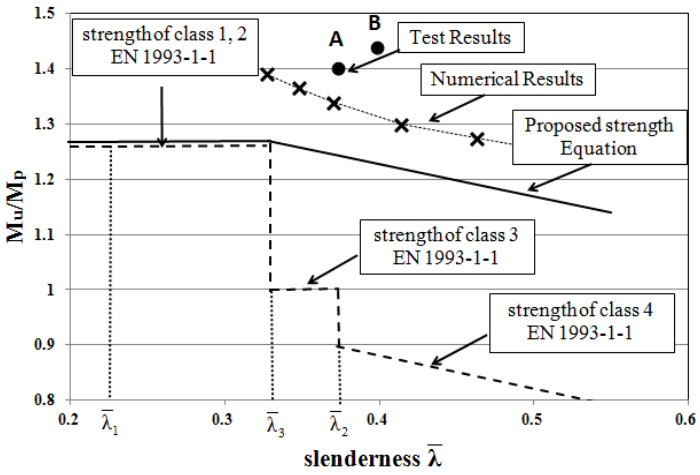

Fig.3b Axial load capacity versus shell slenderness (Pappa & Karamanos, 2012).

c. Strength of CHS columns

The strength of tubular members under combined loading of axial load and bending is calculated from the interaction curve proposed by EN-1993-1-1 paragraph 6.3 (EN1993-1-1, 2005):

$$\frac{N_{Ed}}{\chi N_{Rk}} + k\frac{M_{Ed}}{M_{Rk}} = 1 \tag{7}$$

where M_{Ed} and N_{Ed} are the acting axial and bending loads, and N_{Rk}, M_{Rk} represent the cross sectional axial and bending strength respectively (defined above). The k factor is a coefficient that depends on axial load and the shape of the bending moment diagram along the members, defined in Annex A or B of EN1993-1-1. The buckling reduction factor χ depends on column slenderness

$$\lambda = \sqrt{\frac{N_{Rk}}{N_e}} \tag{8}$$

where N_e is the elastic buckling load of the tubular column. Note that the above definition of λ accounts for CHS sections which may not reach the full plastic axial load. Finally, it is recommended to use curve α_0, for the reduction factor $\chi(\lambda)$ as defined in EN1993-1-1 (EN1993-1-1, 2005).

d. Conclusions from experimental results

The following remarks should be kept in mind for the design of HSS CHS columns at room temperature:

(1) The material and geometrical imperfections of the products studied in this project are very small in magnitude and them behaviour at room temperature is not influenced by.

(2) Cross sectional classification of HSS is not confirmed by experimental evidences, in particular for slenderest cross sections tested in this project (namely cross section B) large safety margin is available. Hence HSS cross sections classified as Class 4 are proposed to be in Class 3.

VIII.8.3.2. Design of HSS CHS columns at elevated temperature

The following remarks should be kept in mind for the design of these columns in fire conditions (elevated temperature).

(1) The design of circular columns made of HSS under fire action should be based on Eurocodes 3, part 1-2 (EN1993-1-2, 2004), and Eurocode 4, part 1-2 (EN1994-1-2, 2004) for steel and composite columns respectively.

(2) The use of stress-strain relationship at elevated temperature initially developed for carbon steel provided results that well reproduced the prediction of vertical displacements, if compared to the experimental results. Also, for the circular filled tube column, the fire resistance predicted with the Eurocode rules was in good agreement with that found experimentally.

(3) However, the fire resistance of the tested steel columns was overestimated using the material model of Eurocode 3, part 1-2 (EN1993-1-2, 2004); the so-obtained predictions are significantly influenced by the considered initial imperfection. To obtain a fire resistance in line with the experimental evidence, the imperfection shall not be taken less than L/200, which is not in line with the recommended initial imperfection for such elements. This aspect should be investigated in more details, what constitutes a perspective to the present project.

VIII.8.4. Design of column bases subjected to combined bending moment and axial force

VIII.8.4.1. Static column-base joints under static loading

a. Introduction

(1) Three parts should be considered at the level of the column base:

- column (steel tube);
- tube-to-plate weld;
- end plate in bending, anchor bolts in tension and concrete in compression.

(2) The bending moment-axial resistance interaction zone for the whole column base is defined from the ones of the joint components (Figure 71). The way to characterise these components is given here below.

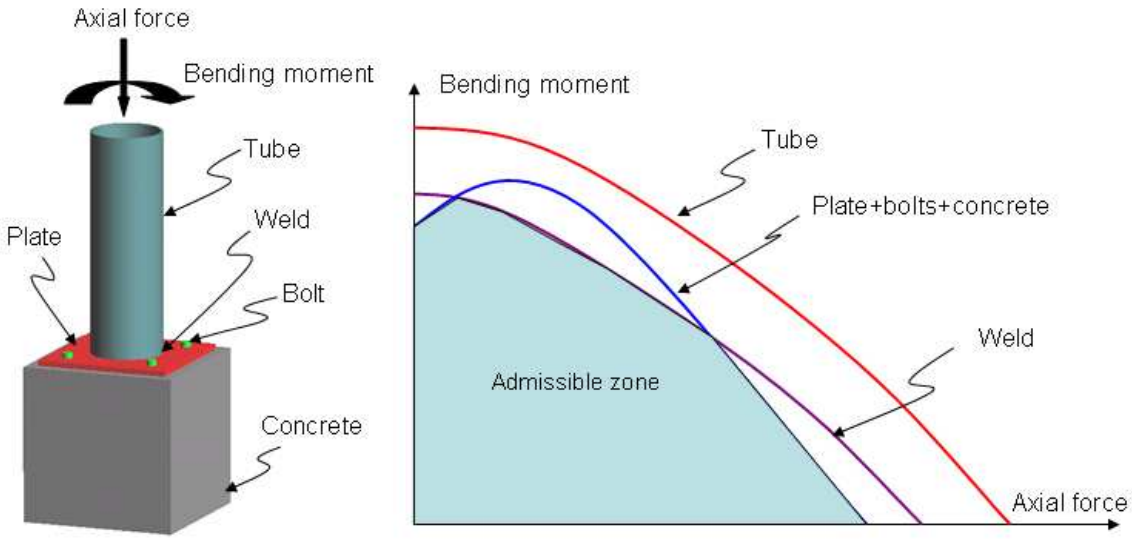

Fig.4

Figure 71. Design guidelines for column bases

b. Tube and tube-to-plate weld

Resistance of the components “tube” and “tube-to-plate weld” can be calculated using Eurocode 3, part 1.1 (EN1993-1-1, 2005). The bending moment-axial resistance interaction curves for these components can be easily established knowing their geometrical and material characteristics.

c. Plate in bending, bolts in tension and concrete in compression

(1) The applied moment (M_{Ed}) and axial force (N_{Ed}) are equilibrium by the “concrete in compression” (f_i) and “plate in bending, bolts in tension” (F_t) components (Figure 72). The interaction curve of bending moment and axial force (Figure 71) can be established using two equilibrium equations for the bending moment and axial force.

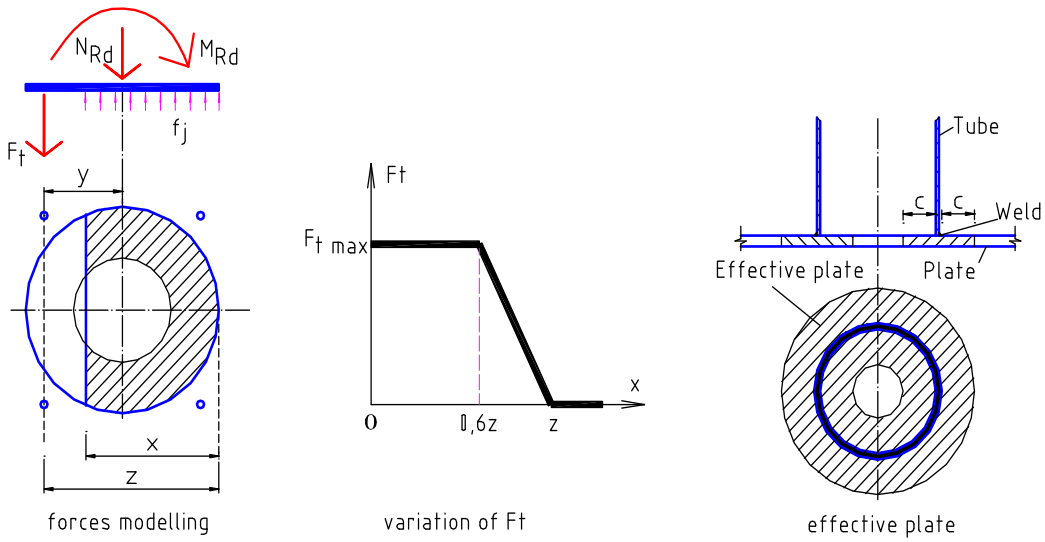

Figure 72. Column base - Assembly of plate, anchor bolts and concrete block components

(2) “Concrete in compression” component: a concentration effect has to be considered to compute the resistance of the concrete in compressing by using the “concentration ratio”. Moreover, to characterise this component, the flexibility of the end plate should also be taken into account through the definition of an effective rigid plate, see Figure 72. The details to characterise this component can be found in Deliverable D 6.

(3) “Plate in bending, bolts in tension” component: this component is modelled by a force (F_t) at the bolt position (Figure 72). This force varies according to the width of the compression zone, and their relation proposed in (Guisse et al, 1996) can be applied here, as illustrated in Figure 72. The maximal value of F_t ($F_{t,max}$) may be calculated by Eq. (9) as follows:

$$F_{t,\max} = (M_{p,\min} - bm_p)/w \qquad (9)$$

with $M_{p,min}$ is the minimum value of M_{pi} (i=1-8) given in Table 21; b and m_p are the width and the unit plastic moment of the end plate, respectively. In Table 21: all geometric quantities are defined on Fig.6; B is the yield force per bolt; the coefficients α_1, α_2, and α_2 are given in Deliverable 6, depend on the geometries of the end plate and the bolt positions.

Noting that M_{pi} in Table 21 is furnished from a limit analysis of the “plate in bending and bolts in tension” component on the rigid foundation (Figure 73). Kinematical approach is applied with seven (7) licit mechanisms is in considering (Figure 74). It should be noted that: the calculation of the two local mechanisms (Figure 74.a and Figure 74.b) can be found in Eurocode 3, part 1.8 (EN1993-1-8, 2003). The length of the yield lines in three mechanisms (Figure 74.c, Figure 74.d and Figure 74.g) are fixed (equal to the flange width) so that the corresponding capacities of these modes can be directly computed. On the other hand, the methods for the calculation of the two mechanisms (Figure 74.e and Figure 74.f) have been developed within this project and are reported Deliverable D6.

Table 21. Determination of M_{pi}

Yield pattern	Failure mode	Plastic moment (M_{pi})
Circular (Fig.7a)	Mode 1– thin plate	$M_{p1} = [8\pi w' + b]m_p$
Circular (Fig.7b)	Mode 1 – thin plate	$M_{p2} = [4(\pi + e/n')w' + b]m_p$
Noncircular (Fig.7c)	Mode 1– thin plate	$M_{p3} = 2(d'/s' + 1)bm_p$
Noncircular (Fig.7d)	Mode 2 – intermediate plate	$M_{p4} = \left(\frac{d'}{e_1 + s'} + 2\right)bm_p + \frac{2e_1 d'}{e_1 + s'}B$
Noncircular (Fig.7e)	Mode 1- thin plate	$M_{p5} = \alpha_1 bm_p$
Noncircular (Fig.7f)	Mode 2 – intermediate plate	$M_{p6} = (\alpha_2 m_p + 2\alpha_3 B)b$
Noncircular (Fig.7g)	Mode 3 – thick plate	$M_{p7} = bm_p + 2w'B$
$d' = d + 2*0.8*\sqrt{2}a$; $s' = s - 0.8\sqrt{2}a$; $w' = w + 0.8\sqrt{a}$; other symbols are defined on Fig.6.		

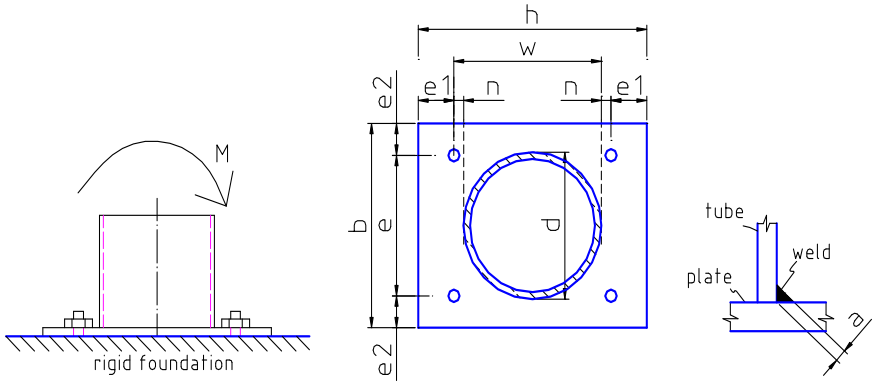

Figure 73. Column base – model for limit analysis of plate and bolts

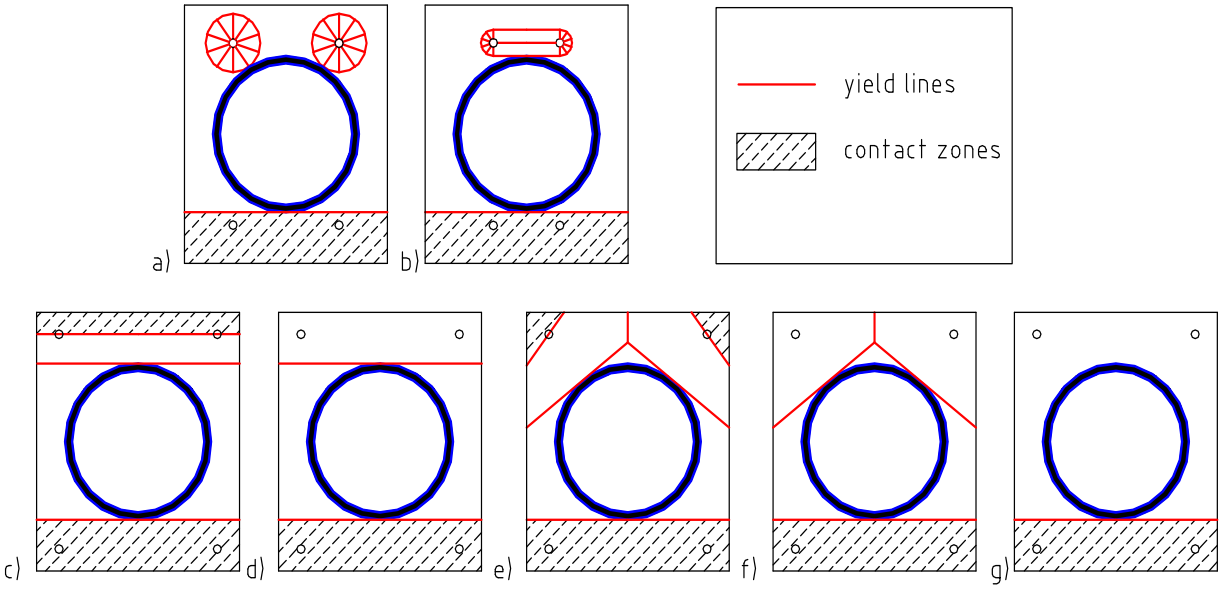

Figure 74. Column base - considered mechanisms for the end plate

VIII.8.4.2. Static column bases at elevated temperature (fire)

The design guidelines given for the column base at normal temperature can be used in case of fire loading; only material characteristics (yield strength and Young modulus) must be adapted according to the variation of temperature.

Advices on how to determine the temperature in the different component are given in Deliverable 5.

VIII.8.4.3. Seismic column-base joints

Both the standard and the innovative solution showed in Figure 70, can be designed coping with the capacity design rules suggested by EN1998-1-1 (2005). Along this line, the strength requested by EN1998-1-1 (2005) for foundation elements was calculated via the following formula:

$$E_{Fd} = E_{FG} + \gamma_{Rd} \cdot \Omega \cdot E_{FE},$$

considered in what follows.

a. Standard seismic column-base joints

The use of the above-mentioned formula permits to obtain a base joint characterized by adequate stiffness and strength to transfer the action of the column to the foundation. The proper design of stiffeners permits to locate the plastic hinge far from the weld between the column and the base plate, thus avoiding brittle failure. In fact, the response of this base-joint under cyclic tests exhibited a ductile behaviour without stiffness and strength degradation. The collapse of the joint was due to the anchor bolts after the activation of the plastic hinge associated with plastic rotations of about 45 mrad.

b. Innovative seismic column-base joints

The innovative seismic base joint realized by means of a column embedded in the foundation permits a cheap solution to be obtained, characterized by stiffness and strength higher than the standard solution. The behaviour of this base joint is like the one employed for pocket foundations. The only function for both, of the base plate and of the anchor bolts, is to permit the column to be vertically erected. This joint exhibited ductile behaviour characterized by large plastic rotation of about 45 mrad with brittle failure on weld between the column and the base plate, due to phenomena of local instability in the wall of the column. To avoid the brittle failure, it is possible to weld some stiffeners in order to govern the zone of instability from the weld of the column to the base plate. The design of this joint regarded only the foundation that can be designed according to the Strut & Tie mechanism proposed for prefabricated concrete constructions, according to EN 1992-1-1 (2005). In detail, both test results and numerical analyses by FE modelling with Abaqus indicate that three struts are present in the plinth. Figure 75 shows both the geometry of the struts in the plinth obtained via numerical analysis and the distribution of compressive principal stresses.

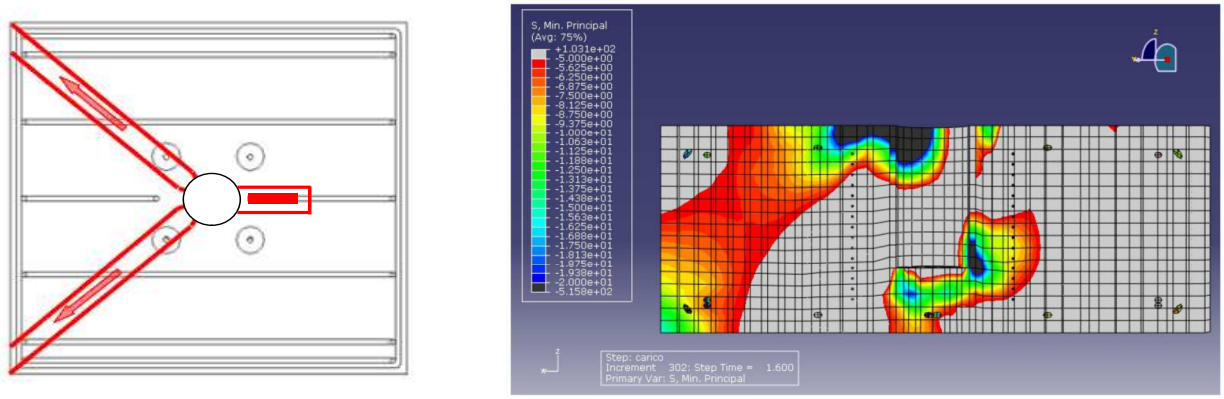

Figure 75. FE results relevant to the plinth of the innovative column-base joint: a) strut & tie mechanism; b) distribution of compressive principal stresses.

VIII.8.4.4. Seismic column bases at elevated temperature (fire)

In fact, the experimental evidence highlighted that the failure occurred in both specimens owing to the collapse of the column that lost its capacity to withstand the applied load because of the degradation of

its mechanical properties with high temperatures. The parts constituting the joint between the foundation and the column did not undergo severe damage: in CB2 the bolts, the vertical stiffeners and the end plate were only slightly damaged whereas in CB3 no major damage was detected.

The detailing of the joint zone shall be carefully designed to avoid problems in case of fire. In particular, the rebars inside the composite HSS tube that end in the foundation, as well as the tube itself in the case of CB3, shall be adequately drowned in the concrete base by providing a sufficient anchorage length. With such a detailing, the fire resistance of the column base can be seen as the resistance of a composite column subjected to fire.

VIII.8.5. Design of beam-to-column joints

VIII.8.5.1. Static beam-to-column joints at normal and elevated temperature

a. General

The bending moment-rotation curve of the joints can be defined by characterising the following components (Figure 76):

- longitudinal slap reinforcement in tension (K1 in Figure 76);
- bolts in shear (K2 in Figure 76);
- plate in bearing (K3 in Figure 76);
- through plate and column in diagonal compression (K4 in Figure 76);

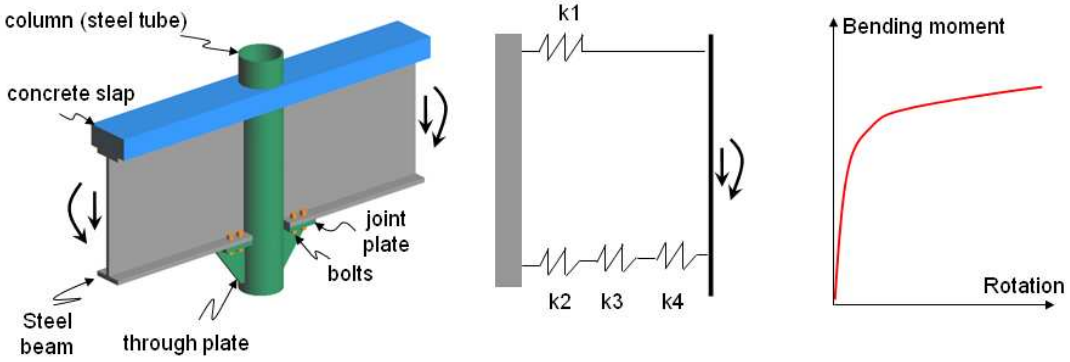

Figure 76. Proposed beam-to-column joint and components to be characterised

b. Longitudinal slap reinforcement in tension, bolts in shear and plate in bearing

The detail calculation for the characterization of the component “longitudinal slap reinforcement in tension” can found in (Anderson, 1999), while the components “bolts in shear” and “plate in bearing” can be found in (EN1993-1-8, 2003).

c. Through plate and column in diagonal compression

The method to characterise this component loaded as illustrated in Fig. 10 has been developed within the present project; the details are reported in Deliverable D6, some remarks are presented in the following. The through plate is devised into two parts, inside part (inside the column) and outside parts (outside the column), the buckling theory of plate is applied to study the strength of each part. The traditional formula of the elastic buckling is used while the plasticity and the initial imperfection are taken into account by a parameter that is determined from a numerical analysis (parametric study). Finally, the safety verification of the through plate may be performed by the following formula:

$$\begin{cases} \dfrac{V_{Ed}}{th} \le \kappa\mu_1 \dfrac{\pi^2 E}{12(1-\upsilon^2)}\left(\dfrac{t}{b}\right)^2 / \gamma_{M1}; \\ \dfrac{4F_{Ed}}{th} + \dfrac{4V_{Ed}b}{th^2} \le \mu_2 \dfrac{\pi^2 E}{12(1-\upsilon^2)}\left(\dfrac{t}{h}\right)^2 / \gamma_{M1}. \end{cases} ; \quad (10)$$

with V_{Ed} and F_{Ed} are the vertical and horizontal components of the applied load (Figure 77); E and υ are the Young modulus and Poisson ratio of the material, respectively; γ_{M1} is the partial factor according to EN1993-3-1 (EN1993-1-1, 2005); κ= 1.0 for the rectangular outside part and κ = 0.9 for the triangular outside part; μ_1 and μ_2 are given in Deliverable D6, depend on the load direction (α - ratio between the vertical and the horizontal loads), the column diameter (D), the plate dimensions (thickness (t), width (b), and height (h)), and the material characteristics; all geometries of the plate are defined on Figure 77.

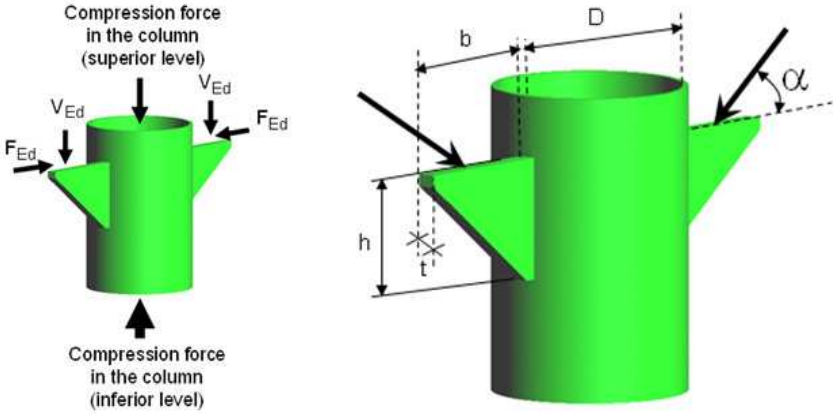

Figure 77. Beam-to-column joints - through plate component

d. In elevated temperature conditions (fire)

The design guidelines given for the column base at normal temperature can be used in case of fire loading; only material characteristics (yield strength and Young modulus) must be adapted according to the variation of temperature.

Advices on how to determine the temperature in the different component are given in Deliverable 5.

VIII.8.5.2. Seismic beam-to-column joints

The innovative beam-to-column joint realized by bolted connections between the beam and weld plate at the column exhibit a ductile behaviour, see Figure 70. The joint can be designed in agreement with EN1993-1-1 (2005), EN1994-1-1 (2005) and EN1998-1-1 (2005) respecting the concept of the capacity design with plastic hinge located on weak section between the end of the beam and the plate welded on the column. The design of beam-to-column joints with the shear connectors only on the upper flange of the beam permits to obtain a cheap solution. In agreement with the component method and test results, the innovative solution shows a ductile behaviour characterized by slip in bolted connections for high value of displacement and force, in agreement with the type of bolted connection, category B; please see EN1993-1-8 (2005).

The design by the component method requires the simulation of the joint by means of a series of different components. Each component was represented by an elastic spring characterised by a specific stiffness and strength, as highlighted in Figure 78. The appropriate coupling in parallel and series of these springs provides the global stiffness of the joint. As far as the global connection strength was concerned, different failure mechanisms were identified, the minimum value of failure loads being the design resistance of the connection. The components considered are reported in Table 22.

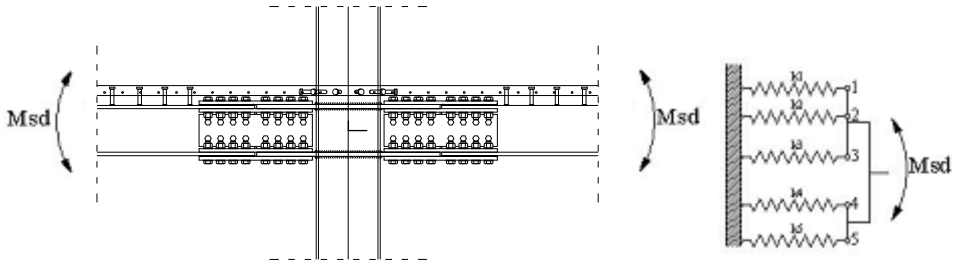

Figure 78. A steel-concrete composite bolted beam-to-column joint and its mechanical model.

The composite column was assumed to be infinitely rigid during the application of the component method. In greater detail, beam-to-column joints were rigid and full-strength joints. The joint overstrength can be guaranteed by the following relation

$$M_{j,Rd} \geq 1.1 \cdot \gamma_{ov} \cdot M_{b,pl,Rd}$$

where $M_{j,Rd}$ defines the resisting moment of the beam-to-column joint assumed to be full strength and $M_{b,pl,Rd}$ represents the resisting moment of the adjacent composite beam.

Table 22. Joint components relevant to sagging and hogging bending moment

Sagging Bending Moment	Hogging Bending Moment
Concrete slab in compression	Longitudinal rebars in tension
Upper horizontal plate in compression	Upper horizontal plate in tension
Vertical plate in bending	Vertical plate in bending
Lower horizontal plate in tension	Lower horizontal plate in compression

VIII.9. WP7 – Project coordination

Four tasks were planned within this work package:

- Task 7.1: Definition of standard protocols
- Task 7.2: Monitoring of the activities of each research unit
- Task 7.3: Global evaluation of the research project
- Task 7.4: Final report of the research activities

Meetings for the ATTEL project were organised in Liège, Moena, Volos, Bolzano, Pula, Asturias and Roma during the project. Minutes for these meetings are available.

At the beginning of the project, an FTP server for the ATTEL project was created. In agreement with the partners of another RFCS project entitled HITUBES (RFSR-CT-00035) in which all the partners of ATTEL are involved, it was agreed to merge the two FTP servers initially created separately for the two projects in one FTP server. The requested information to be connected to this server are given here below:

- Address: ftp://msmsr05.gciv.ulg.ac.be
- Username: HITEL
- Password: HSS590

In particular, directories for the collection of interesting articles, reports and documents have been created on the FTP server according to different domains identified during the kick-off meeting in Liège and updated during the second meeting in Moena.

VIII.10. Conclusions

The use of high strength steel (HSS) circular hollow sections (CHS) is still limited in the construction industry despite their excellent structural and architectural properties and the fast development of end-preparation machines. Moreover, although EC3-1-12 extends its scope to steel grades up to S690/S700MC, limitations exist at the material, structural and design levels.

The project ATTEL intended to develop both analytical and experimental know-how in order to support new design criteria for the exploitation of HSS and steel-concrete composite circular hollow sections for columns and connections subjected to exceptional loads, like earthquakes and fire.

The investigations have been experimental (through testing of tubular members and connections), analytical and numerical (through the use of the component method and advanced finite element simulations).

Globally, but also looking to details, it can be concluded that the different investigations were successfully conducted and the different objectives of the ATTEL project were met. The main achievement of the project is obviously the proposal of design recommendations for structures using HSS tubular columns and for structural elements made of HSS such as columns, beam-to-column joints and column bases in fire conditions and/or under seismic actions.

The exploitation of the results and the possible impacts of the present research will be presented in § VIII.11 here below.

VIII.11. Exploitation and impact of the research results

The main outcomes of the project are:

- the well documented experimental results and;
- the design recommendations for structures and structural elements using HSS tubular columns.

Concerning the first outcome, i.e. the experimental results, the possible exploitation and impact is mainly for the scientific committee. Indeed, most of the performed tests were innovative and these results are useful for people who would like to calibrate and validate analytical or numerical tools.

Concerning the second outcome, i.e. design recommendations, this constitutes the main outcome for engineers in design offices. Indeed, the use of HSS tubular elements is not yet well covered by the codes and standards and, in particular, by the Eurocodes. Accordingly, a designer has to face a lack of information in the codes when he wants to use such structural elements.

A second aspect that the designer has to face is the difficulty to design and to characterise joints (i.e. beam-to-column joints and column bases) when HSS tubular are used. This difficulty is increased when the joints have to respect the criteria for a capacity design in seismic zone as specified in Eurocode 8. Indeed, if so, it is compulsory to design full strength joints with a sufficient overstrength if compared to the beam resistance.

The ATTEL project brings solutions to these difficulties by proposing:

- structural solutions for which the use of HSS can lead to an economical interest;
- design solutions for joints in seismic and non-seismic regions;
- design recommendations for the characterisation of main structural elements, i.e. the columns, the beam-to-column joints and the column bases, both in non-seismic and seismic zones considering a possible fire action.

In details, guidelines in the fields listed here below have been produced as an outcome of WP 6:

- Possible structural solution and recommendations for the structural analysis for:
  - Building in low-seismicity areas
  - Building in high- seismicity areas
- Recommendations for the design of high-strength steel CHS columns:
  - at normal temperature (cross-sectional strength for axial loading, cross-sectional strength for bending loading, strength of CHS columns)
  - at elevated temperature
- Design recommendations for column base subjected to combined bending moment and axial force (at room and elevated temperatures):
  - column-bases in buildings in low-seismicity areas
  - column- bases in buildings in high-seismicity areas (standard and innovative solutions)
- Design recommendations for beam-to-column joints:
  - in building in low-seismicity areas
  - in building in high-seismicity areas

Through the proposed recommendations, it is now possible to perform an optimized and economical design of the structural elements considered within the present project, taking full advantage of the properties of HSS. Most of these recommendations have been developed respecting the Eurocode philosophies and principles. Accordingly, the implementation of proposed rules within the Eurocodes could be contemplated.

Beyond that, the project provides also to designers key information related to the economical fields of application of HSS in structures subjected to fire and static or seismic loading.

IX. List of figures

X. List of tables

XI. References

AISC-LRFD (2000). “Load Resistance Factor Design Specification for steel hollow structural sections”. American Institute of Steel Construction, Chicago, Illinois.

American Institute of Steel Construction, 2005, “Steel Construction Manual - Thirteenth Edition”, AISC 325-05

American Petroleum Institute (1993). “Recommended Practice, Designing and Constructing Fixed Offshore Platforms-Load and Resistance Factor Design”. Recommended practice 2A-LRFD, 1st Edition. Washington.

Anderson D (ed). “COST C1 - Composite steel-concrete joints in frames for buildings: Design provisions”. Brussels – Luxembourg, 1999.

Beg, Hladnik. “Slenderness limit of Class 3 I cross-sections made of high strength steel”, Journal of Constructional Steel Research, Volume 38, Number 3, July 1996 , pp. 201-217

British Standard, 2000. “Structural use of steelwork in building. Code of practice for design. Rolled and welded sections" BS 5950-1:2000

Bursi et al. (2008). “Analysis of steel-concrete composite beam-to-column joints: bolted solutions”, Proceedings of composite construction in steel and concrete VI, Engineering Conferences International, Devil's Thumb Ranch, Colorado (USA)

Bursi O. S., Zandonini R., Salvatore W., Caramelli S., and Haller M. (2006). "Seismic Behavior of a 3D Full-Scale Steel-Concrete Composite Moment Resisting Frame Structure", Composite Construction in Steel and Concrete V, 641 - 652. Proceedings of the 5th International Conference,ASCE,.

Bursi O., Caramelli S., Fabbrocino G., Molina J., Salvatore W., Taucer F. and Zandonini R. (2004). “3D Full-Scale Seismic Testing of a Steel-Concrete Composite Building at ELSA”, EUR 21299 EN.

Chen e Young. “Design of high strength steel columns at elevated temperatures” J. of Constructional Steel Research, Volume 64, 2008, pp.689-703.

Chin-Tung Cheng, Lap-Loi Chung (2003). “Seismic performance of steel beams to concrete-filled steel tubular column connections”. Journal of Constructional Steel Research, Volume 59, Issue 3, Pages 405-426

CIDECT (1992). “Structural Stability with Hollow Sections”. CIDECT design guide No. 2, Springer-Verlag.

E. de M. Batista, F.C. Rodriguez. “Residual Stress Measurements on Cold-formed profiles”. Experimental Techniques Vol. 16 No. 5 pp. 25-29. September/October 1992.

Elchalakani M, Zhao XL, Grzebieta RH. “Cyclic bending tests to determine fully ductile slenderness limits for cold-formed circular hollow sections”. J Struct Engrg ASCE 2004;130(7):1001–10.

EN 12010-2:2006- “Hot finished structural hollow sections of non-alloy and fine grain steels Part 2: Tolerances, dimensions and sectional properties”.

EN 1991-1-1. "Eurocode 1: Action on structures - Part 1-1: General action - Densities, self-weight, imposed loads for buildings", CEN, Bruxelles, 2004.

EN 1992-1-1. "Eurocode 3: Design of concrete structures - Part 1-1: General rules and rules for buildings", CEN, Bruxelles, 2005.

EN 1993-1-1. “Eurocode 3: Design of steel structures, Part 1-1: General rules and rules for buildings”. Brussels, 2005.

EN 1993-1-12. "Eurocode 3: Design of steel structures - Part 1-12: Additional rule for te extension of EN 1993 up to steel grades S700", CEN, Bruxelles, 2007.

EN 1993-1-2. "Eurocode 3: Design of steel structures - Part 1-2: General rules - Structural fire design", CEN, Brussels, 2005.

EN 1993-1-2. “Eurocode 3: Design of steel structures, Part 1-2: General rules - Structural fire design”. CEN, Brussels, 2004.

EN 1993-1-6. “Eurocode 3: Design of steel structures - Part 1-6: Strength and Stability of Shell”. Structures. Brussels, 2007.

EN 1993-1-8. “Eurocode 3: Design of steel structures - Part 1-8: Design of joints”. Brussels, 2003.

EN 1994-1-1. “Eurocode 4: Design of composite steel and concrete structures, Part 1-1: General rules and rules for buildings”. Brussels, 2004.

EN 1994-1-2. “Eurocode 4: Design of composite steel and concrete structures, Part 1-2: General rules - Structural fire design”. Brussels, 2004.

EN 1998-1. "Eurocode 4: Design of structures for earthquake resistance - Part 1-1: General rules and rules, seimic actions and rule for buildings ", CEN, Bruxelles, 2005.

EN ISO 6892-1:2009. “Metallic materials – Tensile testing – Part 1: Method of test at room temperature”.

EN1992-1-1 (2005)."Eurocode 3: Design of concrete structures - Part 1-1: General rules and rules for buildings", CEN, Bruxelles

Franssen J.M. (2005). “SAFIR. A Thermal/Structural Program Modelling Structures under Fire”, Engineering Journal, A.I.S.C., 42(3), 143-158.

Furlong, R. W. (1967), ‘‘Strength of steel-encased concrete beam-columns.’’ J. Struct. Div. ASCE, 93 (5), 113–124.

Guisse S, Vandegans D, Jaspart JP. “Application of the component method to column bases – experimentation and development of a mechanical model for characterization”. Research Centre of the Belgian Metalworking Industry, 1996.

Hoang VL et al. “Field of application of high strength steel circular tubes for steel and composite columns from an economic point of view”. Journal of Constructional Steel Research, (67):1001-1021, 2011.

Karl F., Helmut K., Robert S., (1997), “Protocol for fabrication, inspection, testing, and documentation of beam-column connection tests and other experimental specimens”, Report No.SAC/BD-97/02, SAC joint Venture, Sacramento, California, U.S.A.

Kodur V.K.R (2007). “Guidelines for Fire Resistance Design of Concrete-Filled Steel HSS Columns-State-of-the-Art and Research Needs”, Internation journal of Steel Structures KSSC (Korean Society of Steel Construction) Vol. 7(3)(2007)

Mohamed Elchalakani, Xiao-Ling Zhao and Raphael Grzebieta (2004). “Concrete-filled steel circular tubes subjected to constant amplitude cyclic pure bending”, Engineering Structures 26, 2125–2135

Pappa, P., and Karamanos, S. A. “Buckling of High-Strength Steel CHS Tubular Members under axial compression and bending,” 14th International Symposium on Tubular Structures, Paper No. 104, London, UK, 2012.

Pournara A.E., Karamanos S.A., Ferino J., Lucci A. “Strength and stability of high-strength steel tubular beam-columns under compressive loading,” 14th International Symposium on Tubular Structures, Paper No. 103, London, UK, 2012.

Rasmussen, Hancock “Test of High Strength Steel Columns” J. Construct Steel Research 34 (1995), 27-52.

Richter, Hanus, Wolf. “Structural Steels of 690 MPa Yield Strength – a State of Art”, 2nd International Symposium on High Strength Steel, Stiklestad, Verdal 23-24 April, 2002.

Ronald D. Ziemian. “Guide to Stability design criteria for Metal Structures”. Sixth Edition (2010) by. Jhon Wiley & Sons, inc.

S. Kyriakides, P.K. Shaw. “Inelastic buckling of tubes under cyclic loads,” ASME J. Press. Vessel Technol., 109 (1987), pp. 169–178

Sivakumaran K.S., Bing Y. “Slenderness limit and ductility of high strength steel sections”, Journal of Constructional Steel Research, Volume 46, Number 1, April 1998 , pp. 149-151

Standards Association of Australia, 1990, “AS 4100-1990 Steel Structures”, Standards Australia

Stephen P. Schneider, Yousef M. Alostaz (1998). “Experimental Behaviour of Connections to Concrete-filled Steel Tubes”, Journal of Constructional Steel Research, Volume 45, Issue 3, Pages 321-352

Treuting, Wishart, Lynch and Richards. “Residual stress measurements”. American Society for Metals (1952).

XII. Signed Technical annex

EUROPEAN COMMISSION
RESEARCH DIRECTORATE-GENERAL

Research Fund for Coal and Steel

ANNEX I
Form 1-1
OBLIGATORY AT THE SUBMISSION STAGE

TECHNICAL ANNEX

Project acronym: ATTEL
Proposal No[2]: RFS-PR-07043
Contract No: RFSR-CT-2008-00037

TITLE: ***Performance-based approaches for high strength tubular columns and connections under earthquake and fire loadings***

PROJECT OBJECTIVES

The project ATTEL intend to develop both analytical and experimental know-how in order to support new design criteria for the exploitation of HSS and steel-concrete composite circular hollow sections for columns and connections subjected to exceptional loads, like earthquakes and fire.

The investigation will be both experimental, through testing of tubular members and connections, analytical and numerical, through the use of the component method and advanced finite element simulations, in order to make full use of high strength steel ranging from S500Q/ S500MC to S690Q/S700MC according to the new Eurocode 3 Part 1-12, for structural tubes ranging from 2 in to 24 in, with D/t > 30 which represents nowadays an upper limit for structural applications. The ambitious targets are to increase structural performance of steel structures, reduce weights and construction costs for buildings subjected to exceptional loadings; in a greater detail, over-design based approaches are going to be applied for:

1. Steel and composite CFT columns made of HSS;
2. Welded or bolted composite beam-to-CFT column joints made of HSS;
3. CFT column base-joints made of HSS.

1/20

ANNEX I
Form 1-2
OBLIGATORY AT THE SUBMISSION STAGE

WORK PACKAGE DESCRIPTION

WP No	1

Work package Title	Collection and evaluation of test data and design procedures on HSS tubular members and connections subjects to earthquake and fire loadings	Number of man hours[29]
WP Leader (full name & acronym)	UNIVERSITY OF THESSALY - UNITH	300
Contractor (s) (full name & acronym)	UNIVERSITY OF LIEGE - UNILG	120
	CENTRO SVILUPPO MATERIALI - CSM	90
	STAHLBAU PICHLER - STBPI	60
	UNIVERSITÀ DEGLI STUDI DI TRENTO - UNITN	300
Total		**870**

1 - Objectives

- evaluation of existing methodologies for low-cycle fatigue design of members and joints;
- collection and evaluation of experimental test data on steel and composite steel-concrete tubular members and connections under earthquake and fire loadings;
- collection and evaluation of experimental test data on HSS, HSS-concrete composite joints and HSS tubular elements subjects to earthquake and fire loadings;
- collection and evaluation of design procedures on over-design approach, capacity design and displacement based design applicable on HSS-concrete composite joints.

2 - Work programme and distribution of tasks with indication of participating contractors

The work package is made up of 2 tasks:

- Task 1.1: Collection and evaluation of experimental test on HSS, HSS-concrete composite joints and CHS elements subjected to earthquake and fire loadings (UNILG, CSM, STBPI, UNITH, UNITN, IP).

  → Emphasis on mechanical behaviour, lack of data and lack in the standard European Norms.

- Task 1.2: Collection and evaluation of design procedures on over-design approach, capacity design and displacement based design usable on HSS-concrete composite joints (UNILG, UNITH, UNITN).

  → Collection and evaluation of type, details and mathematical displacements-based models usable on HSS and HSS-concrete columns and joints.

One state-of-the-art report on the two aforementioned subjects will be produced (D1.1).

3 - Interrelation with other work packages (please give WP No)

WP2, WP5, WP6 and WP7

4 - Deliverables and milestones

- M1.1: Collection and evaluation of experimental test on HSS, Steel-concrete composite joints and CHS elements subjected to earthquake and fire loadings;
- M1.2: Collection and evaluation of design procedures on displacement based design applicable on HSS, Steel-concrete composite joints and CHS elements subjected to earthquake and fire loadings.

- D1.1: State-of-the-art report on collection and evaluation of experimental test data and design procedures.

3/20

ANNEX I
Form 1-2

WORK PACKAGE DESCRIPTION

WP No	2

Work package Title	Design of specimens	Number of man hours[29]
WP Leader (full name & acronym)	STAHLBAU PICHLER - STBPI	600
Contractor (s) (full name & acronym)	UNIVERSITY OF LIEGE - UNILG	150
	CENTRO SVILUPPO MATERIALI - CSM	200
	UNIVERSITY OF THESSALY - UNITH	600
	UNIVERSITÀ DEGLI STUDI DI TRENTO - UNITN	400
Total		**1950**

1 – Objectives

- choice and optimization of the specimens to be tested;
- design and numerical modelling of HSS column and HSS-CFT column to be tested under earthquake and fire loadings;
- selection and design of HSS-concrete composite beam-to-column joints to be tested under earthquake and fire loadings;
- selection and design of base joints to be tested
- estimation of specimens characteristics by means of F.E. models and calibration of models.

2 - Work programme and distribution of tasks with indication of participating contractors

The work package is made up of 4 tasks:

- Task 2.1: Definition of 2D frame models (UNITH, UNITN).

  → Selection of 2D frame models to be used in the design process of the specimens.

- Task 2.2: Selection, design and numerical modelling of base-joints to be tested (UNILG, UNITH, UNITN).

  → Design and modelling (3D local model) of column-base HSS joint specimens to be tested under cyclic load (UNITN) and fire (UNILG). In particular 3 different types of specimen of column-base joints will be designed.

- Task 2.3: Selection, design and numerical modelling of HSS-CHS columns and HSS-CFT columns to be tested (UNILG, CSM, UNITH).

  → Selection of specimens and mechanical (CSM) and fire (UNILG) evaluation of their properties, by means of 3D numerical models. In particular 3 different types of specimen, both for HSS columns and HSS-CFT columns with different diameter/width ratios and same boundary conditions will be designed.

- Task 2.4: Selection, design and numerical modelling of HSS-concrete composite beam-to-column joints to be tested (UNILG, STBPI, UNITH).

→ Selection of a HSS-concrete composite beam-to-column joint easy to erect (STBPI), design and modelling (3D local model) of specimens to be tested under cyclic load (UNITH) and fire (UNILG). In particular 2 different types of specimens of beam-to-column joints (one welded joint and one bolted joint) will be designed.

One report on the design process will be produced (D2.1).

One report on the definition of practical solution for the selected typologies will be produced (D2.2).

3 - Interrelation with other work packages (please give WP No)

WP1, WP3, WP4, WP5 and WP7

4 - Deliverables and milestones

- M2.1: definition of 3D local model;
- M2.2: Selection, design and numerical modelling of base joint;
- M2.3: Selection, design and numerical modelling of HSS column and Steel-concrete composite column;
- M2.4: Selection, design and numerical modelling of HSS-concrete composite beam-to-column joint.

- D2.1: report on the design of specimens;
- D2.2: definition of practical solution for the selected typologies of base-joints, of HSS-CHS columns and HSS-CFT columns and of HSS-concrete composite beam-to-column joints.

5/20 AS

ANNEX IV
Form 1-2

WORK PACKAGE DESCRIPTION

WP No	3

Work package Title	Cyclic testing	Number of man hours[29]
WP Leader (full name & acronym)	CENTRO SVILUPPO MATERIALI - CSM	2400
Contractor (s) (full name & acronym)	STAHLBAU PICHLER - STBPI	1550
	UNIVERSITY OF THESSALY - UNITH	2500
	UNIVERSITÀ DEGLI STUDI DI TRENTO - UNITN	2100
Total		8550

1 - Objectives

- experimental investigation of the mechanical behaviour of designed HSS-CHS columns and HSS-CFT columns;
- experimental investigation of the mechanical behaviour of HSS-concrete composite beam to column joints;
- experimental investigation of the mechanical behaviour of base joints.

2 - Work programme and distribution of tasks with indication of participating contractors

The work package is made up of 4 tasks:

- Task 3.1: Mechanical characterization of materials (CSM).

  → Before the true effective experiments, the material (supplied by IP) of the specimens will be tested trough axial monotonic and cyclic tests in order to better calibrate the models developed in WP2.

- Task 3.2: Tests on base-joint specimens (STBPI, UNITN).

  → 3 specimens for each (3) designed type of HSS base joints will be tested under monotonic load (1 specimen), cyclic load (according to ECCS-1986, 1 specimen) and by the use of generated ground acceleration time-histories (1 specimen) (UNITN).

  → Specimen will be supplied and manufactured by STBPI, whilst concrete casting will be executed in UNITN.

- Task 3.3: Tests on column specimens (CSM, STBPI).

  → 3 specimens for each (3) designed type of HSS-CHS column will be tested under monotonic load (1 specimen), cyclic load (according to ECCS-1986, 1 specimen) and by the use of generated ground acceleration time-histories (1 specimen).

  → 3x3 tests will be also performed on the HSS-CFT columns (CSM).

  → Specimens will be supplied and manufactured by STBPI, whilst concrete casting will be executed in CSM.

- Task 3.4: Tests on beam-to-column joint specimens (STBPI, UNITH).

6/20

→ 3 specimens for each (welded and bolted) designed type of HSS-concrete composite beam to column joint will be tested under monotonic load (1 specimen), cyclic load (according to ECCS-1986, 1 specimen) and by the use of generated ground acceleration time-histories (1 specimen) (UNITH).

→ Specimen will be supplied and manufactured by STBPI, whilst concrete casting will be executed in UNITH.

1 report on the cyclic tests will be produced (D3.4)

3 - Interrelation with other work packages (please give WP No)

WP2, WP5, WP6 and WP7

4 - Deliverables and milestones

- M3.1: Results of material characterization;
- M3.2: Manufacturing and experimental set-up of base-joint specimens;
- M3.3: Manufacturing and experimental set-up of column specimens;
- M3.4: Manufacturing and experimental set-up of beam-to-column joint specimens.

- D3.1: monotonic and cyclic test data on base-joint specimens;
- D3.2: monotonic and cyclic test data on column specimens;
- D3.3: monotonic and cyclic test data on beam-to-column joint specimens;
- D3.4: cyclic test results laboratory report.

7/20

ANNEX IV
Form 1-2

WORK PACKAGE DESCRIPTION

WP No	4

Work package Title	Fire testing	Number of man hours[29]
WP Leader (full name & acronym)	UNIVERSITY OF LIEGE - UNILG	1900
Contractor (s) (full name & acronym)	STAHLBAU PICHLER - STBPI	900
Total		**2800**

1 - Objectives

- experimental investigation of the fire behaviour of designed HSS-CHS columns and HSS-CFT columns;
- experimental investigation of the fire behaviour of HSS-concrete composite beam-to-column joints;
- experimental investigation of the fire behaviour of base-joints.

2 - Work programme and distribution of tasks with indication of participating contractors

The work package is made up of 4 tasks:

- Task 4.1: Thermal characterization of materials (UNILG).

  Tests for the characterisation of the thermal properties of the high strength steel will be performed on small coupon elements extracted from the various connections, columns and column bases to be tested in Tasks 4.2 to 4.4. These specimens will be tested in a furnace at a constant temperature. In total, 6 components composed of HSS are identified within the specimens (3 tubular columns, 1 end-plate for the column bases, 2 plates for the beam-to-column joints); the "normal" carbon steel used within the other elements of the tested specimen will not be experimentally characterised at high temperature as their behaviour is already well known from the literature. For each identified component, it is intended to perform tests at 5 different temperatures; so, in total, 30 tests will be performed.

  Within the project, it is intended that Stahlbau Pichler provides "ready to test" coupons fabricated according to the requirements of ULg. So, the 100 hours will only be dedicated to the performance of the 30 experimental tests; so, more or less 3 hours are available for each test and 10 hours for the preparation of the test equipment.

  The objective is just to characterise the thermal behaviour of the steel material used for the connections, columns and columns bases tested in Tasks 4.2 to 4.4. In other words, this means that a full parametrical study of the thermal properties of high strength steel, which would involve many more tests, is not planned within the project.

- Task 4.4: Tests on base-joint specimens (UNILG, STBPI).

  → 1 specimen for each (3) designed type of HSS base-joints will be tested under ISO fire tests (UNILG).

  → Specimen will be supplied and manufactured by STBPI, whilst concrete casting will be executed in UNILG.

9/20

- Task 4.2: Tests on column specimens (UNILG, STBPI).
  - → 1 specimen for each (3) designed type of HSS-CHS columns will be tested under ISO fire test (UNILG).
  - → 1 test will be also performed on the HSS-CFT columns (UNILG).
  - → Specimen will be supplied and manufactured by STBPI, whilst concrete casting will be executed in UNILG.
- Task 4.3: Tests on beam-to-column joint specimens (UNILG, STBPI).
  - → 1 specimen for each (welded and bolted) designed type of HSS-concrete composite beam-to-column joints will be tested under ISO and natural fire tests (UNILG).
  - → Specimen will be supplied and manufactured by STBPI, whilst concrete casting will be executed in UNILG.

1 report on the fire tests will be produced (D4.4).

3 - Interrelation with other work packages (please give WP No)

WP2, WP5, WP6 and WP7

4 - Deliverables and milestones

- M4.1: Results of material characterization;
- M4.2: Manufacturing and experimental set-up of base-joint specimens;
- M4.3: Manufacturing and experimental set-up of column specimens;
- M4.4: Manufacturing and experimental set-up of beam-to-column joint specimens;

- D4.1: fire test data on base-joint specimens;
- D4.2: fire test data on column specimens;
- D4.3: fire test data on beam-to-column joint specimens;
- D4.4: fire test results laboratory report.

9/20 45.

ANNEX IV
Form 1-2

WORK PACKAGE DESCRIPTION

WP No	5

Work package Title	Model Calibration	Number of man hours[29]
WP Leader (full name & acronym)	UNIVERSITÀ DEGLI STUDI DI TRENTO - UNITN	1300
Contractor (s) (full name & acronym)	UNIVERSITY OF LIEGE - UNILG	600
	CENTRO SVILUPPO MATERIALI - CSM	600
	UNIVERSITY OF THESSALY - UNITH	1800
Total		**4300**

1 - Objectives

- provide stability curves to be applied with HSS according to test results of WP3;
- provide mathematical formulation and calibration by means of the results obtained experimentally in WP3 and WP4;
- provide prequalification data and design procedures for HSS columns and joint tested.

2 - Work programme and distribution of tasks with indication of participating contractors

The work package is made up of 3 tasks:

- Task 5.1: Definition of stability curves (CSM,UNITH).

  → Stability curves as a function of member slenderness and rotation capacity of the HSS tubular members used in the tests will be identified.

- Task 5.2: Calibration of 2D-3D numerical model (UNILG, UNITH, UNITN).

  → Mathematical formulation and calibration of 2D frame models and 3D local models developed by means of the results obtained experimentally in WP3 and WP4.

- Task 5.3: Parametric numerical analyses (UNILG, UNITH, UNITN).

  → Parametric analyses will be performed after the calibration of models in order to optimize design process.

  → Parametric analyses will be performed with natural earthquake and fire will be performed.

  → Prequalification data and design procedures for HSS columns and joint tested will defined.

One report on the numerical modelling relevant to the stability curve formulation will be produced (D5.1)

One report on the numerical model calibration relevant to the selected specimen typologies will be produced (D5.2)

One report on the parametric analyses will be produced (D5.3)

3 - Interrelation with other work packages (please give WP No)

WP1, WP3, WP4, WP6 and WP7

4 - Deliverables and milestones

- M5.1: Calibration of 2D frame and 3D local mechanical models;
- M5.2: Parametric numerical analyses.

- D5.1: Definition of stability curves;
- D5.2: simulation data relevant to the selected typologies of base-joints, of HSS-CHS columns and HSS-CFT columns and of HSS-concrete composite beam-to-column joints;
- D5.3: report on parametric numerical analyses.

ANNEX IV
Form 1-2

WORK PACKAGE DESCRIPTION

WP No	6

Work package Title	Design guidelines	Number of man hours[29]
WP Leader (full name & acronym)	UNIVERSITY OF THESSALY - UNITH	600
Contractor (s) (full name & acronym)	UNIVERSITY OF LIEGE - UNILG	300
	CENTRO SVILUPPO MATERIALI - CSM	350
	STAHLBAU PICHLER - STBPI	300
	UNIVERSITÀ DEGLI STUDI DI TRENTO - UNITN	390
Total		**1940**

1 - Objectives

- development of design guidelines and recommendations endowed with HSS and HSS-CFT columns under earthquake and fire loading;
- development of design guidelines and recommendations endowed with HSS tested beam-to-column joints under earthquake and fire loading;
- development of design guidelines and recommendations endowed with HSS tested base-joints.

2 - Work programme and distribution of tasks with indication of participating contractors

The work package is made up of 3 tasks:

- Task 6.1: Definition of design rules and proposal for EC3, EC4 and EC8 relevant to HSS base-joints (UNILG, UNITN, STBPI).

  → Seismic design rules and methods of HSS base-joints computation based on the displacement-based method will be provided.

  → Design rules related on zones of strong (hot-spot) stress concentrations will be provided.

- Task 6.2: Definition of design rules and proposal for EC3, EC4 and EC8 relevant to HSS and HSS-CFT columns (UNILG, CSM, UNITH, STBPI).

  → Stability curves as a function of member slenderness and rotation capacity of tested HSS tubular members will be provided.

  → Rules related to mechanical and fire behaviour of HSS-CFT columns will be provided.

- Task 6.3: Definition of design rules and proposal for EC3, EC4 and EC8 relevant to HSS composite beam-to-column joints (UNILG, UNITH, STBPI).

  → Seismic design rules and methods of HSS joints computation based on the displacement-based method will be provided.

  → Fire design rules and methods of HSS joints will be provided.

12/20

→ Design rules related on zones of strong (hot-spot) stress concentrations will be provided.

One report on the design rules and proposal for EC3, EC4 and EC8 will be produced (D6.4)

3 - Interrelation with other work packages (please give WP No)

WP1, WP5 and WP7

4 - Deliverables and milestones

- M6.1: Collection of experimental data and simulations related to column base-joints;
- M6.2: Collection of experimental data and simulations related to HSS and HSS-CTF columns;
- M6.3: Collection of experimental data and simulations related to HSS composite beam-to-column joints;

- D6.1: definition of design rules and proposal for EC3, EC4 and EC8 for column base-joints;
- D6.2: definition of design rules and proposal for EC3, EC4 and EC8 for HSS and HSS-CTF columns;
- D6.3: Definition of design rules and proposal for EC3, EC4 and EC8 for HSS composite beam-to-column joints;
- D6.4: report on the design rules and proposal for EC3, EC4 and EC8.

13/20

ANNEX IV
Form 1-2

WORK PACKAGE DESCRIPTION

WP No	7

Work package Title	Project coordination	Number of man hours[29]
WP Leader (full name & acronym)	UNIVERSITY OF LIEGE - UNILG	1000
Contractor (s) (full name & acronym)		
Total		1000

1 - Objectives

- guarantee a continuous interaction among the activities carried out by each contractor.
- Definition and implementation of a strong co-ordination procedure in order to enhance the efficiency and effectiveness of the work, via support and stimulation of synergies. More specifically, standard protocols will be agreed relevant to:
- execution of physical tests;
- set of a database to allow the collection and the exchange of experimental data;
- evaluation procedures of analytical/numerical models;

Moreover standard formats are established relevant to:

- state-of-the art documents;
- laboratory test reports;
- intermediate and final reports.

The activity of each contractor will be monitored through visits and meetings each six months among the persons in charge of each research unit.

2 - Work programme and distribution of tasks with indication of participating contractors

The work package is made up of 4 tasks:

- Task 7.1: Definition of standard protocols (UNILG).

  → Standard protocols will be agreed, relevant to: execution of physical tests; set of a database to allow the collection and the exchange of experimental data; evaluation procedures of analytical/numerical models. Moreover, common formats will be established relevant to: state-of-the-art documents; laboratory test reports; intermediate and final research reports. All the aforementioned documents will be available on a web site at the project end. As a result, their diffusion and use by the scientific community will be enhanced.

- Task 7.2: Monitoring of the activities of each research unit (UNILG).

  → The activities of each research unit will be monitored through the co-ordination meetings approximately each six months among the persons in charge of each unit. Intermediate results will be thoroughly discussed and presented in reports, which will enable internal and external monitoring of the project advances, and of the degree of fulfilment of the objectives set for the various phases.

14/20

- Task 7.3: Global evaluation of the research project (UNILG).

  → The global evaluation of the research project must take into account both the co-ordination activity and the effectiveness of the work of each research unit, measured on the basis of the degree of fulfilment of the project objectives. The Co-ordinator will check the activities and will perform the internal evaluation of the whole project.

- Task 7.4: Final report of the research activities (UNILG).

  → A final report of the research activities will follow.

Three reports on the activities undertaken will be produced (D7.1, D7.2, D7.3)

3 - Interrelation with other work packages (please give WP No)

WP1, WP2, WP3, WP4, WP5 and WP6

4 - Deliverables and milestones

- M7.1: Definition of standard protocols;
- M7.2: Collection of data on activities and meetings related to first year; evaluation of research project course state;
- M7.3: Collection of data on activities and meetings related to second year; evaluation of research project course state;
- M7.4: Draft of Final report on the research activities.

- D7.1: First year report on activities, meetings and evaluation of research project course state;
- D7.2: Second year report on activities, meetings and evaluation of research project course state;
- D7.3: Final report on the research activities.

ANNEX IV
Form 1-3

PROGRAMME BAR CHART (TASK, PARTNER, DELIVERABLES, MILESTONES)

Work packages	*Work packages' title*	*Deliverables*	Hours on project/ Contractor(s)					1st year				2nd year				3rd year				4th year	
			1	2	3	4	5	I	II	III	IV	I	II	III	IV	I	II	III	IV	I	II
WP 1	**Collection and evaluation of test data and design procedures**		**120**	**90**	**60**	**300**	**300**														
Task 1.1	Collection and evaluation of experimental test on HSS, HSS-composite joints and CHS elements subjected to earthquake and fire loadings	D1	60	90	60	150	150	M1.1	D1.1												

1 2 3 4 5

Task **1.2**	collection and evaluation of design procedures on over-design approach, capacity design and displacement based design usable on HSS-concrete composite joints		60			150	150	M1.2												
WP 2	**Design of specimens**		**150**	**200**	**600**	**600**	**400**													
Task **2.1**	Definition of 2D frame and 3D local models	D2.1				100	100	M2.1												
Task **2.2**	Selection, design and numerical modelling of base-joints to be tested	D2.1, D2.2	50		150	200	300		M2.2		D2.1 D2.2									
Task **2.3**	Selection, design and numerical modelling of HSS-CHS columns and HSS-CFT columns to be tested	D2.1, D2.2	50	200	150	200			M2.3											

Task **2.4**	Selection, design and numerical modelling of HSS-concrete composite beam-to-column joints to be tested	D2.1, D2.2	50		300	100				M2.4											
WP 3	**Cyclic testing**		**0**	**2400**	**1550**	**2500**	**2100**														
Task **3.1**	Mechanical characterization of materials			300							M3.1										
Task **3.2**	Tests on base-joint specimens	D3.1, D3.4			450		2100					M3.2			D3.1						
Task **3.3**	Tests on column specimens	D3.2, D3.4		2100	450								M3.3		D3.2	D3.4					
Task **3.4**	Tests on beam-to-column joint specimens	D3.3, D3.4			650	2500								M3.4	D3.3						
WP 4	**Fire testing**		**1900**	**0**	**900**	**0**	**0**														
Task **4.1**	Thermal characterization of materials		100							M4.1											
Task **4.2**	Tests on base-joint specimens	D4.1, D4.4	600		275						M4.2				D4.1	D4.4					
Task **4.3**	Tests on column specimens	D4.2, D4.4	600		275							M4.3			D4.2						
Task **4.4**	Tests on beam-to-column joint specimens	D4.3, D4.4	600		350								M4.4		D4.3						
WP 5	**Model calibration**		**600**	**600**	**0**	**1800**	**1300**														

Task **5.1**	Definition of stability curves	D5.1, D5.3		600		500													D5.1		
Task **5.2**	Calibration of 2D-3D numerical model	D5.2, D5.3	400			600	600										M5.1		D5.2	D5.3	
Task **5.3**	Parametric numerical analyses	D5.2, D5.3	200			700	700											M5.2			
WP 6	**Design guidelines**		**300**	**350**	**300**	**600**	**390**														
Task **6.1**	Definition of design rules and proposal for EC3, EC4 and EC8 relevant to HSS base-joints	D6.1, D6.4	100		100		390												M6.1	D6.1	
Task **6.2**	Definition of design rules and proposal for EC3, EC4 and EC8 relevant to HSS and HSS-CFT columns	D6.2, D6.4	100	350	100	300													M6.2	D6.2	D6.4
Task **6.3**	Definition of design rules and proposal for EC3, EC4 and EC8 relevant to HSS composite beam-to-column joints	D6.3, D6.4	100		100	300													M6.3	D6.3	

1 2 3 4 5

WP 7	**Project coordination**		1000	0	0	0	0														
Task 7.1	Definition of standard protocols		100						M7.1												
Task 7.2	Monitoring of the activities of each research unit	D7.1, D7.2, D7.3	300								M7.2	D7.1				M7.3	D7.2				
Task 7.3	Global evaluation of the research project	D7.1, D7.2, D7.3	300																	M7.4	D7.3
Task 7.4	Final report of the research activities	D7.3	300																		
Total Hours on project			**4070**	**3640**	**3410**	**5800**	**4490**														

WP 7	**Project coordination**		**1000**	**0**	**0**	**0**	**0**														
Task **7.1**	Definition of standard protocols		100						M7.1												
Task **7.2**	Monitoring of the activities of each research unit	D7.1, D7.2, D7.3	300								M7.2	D7.1			M7.3	D7.2					
Task **7.3**	Global evaluation of the research project	D7.1, D7.2, D7.3	300																	M7.4	D7.3
Task **7.4**	Final report of the research activities	D7.3	300																		
Total Hours on project			**4070**	**3640**	**3410**	**5800**	**4490**														

EUROPEAN COMMISSION
RESEARCH DIRECTORATE-GENERAL

Ref. ARES (2010)970266 - 26/11/2010

rtd.k.4(2010)921871

UNIVERSITE DE LIEGE*
Prof Jean-Pierre JASPART
Sart Tilman, Allée des Chevreuils, 1 B52/3
BE-4000 LIEGE
BELGIQUE

REGISTERED LETTER

AMENDMENT No (2)
TO CONTRACT No (RFSR-CT-2008-00037)

HAVING REGARD TO contract No (RFSR-CT-2008-00037) signed on 28/07/2008 and amendment n°1
(hereinafter called the "Contract").

WHEREAS the Coordinator UNIVERSITE DE LIEGE* "ULGG" asked the Commission , by letter of 28/09/2010 for:

- A modification of the Community contribution
- A modification of the Description of work (Annex I)
- An amendment of the table of breakdown of the costs
- A modification of total estimated eligible costs

IT HAS BEEN AGREED as follows:

Article 1.-

Change of the Community contribution

The total maximum Community financial contribution allocated to the Project specified in Article 3.2. of the contract is modified as follows:

Previous contribution(EURO)	New financial contribution(EURO)
689301.00	689297.00

A modification of the Description of work

The WP3 to annex I (technical annex) is modified as attached to this amendment

Amendment of table I of the estimated breakdown of the total estimated allowable costs

The table of estimated breakdown of estimated allowable costs between contractors is modified as attached to this amendment.

Change of the total estimated eligible costs

The **total estimated allowable costs** of the Project specified in Article 3.1. of the contract is modified as follows:

Previous total allowable costs(EURO)	New total allowable costs(EURO)
1148834.00	1148829.00

Article 2.-

All the other provisions of the Contract remain unchanged and shall continue to have full force and effect.

Article 3.-

This amendment, forming an integral part of the Contract, enters into force at the date of dispatch of the registered letter.

I request you to notify all the contractors of the content of the present amendment.

Yours faithfully.

On behalf of the Commission:

Name: Raffaele LIBERALI

Function: Director Directorate K

Signature:

(seal of the organisation)

Date:

Estimated breakdown of the total estimated *allowable costs* and *pre-financing*

Contract No RFSR-CT-2008-00037

NAME	TOTAL ESTIMATED ALLOWABLE COST (euro)	MAXIMUM CONTRIBUTION (euro)	FIRST PRE-FINANCING (euro)	FIRST FINANCIAL GUARANTEE (euro)	SECOND PRE-FINANCING (euro)	AGGREGATED FINANCIAL GUARANTEE (euro)
Coordinator UNIVERSITE DE LIEGE* (ULGG)	241,111.00	144,667.00	57,000.00	0.00	57,000.00	0.00
Principal Contractor CENTRO SVILUPPO MATERIALI SPA (CSM)	217,193.00	130,316.00	52,000.00	0.00	52,000.00	0.00
Principal Contractor STAHLBAU PICHLER SRL* (STAPI)	282,379.00	169,427.00	67,000.00	0.00	67,000.00	0.00
Principal Contractor PANEPISTIMIO THESSALIAS*UNIVERSITY OF THESSALY (UTHESSA)	170,445.00	102,267.00	44,000.00	0.00	37,000.00	0.00
Principal Contractor UNIVERSITA DEGLI STUDI DI TRENTO* (UTRE)	237,701.00	142,620.00	53,000.00	0.00	61,000.00	0.00
TOTAL	1,148,829.00	689,297.00	273,000.00	0.00	274,000.00	0.00

EUROPEAN COMMISSION
RESEARCH DIRECTORATE-GENERAL

Research Fund for Coal and Steel

ANNEX I

to Am° 2 to RFSR-CT-2008-00037

WORK PACKAGE DESCRIPTION

WP No	3

Work package Title	Cyclic testing	Number of man hours[29]
WP Leader (full name & acronym)	CENTRO SVILUPPO MATERIALI - CSM	2400
Contractor (s) (full name & acronym)	STAHLBAU PICHLER - STBPI	1550
	UNIVERSITY OF THESSALY - UNITH	2137
	UNIVERSITÀ DEGLI STUDI DI TRENTO - UNITN	2384
Total		**8470**

1 - Objectives

- experimental investigation of the mechanical behaviour of designed HSS-CHS columns and HSS-CFT columns;
- experimental investigation of the mechanical behaviour of HSS-concrete composite beam to column joints;
- experimental investigation of the mechanical behaviour of base joints.

2 - Work programme and distribution of tasks with indication of participating contractors

The work package is made up of 4 tasks:

- Task 3.1: Mechanical characterization of materials (CSM).

  → Before the true effective experiments, the material (supplied by IP) of the specimens will be tested trough axial monotonic and cyclic tests in order to better calibrate the models developed in WP2.

- Task 3.2: Tests on base-joint specimens (STBPI, UNITN, UNITH).

  → 6 tests: three different types of HSS base joints will be tested under cyclic load (3 specimens) and by the use of generated ground acceleration time-histories (3 specimens) (UNITN).

  → 3 tests on components extracted from HSS column bases will be performed under monotonic load (UNITH).

  → Specimen will be supplied and manufactured by STBPI, whilst concrete casting (if necessary) will be executed in UNITN and UNITH.

- Task 3.3: Tests on column specimens (CSM, STBPI).

  → 18 specimens on short and slender HSS-CHS columns with two different cross-sections will be tested under monotonic load so as to investigate the aspects of stability and cross-section resistance (CSM).

  → Specimens will be supplied and manufactured by STBPI.

- Task 3.4: Tests on beam-to-column joint specimens (STBPI, UNITN, UNITH).

  → 3 test: a HSS-concrete composite beam-to-column joint (used in a seismic zone) will be tested under monotonic load (1 specimen), cyclic load (according to ECCS-1986, 1 specimen) and by the use of generated ground acceleration time-histories (1 specimen) (UNITN).

  → 8 tests on components extracted from HSS-concrete composite beam-to-column joints will be performed under monotonic load (7 specimens) and cyclic load (1 specimen) (UNITH).

  → Specimens will be supplied and manufactured by STBPI, whilst concrete casting will be executed in UNITH and UNITN.

1 report on the cyclic tests will be produced (D3.4)

3 - Interrelation with other work packages (please give WP No)

WP2, WP5, WP6 and WP7

4 - Deliverables and milestones

- M3.1: Results of material characterization;
- M3.2: Manufacturing and experimental set-up of base-joint specimens;
- M3.3: Manufacturing and experimental set-up of column specimens;
- M3.4: Manufacturing and experimental set-up of beam-to-column joint specimens.

- D3.1: monotonic and cyclic test data on base-joint specimens;
- D3.2: monotonic and cyclic test data on column specimens;
- D3.3: monotonic and cyclic test data on beam-to-column joint specimens;
- D3.4: cyclic test results laboratory report.

EUROPEAN COMMISSION
RESEARCH DIRECTORATE-GENERAL

Research Fund for Coal and Steel

ANNEX IV
Form 1-3

PROGRAMME BAR CHART (TASK, PARTNER, DELIVERABLES, MILESTONES)

Work packages	*Work packages' title*	*Deliverables*	Hours on project/ Contractor(s)					1st year				2nd year				3rd year				4th year	
			1	2	3	4	5	I	II	III	IV	I	II	III	IV	I	II	III	IV	I	II
WP 1	**Collection and evaluation of test data and design procedures**		**120**	**90**	**60**	**300**	**300**														
Task **1.1**	Collection and evaluation of experimental test on HSS, HSS-composite joints and CHS elements subjected to earthquake and fire loadings	D1	60	90	60	150	150	M1.1	D1.1												
Task **1.2**	collection and evaluation of design procedures on over-design approach, capacity design and displacement based design usable on HSS-		60			150	150	M1.2													

16/20 371

	specimens																				
Task **3.4**	Tests on beam-to-column joint specimens and joint components	D3.3, D3.4			650	2137	284							M3.4	D3.3						
WP 4	**Fire testing**		**1900**	**0**	**900**	**0**	**0**														
Task **4.1**	Thermal characterization of materials		100							M4.1											
Task **4.2**	Tests on base-joint specimens	D4.1, D4.4	600		275						M4.2				D4.1	D4.4					
Task **4.3**	Tests on column specimens	D4.2, D4.4	600		275							M4.3			D4.2						
Task **4.4**	Tests on beam-to-column joint specimens	D4.3, D4.4	600		350								M4.4		D4.3						
WP 5	**Model calibration**		**600**	**600**	**0**	**1800**	**1300**														
Task **5.1**	Definition of stability curves	D5.1, D5.3		600		500												D5.1			
Task **5.2**	Calibration of 2D-3D numerical model	D5.2, D5.3	400			600	600										M5.1		D5.2	D5.3	
Task **5.3**	Parametric numerical analyses	D5.2, D5.3	200			700	700											M5.2			
WP 6	**Design guidelines**		**300**	**350**	**300**	**600**	**390**														
Task **6.1**	Definition of design rules and proposal for EC3, EC4 and	D6.1, D6.4	100		100		390												M6.1	D6.1	D6.4

EUROPEAN COMMISSION
RESEARCH DIRECTORATE-GENERAL

Research Fund for Coal and Steel

	EC8 relevant to HSS base-joints																				
Task 6.2	Definition of design rules and proposal for EC3, EC4 and EC8 relevant to HSS and HSS-CFT columns	D6.2, D6.4	100	350	100	300													M6.2	D6.2	
Task 6.3	Definition of design rules and proposal for EC3, EC4 and EC8 relevant to HSS composite beam-to-column joints	D6.3, D6.4	100		100	300													M6.3	D6.3	
WP 7	**Project coordination**		**1000**	**0**	**0**	**0**	**0**														
Task 7.1	Definition of standard protocols		100						M7.1												
Task 7.2	Monitoring of the activities of each research unit	D7.1, D7.2, D7.3	300								M7.2	D7.1			M7.3	D7.2				M7.4	D7.3
Task 7.3	Global evaluation of the research project	D7.1, D7.2, D7.3	300																		
Task 7.4	Final report of the research activities	D7.3	300																		
Total Hours on project			**4070**	**3640**	**3410**	**5437**	**4774**														

July 1st 2008 July 1st 2009 July 1st 2010 July 1st 2011

✓ ✓ ✓ 10290 → 10211, Δ = -79 h

19/20 DH

	concrete composite joints																				
WP 2	**Design of specimens**		**150**	**200**	**600**	**600**	**400**														
Task **2.1**	Definition of 2D frame and 3D local models	D2.1				100	100	M2.1													
Task **2.2**	Selection, design and numerical modelling of base-joints to be tested	D2.1, D2.2	50		150	200	300		M2.2												
Task **2.3**	Selection, design and numerical modelling of HSS-CHS columns and HSS-CFT columns to be tested	D2.1, D2.2	50	200	150	200			M2.3		D2.1 D2.2										
Task **2.4**	Selection, design and numerical modelling of HSS-concrete composite beam-to-column joints to be tested	D2.1, D2.2	50		300	100				M2.4											
WP 3	**Cyclic testing**		**0**	**2400**	**1550**	**2137**	**2384**														
Task **3.1**	Mechanical characterization of materials			300							M3.1						D3.4				
Task **3.2**	Tests on base-joint specimens	D3.1, D3.4			450		2100					M3.2			D3.1						
~~Task 3.3~~	~~Tests on column~~	~~D3.2, D3.4~~		~~2100~~	~~450~~								~~M3.3~~		~~D3.2~~						

XIII. Appendices

XIII.1. Modification of the WP 3 test campaign

TASKS WP3	ORIGINALLY	NOW	JUSTIFICATION OF PROPOSED CHANGES
Task 3.1	Axial monotonic and cyclic tests on materials (CSM)	Axial monotonic and cyclic tests on materials (CSM)	No change

TASKS WP3	ORIGINALLY	NOW	JUSTIFICATION OF PROPOSED CHANGES
Task 3.2	9 tests on column base joints with three different types of connections Monotonic/cyclic/ground acceleration time-histories loadings (UTRE)	6 tests on base joints with three different types of connections Cyclic/ground acceleration time-histories loadings (UTRE) 3 tests on components extracted from column base tests Monotonic loading (UTHESSA)	In order to define the specimens to be tested, it was agreed at the kick-off meeting held in Liège to extract these specimens from "actual" case studies, in order to carry out tests on realistic elements. Accordingly, it was proposed to design three different reference buildings corresponding to different loading conditions: - Building I: static load and fire - Building II: "low and medium" earthquake (<0,25g) and Fire - Building III: "strong" earthquake (>0,25g) and Fire From these study cases the specimens typologies for beam-to-column joints and base-joints were extracted and defined for two specific situations: - "Static" (joint configurations used in Building I); - "Seismic" (joint configurations used in Building II and Building III). The difference both in number and in loading protocol for the tests on base-joint specimens is justified by what follows. In the considered column base joints, only few components will be critical in terms of resistance and ductility; as a consequence, it appears much better to have more information on critical components, which are difficult to characterise in large specimens, and less information on large specimens whose behaviour is partly known. Therefore it is suggested to substitute the 9 initially planned tests on column base joints by 6 tests on full-scale beam-to-column joints and 3 specific tests on components extracted from the full-scale column base joints. These tests will be dedicated to better understanding of the mechanical behaviour of the base plate. The load application protocols that are normally used in experimental structural engineering and recognised from a scientific point of view will be referred to: - monotonic loading; - cyclic loading according to the European ECCS n°45 procedure (1986), sometimes modified by the SAC procedure (1997); - ground acceleration time-histories. They will be applied as foreseen in the original test programme.

TASKS WP3	ORIGINALLY	NOW	JUSTIFICATION OF PROPOSED CHANGES
Task 3.3	9 tests on slender steel columns 9 tests on slender composite columns Monotonic / Cyclic loading (CSM)	18 tests on short and slender steel columns with 2 different cross-sections Monotonic loading (CSM)	<u>Justification from the second six-monthly report</u> Originally, 9 tests on HSS-CHS and 9 tests on HSS-CFT columns were planned. Besides that, few tests were expected to be performed under cyclic loading. After discussion of the full experimental campaign (including tests on columns, beam-to-column joints and column bases) among the partners, it appeared that the number of parameters that should be examined for column tests would require a much higher number of tests with respect to the initially concerned one. As a result, the planning of tests on columns was revised in the following manner: - two cross-sections will be studied (323x10 and 355x12) in accordance with the aforementioned study cases; - half of the tests will be carried out on short columns and different moment to axial force ratios, with the objective to characterise the cross-section resistance M-N curve; - half of the tests will be carried out on long columns and different moment to axial force ratios, with the objective to characterise the buckling resistance of columns under M-N loading. - all tests will be carried out under monotonic loading. This decision can be explained as follows: - on the basis of the tests performed on steel columns, the validation of FEM tools will be achieved and, as a result, it will so be demonstrated that actual tests may be “replaced” by simulations; if this step is successfully crossed, the extending, with a very good confidence, of the use of the numerical tools for the simulation of composite columns appears as quite justified. - in seismic design, the formation of plastic hinges in columns is not acceptable. So the only place where dissipation can take place is at the level of column bases. Because cyclic tests on column bases will be performed in UTRE anyway, the cyclic tests on columns have been preferably replaced by monotonic tests in order to allow a more careful examination of the “M/N interaction” parameter and the member stability aspects.

TASKS WP3	ORIGINALLY	NOW	JUSTIFICATION OF PROPOSED CHANGES
Task 3.4	6 tests on beam-to-column joints with two different connections Monotonic/cyclic/ground acceleration time-histories loadings (UTHESSA)	3 tests on beam-to-column joints with the "seismic" joint configuration Monotonic/cyclic loadings/ ground acceleration time-histories loadings (UTRE) 8 tests on "single-component" beam-to-column "static" joint configurations Monotonic loading (UTHESSA)	In order to define the specimens to be tested, it was agreed at the kick-off meeting held in Liège to extract these specimens from "actual" case studies, in order to carry out tests on realistic elements. Accordingly, it was proposed to design three different reference buildings corresponding to different loading conditions: - Building I: static load and fire - Building II: "low and medium" earthquake (<0,25g) and Fire - Building III: "strong" earthquake (>0,25g) and Fire From these study cases the specimens typologies for beam-to-column joints and base-joints were extracted and defined for two specific situations: - "static" (joint configurations used in Building I); - "seismic" (joint configurations used in Building II and Building III). The difference both in the number and in the loading protocol for the tests on beam-to-column joint specimens is justified by what follows. In fact, in the considered beam-to-column joints, only few components will be critical in terms of resistance and ductility; as a consequence, it appears much better to have more information on critical components and less information on large specimens whose behaviour is partly known. Therefore it is suggested to substitute the 6 initially planned tests on beam-to-column joints by 3 tests on full-scale beam-to-column joints and eight tests on so-called "single-component" beam-to-column joints. These "single-component" joints are full-scale joints in which all the other components exhibit a much higher resistance than the one which is investigated. Tests on such joint configurations allow determining the actual behaviour of the component within the studied joint. The load application protocols that are normally used in experimental field and recognised from a scientific point of view will be referred to: - monotonic loading - cyclic loading according to the European ECCS n°45 procedure (1986), modified by the SAC procedure (1997) - ground acceleration time-histories They will be applied as foreseen in the original test programme

XIII.2. Appendix of WP3 – Cycling tests

XIII.2.1. Task 3.1 - Mechanical characterization of materials

Two (2) different CHS made of HSS nominal strength grade S590 from seamless quenched and tempered products were studied:

Cross-section A diameter (D) = 355 mm thickness (t) = 12 mm

Cross-section B diameter (D) = 323.9mm thickness (t) = 10 mm

XIII.2.1.1. Tensile tests

Two (2) tensile tests each cross-section were performed at room temperature in accordance with 0. Specimens were cylindrical (7 mm in diameter) machined in longitudinal direction. Results are reported in Table 23 and Figure 79 where:

S_0 original cross sectional area

D_0 original cross sectional diameter

L_0 original gauge length

$Rp_{0,2}$ stress at 0.2% of plastic extension

R_m tensile strength

A_g percentage plastic extension at maximum force (percentage of the extensometer length)

A permanent elongation after fracture expressed as a percentage of the original gauge length

Z percentage reduction of area

Table 23. Results of tensile test at room temperature.

Cross section	ID	S_0 mm²	D_0 mm	L_0 mm	$Rp_{0,2}$ MPa	R_m MPa	A_g %	A %	Z %
A	A-1	37.72	6.93	50	746	821	7.2	16	72
	A-2	37.72	6.93	50	733	811	6.8	15	72
B	B-1	38.16	6.97	50	723	805	7.3	16	72
	B-2	37.61	6.92	50	735	813	6.9	15	70

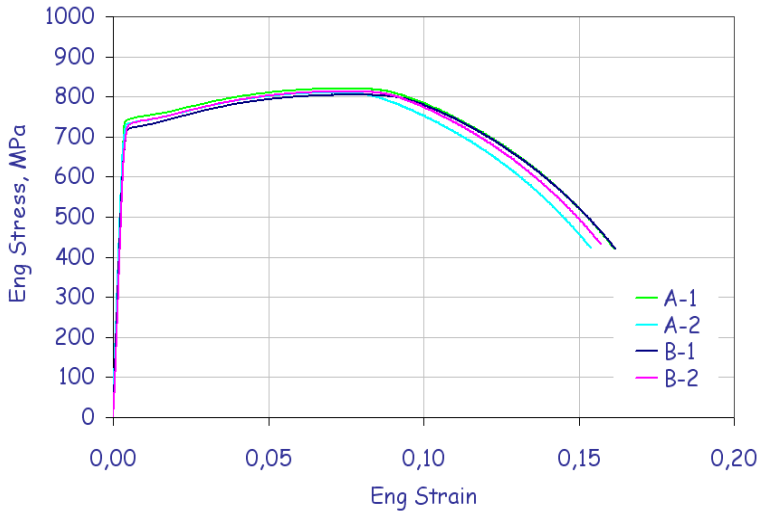

Figure 79. Room temperature tensile tests on CHS: engineering stress vs. engineering strain.

XIII.2.1.2. Cyclic tests

Five (5) cyclic tests each cross-section were performed on cylindrical specimens (6 mm in diameter) machined in longitudinal direction. Testing programme and loading specifications are reported in Table 5 where

ε_y the total strain (elastic + plastic) corresponding to $R_{p0.2}$ of the material

σ_{max} maximum stress of a stress controlled cyclic tests

σ_{min} minimum stress of a stress controlled cyclic tests

Table 24. Testing programme and loading conditions for material cyclic tests.

Cyclic test	**Strain/stress range**	**specimen ID**	
		Cross section A	**Cross section B**
Strain controlled cyclic tests	$\pm 2\ \varepsilon_y$	A-1	B-1
	$\pm 1.5\ \varepsilon_y$	A-2	B-2
Stress controlled cyclic tests	$\sigma_{max} = \sigma\ (2\ \varepsilon_y)$; $\sigma_{min} = 0$	A-3	B-3
	$\sigma_{max} = \sigma\ (2\ \varepsilon_y)$; $\sigma_{min} = -\ 0.4\ \sigma_{max}$	A-4	B-4
	$\sigma_{max} = \sigma\ (2\ \varepsilon_y)$; $\sigma_{min} = -\ 0.8\ \sigma_{max}$	A-5	B-5

Each cyclic test was continued up to 100 cycle were completed, no premature failure was recorded. Whole test data are available up to 30th cycle, after the 30th cycle 1 each 5 cycle performed was recorded. Results are summarized in Table 25 and

Table 26 for strain and stress controlled tests respectively where is it possible to evaluate material stress softening (Table 25) and strain stabilization (Table 26).

Table 25. Results of strain controlled cyclic tests. Strain controlled cyclic test B-1.

specimen ID	σ [MPa]		
	Cycle 0	Cycle 10	Cycle 30
A-1	+747 −741	+729 −739	+702 −716
B-1	+ 755 − 795	+750 −768	+722 −733
A-2	+716 −715	+691 −701	+675 −686
B-2	+760 −766	+732 −751	+709 −724

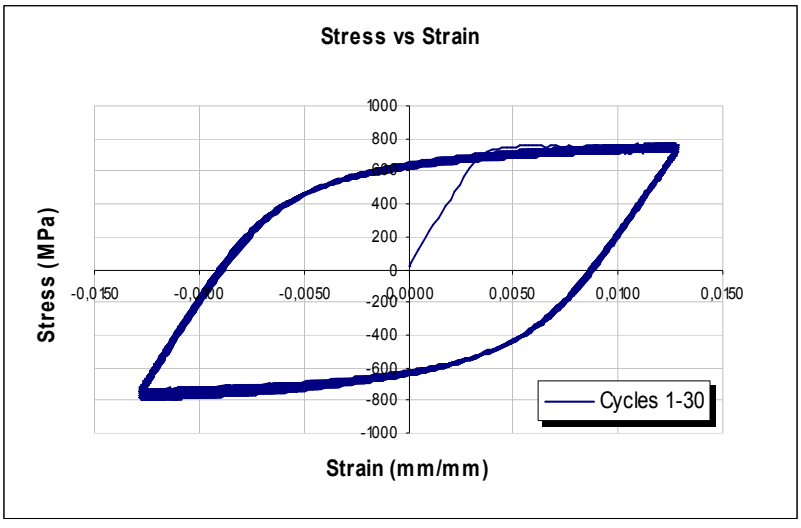

Table 26. Results of stress controlled cyclic tests. Stress controlled cyclic test B-4.

specimen ID	ε x 10^{-2}		
	Cycle 0	Cycle 10	Cycle 30
A-3	+1.08 +0.70	+1.15 +0.77	+1.19 +0.81
B-3	+1.31 +0.90	+1.37 +0.97	+1.40 +1.00
A-4	+1.08 +0.47	+1.20 +0.65	+1.28 +0.73
B-4	+0.31 +0.64	+1.41 +0.81	+1.46 +0.88
A-5	+1.05 +0.072	+1.38 +0.37	+1.87 +0.82
B-5	+1.46 +0.14	+2.01 +0.79	+3.32 +0.19

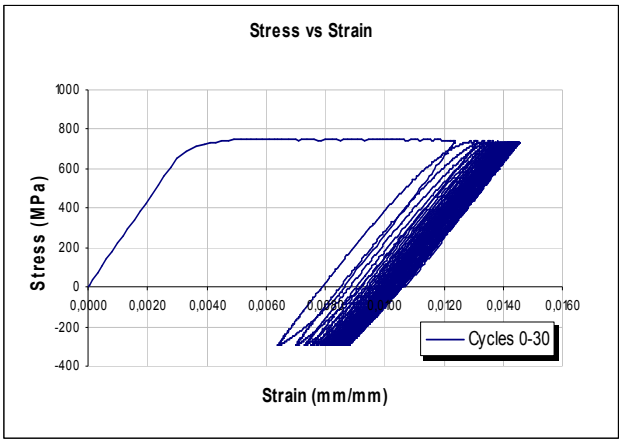

XIII.2.1.3. Residual stresses

Heat treated products as those under study are expected to show very low level of residual stresses (about 5-15% of yield stress).

As first attempt the *hole drilling* technique was applied to measure residual stresses. This technique is a semi-destructive one and measure via electrical strain gauges the evolution of residual strains relaxation while removing a little quantity of material by drilling. Four (4) measurements on each of the two (2) cross sections A and B were performed producing a total of 8 measuring points.

Since higher value than those expected have been measured (about 200MPa) extra investigations were planned. In particular:

- Material characterization to verify the effectiveness of tempering process (chemical composition, metallographic inspections, hardness and thoughness).
- Residual stress measurements applying another technique: the method of sectioning.

a. Material characterization

When substantial variation of residual stresses is expected it should be coupled with variation of metallurgical quantities as grain size and material hardness. Metallographic inspections and hardness HV10 measurements were performed in 4 different positions through each cross-section and 3 different depths each position. Moreover chemical composition and material toughness have performed. The data obtained shown no substantial variation of metallurgical quantities thorough thickness and in the different positions analyzed, that is in accordance with the heat treatment experienced by the material.

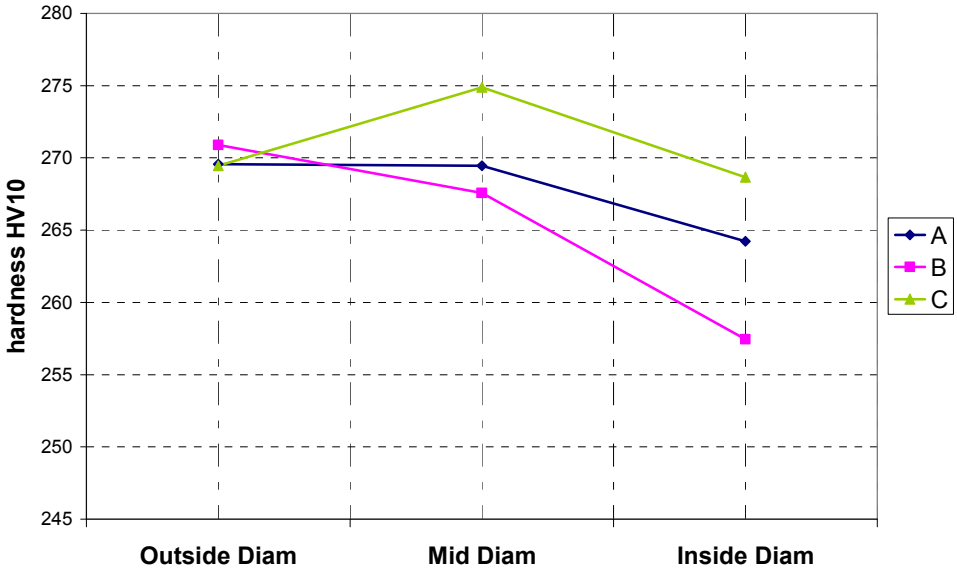

Figure 80. Hardness through thickness of three different CHSs.

Table 27. Impact test Charpy V.

Cross section-ID	Temp. [°C]	Energy [J]	Brittle area [%]
A-1	- 20	172	15
A-2	- 20	175	20
B-1	- 20	162	20
B-2	- 20	178	15
C-1	- 20	148	0
C-2	- 20	147	0

OD	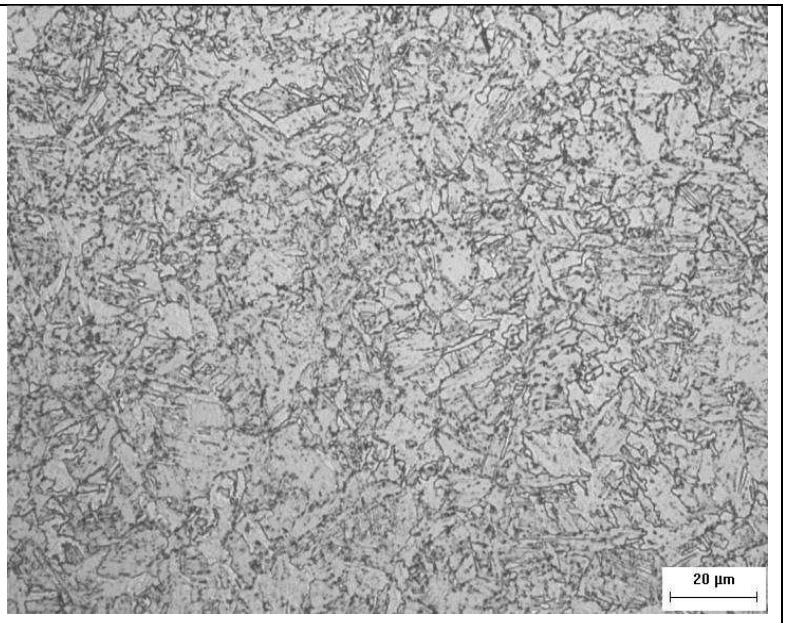
MD	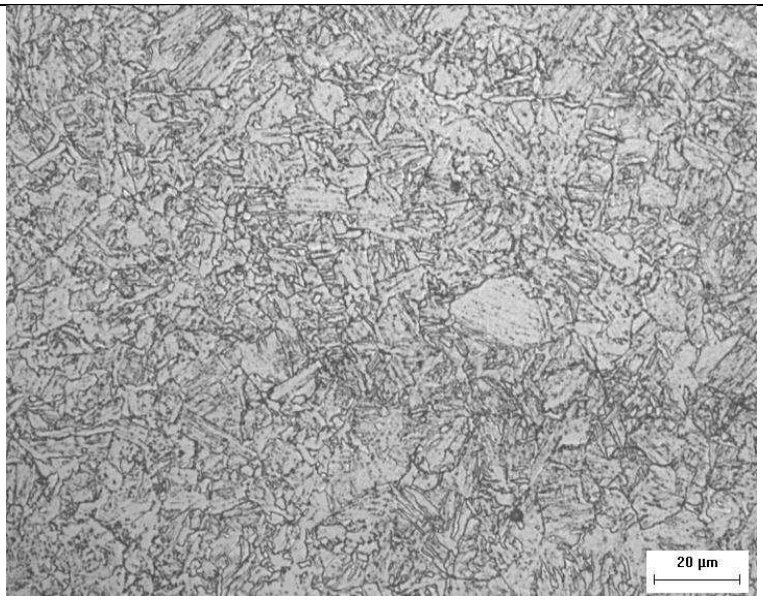
ID	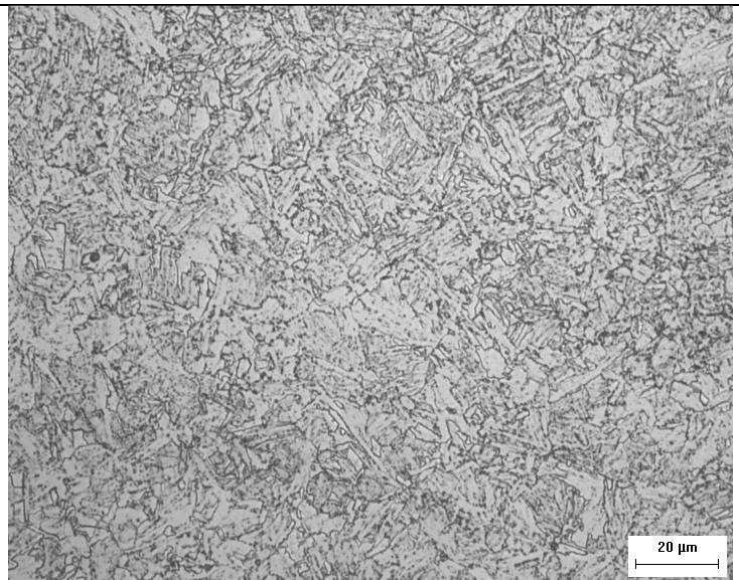

Figure 81. Microstructure analysis of CHS A (355 x 12 mm).

OD	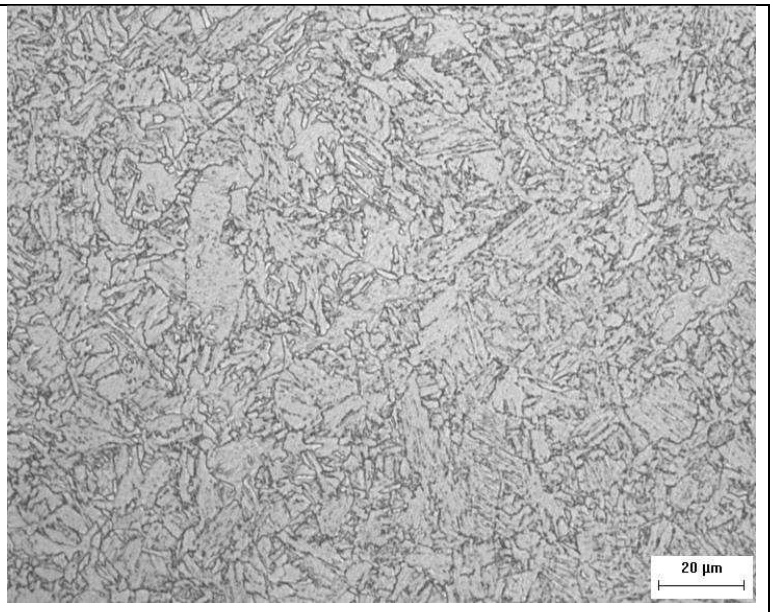
MD	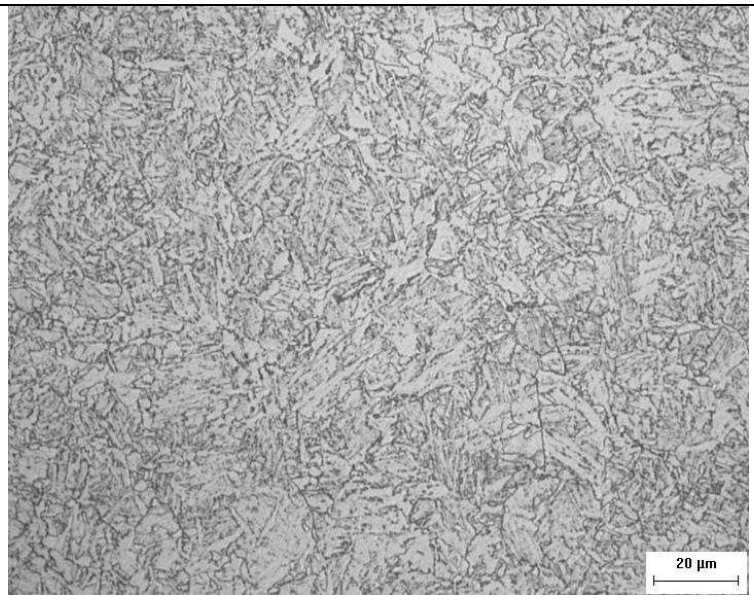
ID	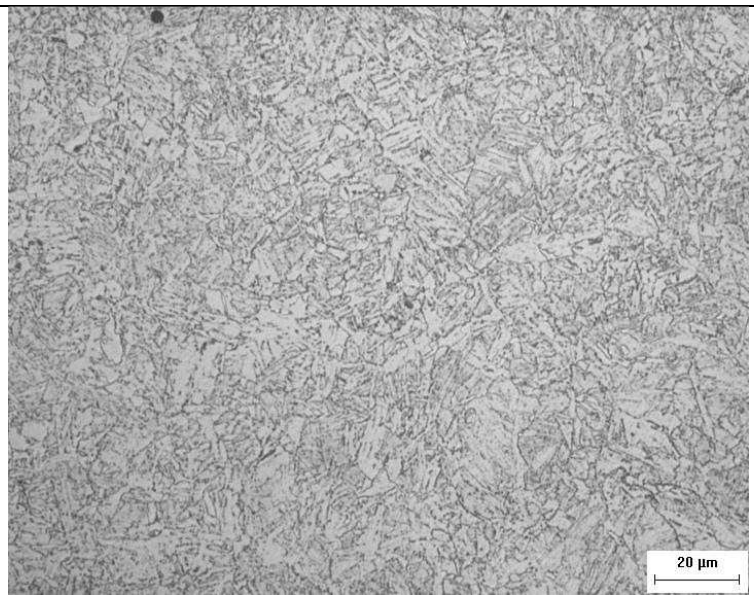

Figure 82. Microstructure analysis of CHS B (323.7 x 10 mm).

b. Sectioning method

The "sectioning method" 0 was selected by the Consortium for a deeper evaluation of longitudinal residual stresses. This method consists of the extraction of a cross-section and its sectioning in several strips. It is based on the principle that internal stresses are relieved by cold-cutting the specimen. The stress distribution over a cross section can be determined with reasonable accuracy by measuring the change in length of each strip and by applying Hooke's Law. Substantial variation through thickness of longitudinal residual stress is detected via measuring eventual deflection of strips after cutting. While historically the change in length of the strips was measured by means of mechanical extensometers recently the application of electrical strain gauges has proved its benefits 0 and the present application refers to the latter.

The sectioning method was applied on cross section A (Figure 83): a 2m long specimen was instrumented with electrical strain gauges on the external surface at mid span; allowing to the record of both longitudinal and transversal strains relaxation during sectioning. Test piece was extracted and subsequently sectioned by cold sawing (Figure 83) and data acquisition was continued during those operations.

Figure 83. Sectioning method: instrumented specimen before during and after sectioning.

Longitudinal residual stresses were measured on the external surface ($\sigma_{res,ext}$) and its distribution through cross section is reported in Figure 84. Longitudinal residual stresses are in the range of (-20 MPa ; + 63 MPa) in accordance with the heat treatment experienced by the products.

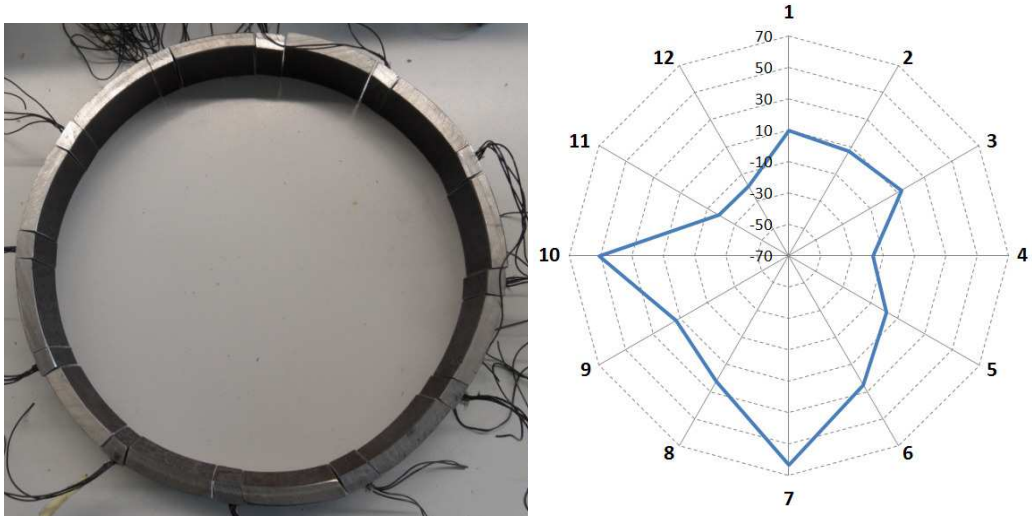

Figure 84. Sectioning method: cross section A after sectioning (left) and longitudinal residual stress distribution through cross section A (right) measured on the external surface.

Flexural displacements due to through thickness variation of residual stresses were evaluated by the application of the method of Anderson-Fahlman 0. It consists on cold cutting a longitudinal strip of appropriate length (l) and measuring its flexural deformation (f), bending residual stress (σ_b) being obtained by the formula:

$$\sigma_b = \frac{Etf}{l^2} \qquad \text{and} \qquad \sigma_{res,ext} = \sigma_b + \sigma_m$$

where:

$\sigma_{res,ext}$ is the residual stress measured on the external surface;

σ_m is the membrane component of residual stress;

σ_b is the bending component of residual stress;

E is the Young modulus of the material;

t is the CHS thickness;

l is the strip length;

f is the flexural deformation.

In the present case two (2) strips 800mm long were milled (Figure 85). On one of the two milled strips 15 MPa of bending residual stress (+ 15MPa on the external surface and – 15MPa on the internal surface) were measured while on the other strip no relevant flexural deformation was detected.

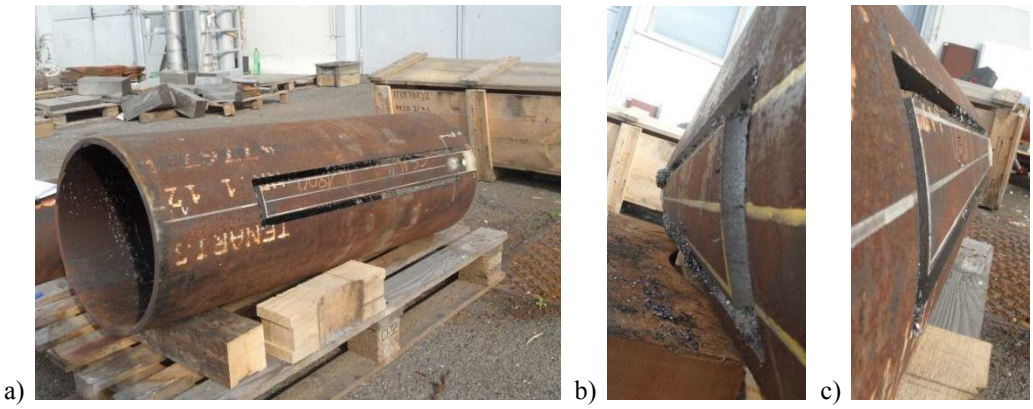

a) b) c)

Figure 85. Application of the method of Anderson-Fahlman: a) specimen; b) deflected strip; c) not deflected strip.

XIII.2.1.4. References (residual stresses)

[1] Guide to Stability design criteria for Metal Structures. Sixth Edition (2010) by Ronald D. Ziemian. Jhon Wiley & Sons, inc.

[2] E. de M. Batista, F.C. Rodriguez. Residual Stress Measurements on Cold-formed profiles. Experimental Techniques Vol. 16 No. 5 pp. 25-29. September/October 1992.

[3] Treuting, Wishart, Lynch and Richards. Residual stress measurements. American Society for Metals (1952).

XIII.2.2. Task 3.2 & 3.4 – Tests on beam-to-column joints and column-base joints

With regard to tests on beam-to-column joints and column-base joints, the loading protocols and the test set-up are here explained. The list of tests performed is reported in Table 28.

Table 28. Specimen nomenclature and test protocol

Number	Label	Test Protocol	Type of Specimen
1	BTCJE	ECCS-SAC	Beam-to-column Joint
2	BTCJR	RANDOM	Beam-to-column Joint
3	BTCJM	MONOTONIC	Beam-to-column Joint
4	CBJSTE	ECCS-SAC	Column-base joint designed for static loads
5	CBJSTR	RANDOM	Column-base joint designed for static loads
6	CBJSEE	ECCS-SAC	Column-base joint designed for seismic loads
7	CBJSER	RANDOM	Column-base joint designed for seismic loads
8	CBJINE	ECCS-SAC	Column-base joint with an improved s. design
9	CBJINR	RANDOM	Column-base joint with an improved s. design

XIII.2.2.1. Types of test

Cyclic and monotonic tests were performed on beam-to-column joints and column-base joints. In detail, the following tests were realized: i) monotonic tests; ii) cyclic tests according to the ECCS procedure (ECCS, 1986); iii) random tests. The aim of tests was to understand the global behaviour of joints and the activation of mechanisms in critical parts. Figure 86 shows the loading protocol applied to beam-to-column joints; the inputs of tests for column-base joints are similar and not shown for brevity.

a. Monotonic test

The monotonic test was realized in order to estimate the maximum force level and the maximum rotational capacity of the joint and the position of plastic hinges. Figure 86 shows the loading protocol applied; test was carried out in displacement control, on beam-to-column joint with maximum displacement imposed of about ±240mm.

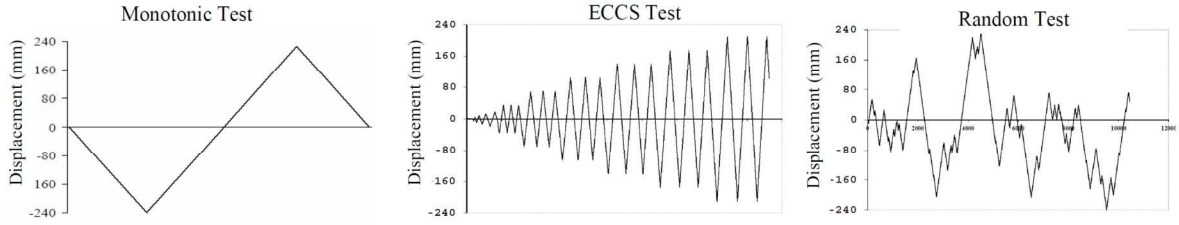

Figure 86. Loading protocols relevant to tested beam-to-column joints

b. Cyclic test

Cyclic tests were performed in order to evaluate the hysteretic behaviour of joints, the degradation of strength and stiffness with the increasing of damage level as well as the rotational capacity under cyclic loadings. The cyclic test was realized according to the ECCS stepwise increasing amplitude loading protocol (ECCS, 1986), modified with the SAC procedure (Karl et al., 1997). The stepwise was evaluated considering an interstory drift angle equal to 5 mrad, in order to evaluate the benchmark displacement $e_y = 0.005h$, where h is the storey height equal to 3.5 m. The loading protocol was divided into the two following parts:

- one cycle in the intervals:
  $e_y^+/4, e_y^-/4; 2, e_y^+/4, 2e_y^-/4; 3e_y^+/4, 3e_y^-/4; e_y^+, e_y^-$
- three cycles in the intervals:
  $2e_y^+, 2e_y^-; 4e_y^+, 4e_y^-; ...; (2+2n)e_y^+, (2+2n)e_y^-$ with $n = 1,2,3,...$

The maximum displacement reached in the test on beam-to-column joint was $12e_y$ equal about to ± 210mm, corresponding to the available stroke of the actuator. Conversely, in the case of column-base

joints it was possible to reach a displacement of $\pm 16e_y$ equal to about ±140mm, due to height of specimens, which is equal to half height of the beam-to-column specimen.

c. Random test

The aim of random tests was the characterization of the actual behaviour and performance of joints under seismic loading. The random tests were performed using as input the interstorey drift provided by the non-linear structural analysis of the 2D frame developed in WP2. The 2D frame was subjected to seismic loading by means of a far field spectrum-compatible accelerogram, in agreement with the EN1998-1 (2005). The value of the peak ground acceleration was increased about to 1,8g, to obtain the displacements in loading protocol comparable to that maximum recorded during the ECCS test. The response of the 2D frame was scaled in time to obtain quasi-static cyclic tests.
Figure 66 shows the 2D frame used to evaluate the loading protocol of the random test by non-linear analysis, considering two plastic hinges in parallel located at beam ends. In detail, the displacement at the middle height of the first story column depicts the input for tests on column-base joints.

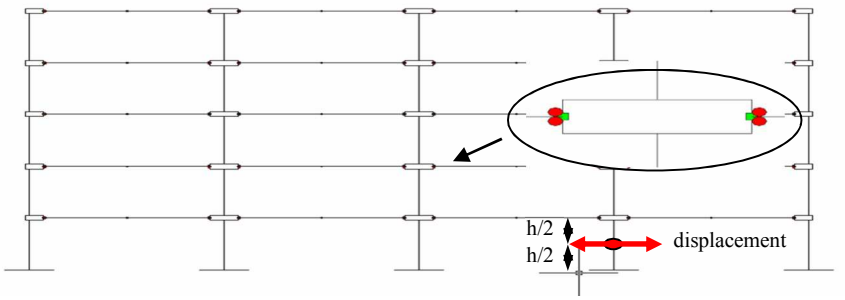

Figure 87. Moment resisting frame model used to evaluate loading protocol for the random test

XIII.2.2.2. Beam-to-column Joint

The instruments used and the correct position is fundamental in order to better understand the behaviour of joints. Briefly the instruments used during the tests and theirs position are showed below.

a. Test equipment

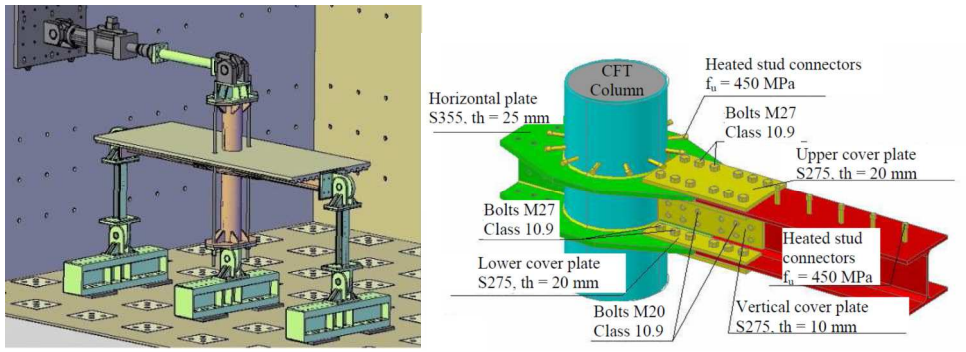

Figure 88. Test set-up and geometry of beam-to-column joints

- Seika Inclinometers that survey the distortion of the joint and the rotations between beam and column.

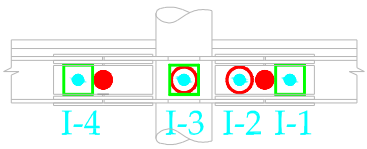

Evaluation of the rotation of the joint and verification of the assumption of rigid joint;

Evaluation of the rotations in plastic hinges;

Plastic hinge

Figure 89. Beam-to-column joint: inclinometers

- Linear Voltage Displacement Transducers (LVDTs) on the steel beam, that survey the displacement between column and slab, beam and slab and the distortion of the joint.

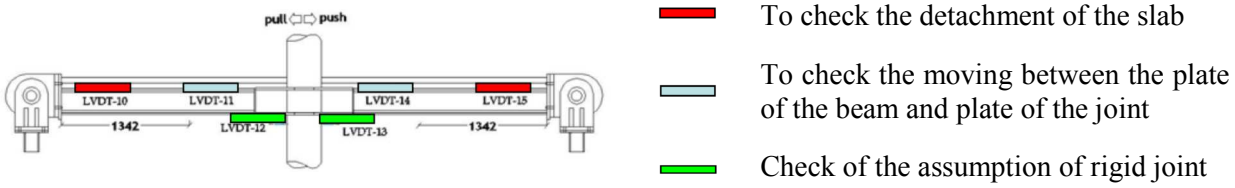

Figure 90. Beam-to-column joint: linear voltage displacement transducers LVDT

- Linear Voltage Displacement Transducers (LVDTs) and Ω Strain Gauges on the concrete slab.

Figure 91. Beam-to-column joint: linear voltage displacement transducers LVDT and Ω strain gauges

- Strain Gauges in the flanges of the beam and in the plates of a joint are showed in Figure 92. They survey the deformation of the steel elements of the composite beams in the zone of the plastic hinges in order: i) to evaluate the strain in the flange of the beam in the plastic zone and in the horizontal plates of the joint; ii) to evaluate the position of the neutral axis.
- Strain Gauges on reinforcement bars (push) as showed in Figure 92, that survey the deformation of the rebars into the slab for the monitoring of the activation of the compression transfer mechanism from the concrete slab into the column. In detail, to observe : i) the yield of the reinforcement bars; ii) the development of the compression transfer mechanism Type 1 and Type 2 in agreement with EN 1998-1 (2005).

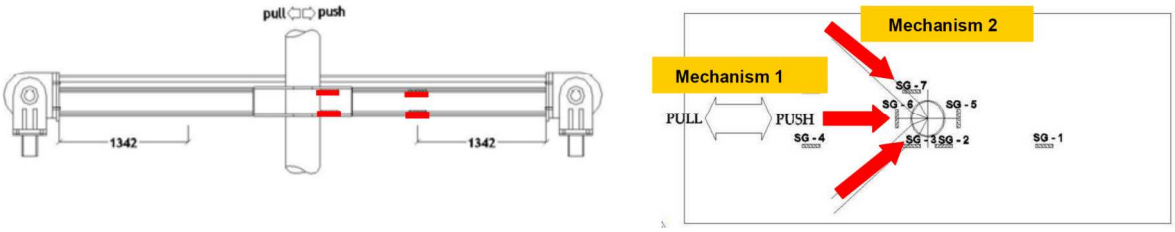

Figure 92. Beam-to-column joint: strain gauges

b. Classification of the beam-to-column joint

In agreement with EN1998-3-8 (2005) the joint is characterized by a connections of Category B where the slip does not occur at the serviceability state and the ultimate shear resistance of the connection is assured by the shear bolt resistance. The plastic hinges in agreement with the design were formed in weak section between the beam ends and the horizontal plates welded at the column. The value of the moment of the plastic hinges is correlated to the slip resistance of the connection. The overstrength of the joint was evaluated considering: i) the moment in the section of the plastic hinge, weak section; ii) the minimum moment resistance of the joint considering a pure steel section with concrete cracked. The minimum overstrength factor of the joint is higher than the value requested to cope with the capacity design rule to assure the overstrength of the joint with respect to the beam, as showed in Figure 93.

$$R_d \geq 1{,}1\gamma_{ov} R_{fy} = 1{,}1 \cdot 1{,}25 \cdot R_{fy} = 1{,}375 \cdot R_{fy} \Rightarrow \frac{R_d}{R_{fy}} \geq 1{,}375$$

$$\frac{M^{+}_{R4}}{M^{+}_{R2}} = \frac{1425\ ,79}{796\ .14} = 1{,}791 \geq 1{,}375$$

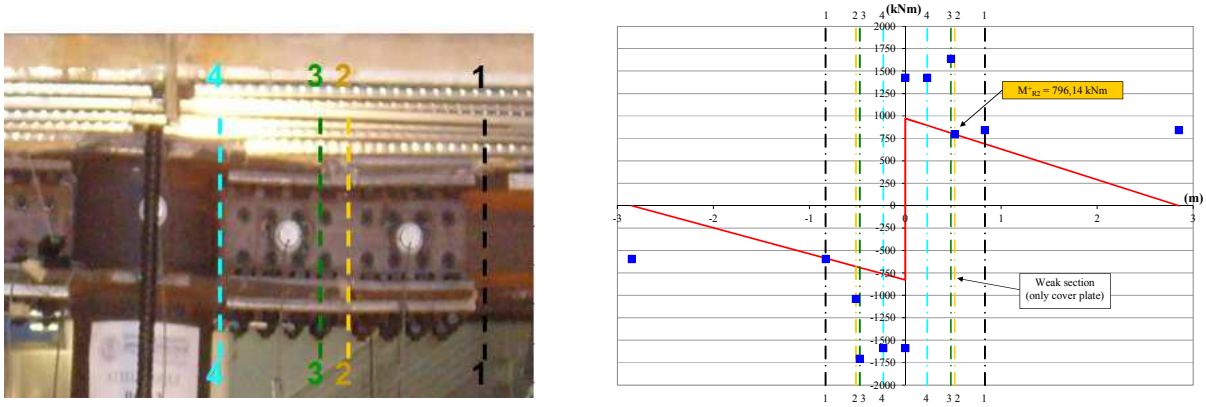

Figure 93. Overstrength of Beam-to-column joint

In agreement with EN1998-3-8 (2005), the beam-to-column joint can be classified as rigid, as show in Figure 94, if the mean value of the beam stiffness is higher than 10 per cent of that of relevant columns for each floor.

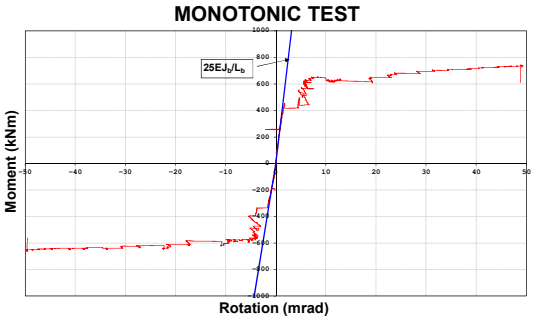

Figure 94. Classification of joint by stiffness

XIII.2.2.3. Column-base Joint

The instruments used and their correct position is fundamental in order to better understand the behaviour of joints. Briefly the instruments used during the tests and their locations are showed below.

a. Test equipment

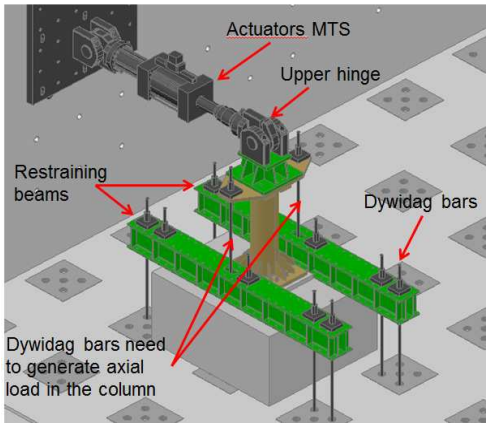

a)

Figure 95. Test set-up of column-base joint

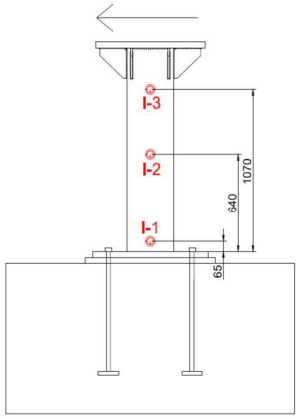

b)

Figure 96. Inclinometers on column-base joint

- Seika Inclinometers, as showed in Figure 96, were used to monitor the flexural deformation of columns and the position of plastic hinges.
- Linear Voltage Displacement Transducers (LVDTs), as shown in Figure 97, were used to monitor the elongation both of anchor bolts and of base plates;

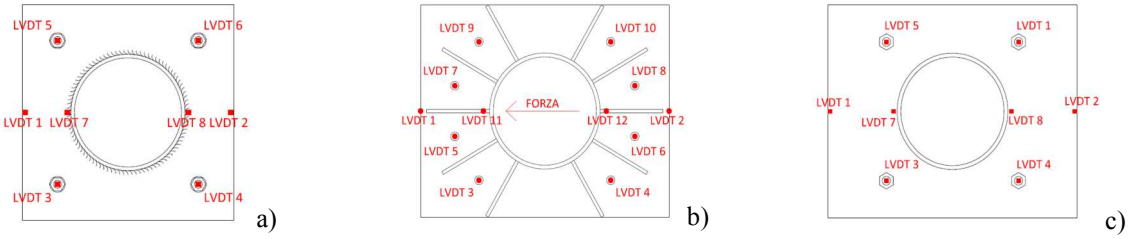

Figure 97. LVDT on Column-base: a) joint designed for static loads; b) standard solution of joint designed for seismic loading c) improvement solution designed for seismic loading

- Strain Gauges have been glued on base plates to monitor their deformation.

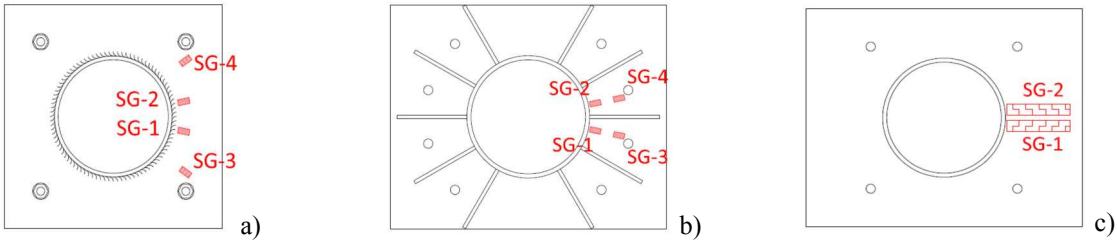

Figure 98. Strain Gauges on the base plates of Column-base joint: a) joint designed for static loads; b) standard solution of joint designed for seismic loads c) improvement solution designed for seismic loading

- Strain Gauges welded on the reinforcing bars within the column, they have the function to record the deformation of these bars during testing.

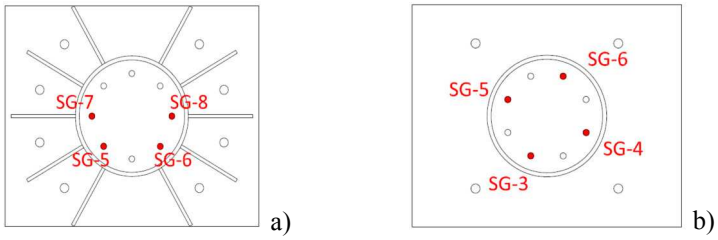

Figure 99. Strain Gauges on re-bars in the column designed for seismic loading: a) standard solution c) improvement solution

- Linear strain gauges were positioned, as shown in Figure 6, on the rebars in the concrete foundations of the innovative seismic column- base joints in order to take into account the activation of the strut&tie mechanisms descripted in WP5.

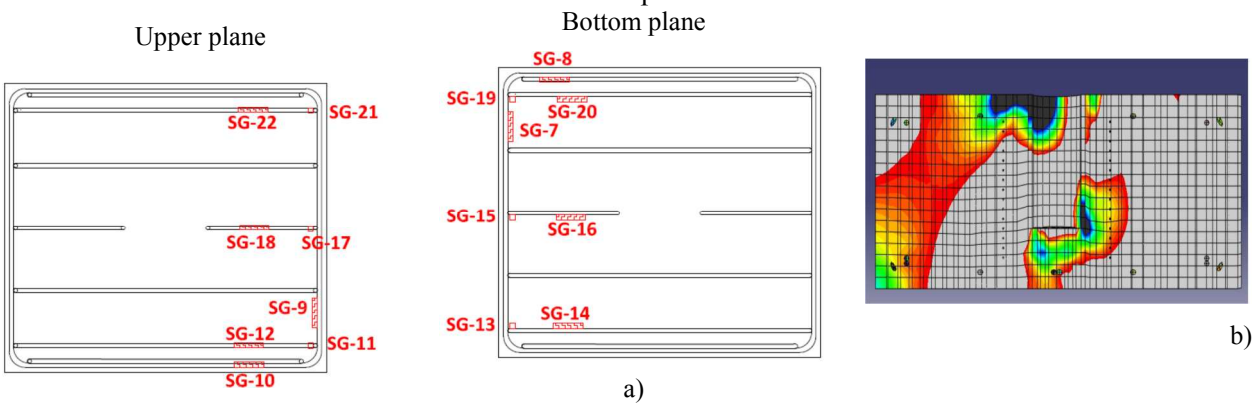

Figure 100. Innovative solution of joint designed for seismic loading: a) strain gauges position inside the plinth; b) distribution of compressive principal stresses

b. Classification of column-base joints

With reference to column-base joints there is not a classification of the stiffness of the joint. In fact, column base joints subject to seismic action have to be designed to full rigid and full strength. In othert European projects, it was observed that both the strength and stiffness of the standard solution depends

of the behaviour of grout and anchor bolts. It is difficult to obtain a rigid and full strength joint. In order to show this, it possible to compare the actual resisting moment of the CFT column with the moment recorder during the test in the plastic hinge. We obtained that: i) the standard solution is not over strength with respect to the column owing to grout cracking and anchor bolt elongation; ii) the innovative solution it is overstrength with respect to the column, in agreement with design. Figure 101 shows the comparison between aformentioned moments.

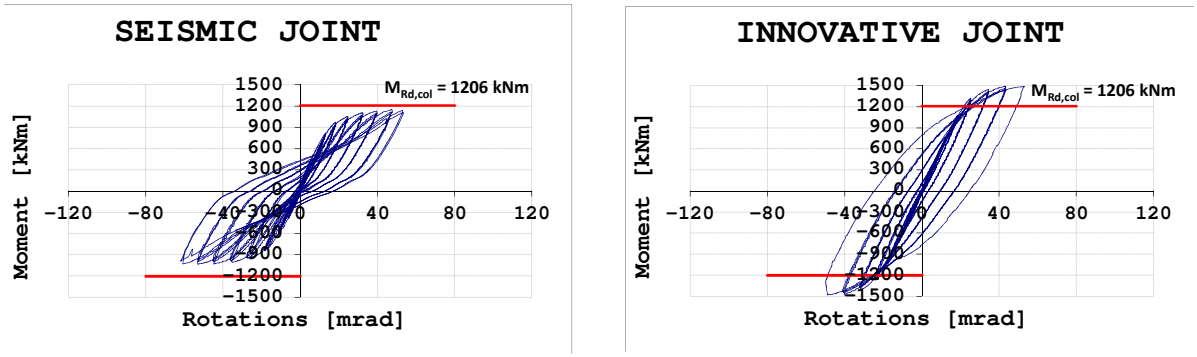

Figure 101. Moment-Rotation of Seismic and Innovative Column-base joints

XIII.2.2.4. References (beam-to-column joints and column-base joints)

Karl F., Helmut K., Robert S., (1997), "Protocol for fabrication, inspection, testing, and documentation of beam-column connection tests and other experimental specimens", Report No.SAC/BD-97/02, SAC joint Venture, Sacramento, California, U.S.A.

ECCS, (1986). "Recommended testing procedures for assessing the behaviour of structural steel elements under cyclic loads", ECCS Publication N.45.

EN1993-1-1 (2005). "Eurocode 3: Design of steel structures - Part 1-1: General rules and rules for buildings", CEN, Bruxelles.

EN1993-1-8 (2005). "Eurocode 3: Design of steel structures - Part 1-8: Design of joints", CEN, Bruxelles

EN1998-1 (2005). "Eurocode 8: Design of structures for earthquake resistance - Part 1-1: General rules and rules, seimic actions and rule for buildings ", CEN, Bruxelles.

XIII.2.3. Task 3.2 – Tests on components of column bases

To determine the bending behavior of the rectangular end plates of a tubular column under 4-point bending, three (3) specimens with plate thicknesses of t_{pl}=14, 16 and 18 mm were tested. The specimens were supported by a double-hinge 'roller' system with ball-joint hinges and the 4-point bending loading was applied to the brace through a steel cross-beam with a system of two special ball-joint hinges and appropriate wooden grips. The instrumentation setup consisted of wire position transducers and DCDT's for measuring load-point and support displacements, respectively, and inclinometers for measuring rotation of the tubes relative to the base (see Figure 102a). Strain gages were placed on the base plates at a distance of 25 mm to measure longitudinal and transverse strains starting at 5 mm away from the weld- toe (see Figure 102b).

Under monotonic loading, the specimens with the larger base plate thickness showed higher flexural resistance at the same flexural deformation (or base rotation) and lower deformation at the same applied bending moment than those with the smaller thickness, as expected. However, the flexural stiffness of the specimens, which is initially the same at about 3÷4 kNm/mm, is approximately constant in the yielding region of the plate at about 0.25 kNm/mm due to the same steel grade used, independently of the plate thickness (see Figure 103). However, the level of the resisted bending moment for each plate increased by about 25 kNm for a 2 mm increase in plate thickness from 14 to16 and 16 to18 mm. Failure occurred in the base plates due to large deformations, as shown in Figure 103. The longitudinal strains along line A and C changed sign from positive close to the weld-toe to negative towards the end of the plate (see Figure 105 and Figure 106) causing reverse curvature in both sections A and C, with an inflection point at a distance of about 35 mm from the plate edge (more or less the line which connects the outside edge of the washers used for the bolts). On the other hand, tensile strains were measured in

the transverse direction of line A (vertical section of plate) and C (horizontal section) with much larger values at the end of the plate than close to the weld-toe, causing 2 to 3 times higher transverse curvature along the vertical section than that in the horizontal section of the plate (axis of applied moment), as shown in Figure 103.

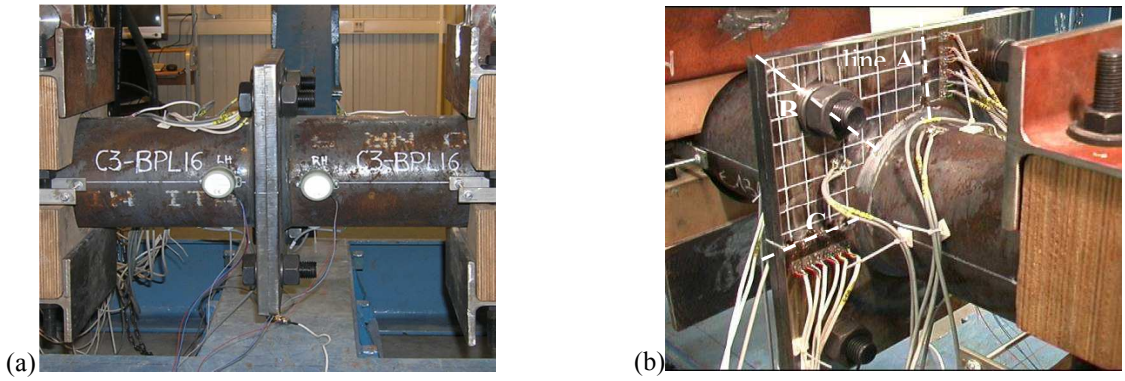

Figure 102. Component 3 base plate instrumentation measuring: (a) base rotation, (b) strain along lines A, B and C.

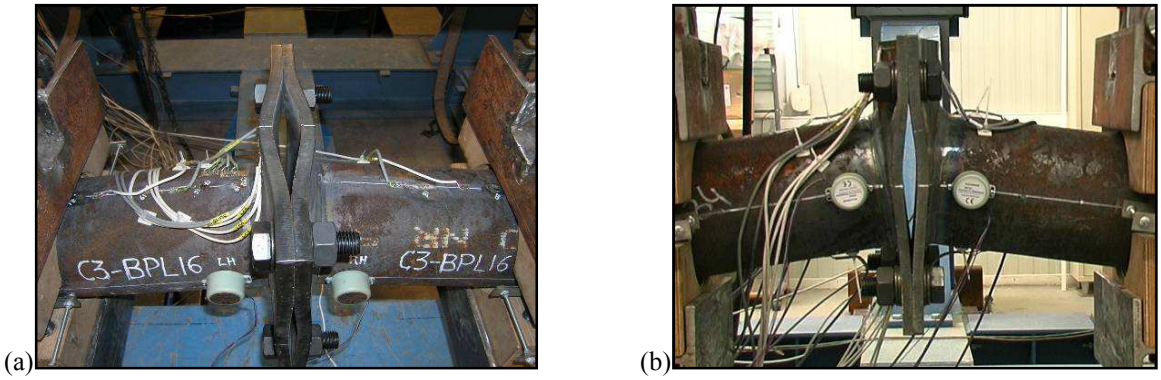

Figure 103. Base plate deformation: (a) top view, (b) side view.

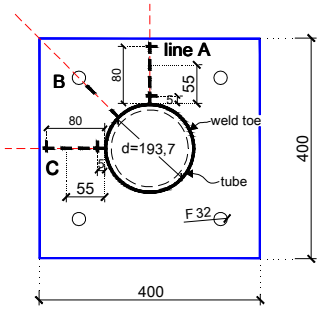

Figure 104. Strain gage instrumentation for base plate.

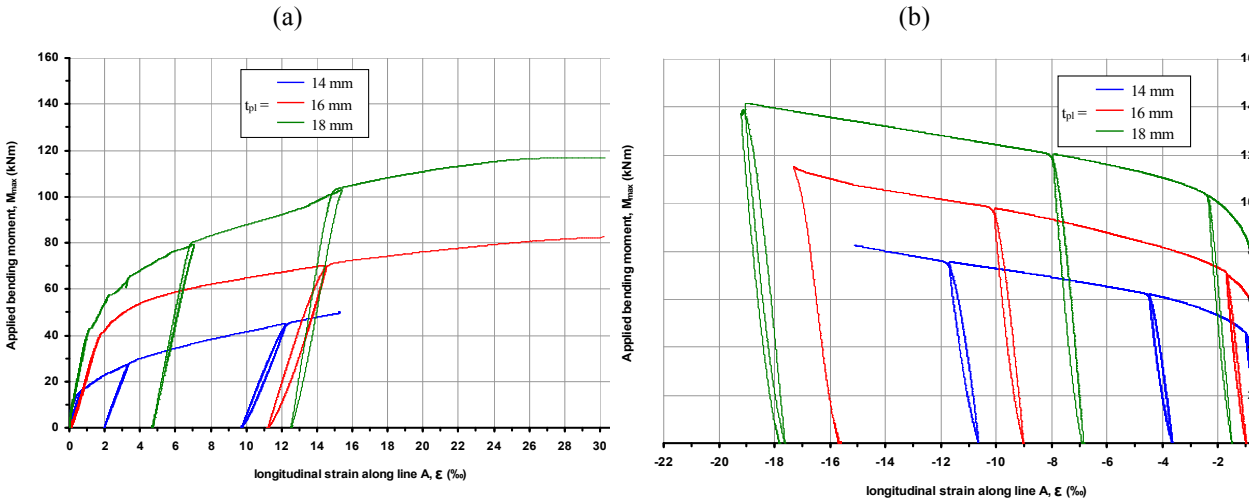

Figure 105. Applied bending moment vs. base-plate strains along line A for each plate thickness, tpl: (a) 5 mm away from the weld-toe, (b) 80 mm away from the weld-toe.

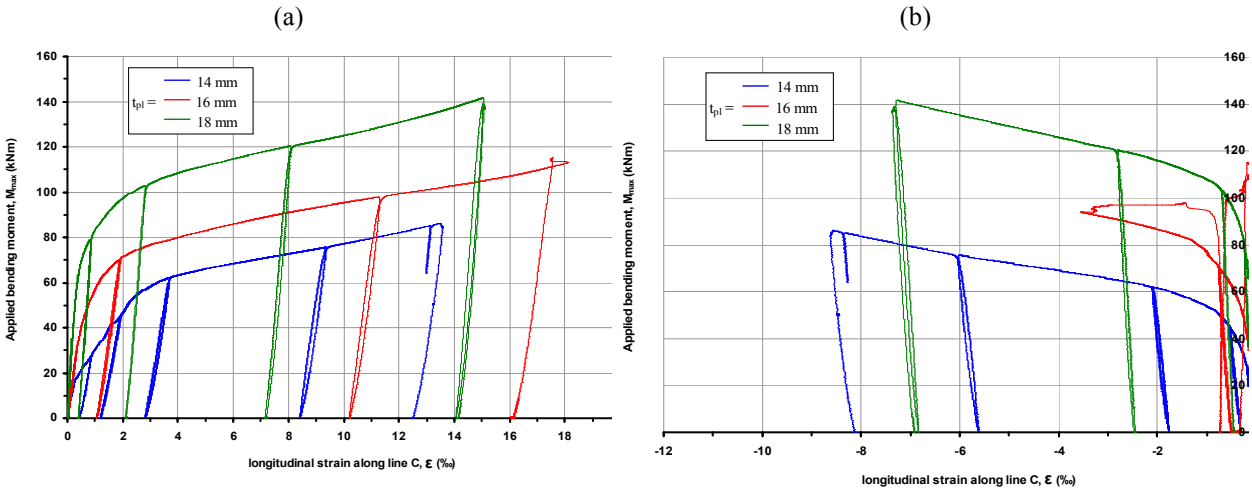

Figure 106. Applied bending moment vs. base-plate strains along line C for each plate thickness, tpl : (a) 5 mm away from the weld-toe, (b) 80 mm away from the weld-toe.

XIII.2.4. Task 3.4 – Tests on beam-to-column joint components

For the experimental study of the beam-to-column joints, eight (8) specimens were tested, four (4) to examine the behavior of concrete composite slabs (denoted as Component 1) under negative bending moment with the slab in tension and four (4) beam-column steel through-plate connections (denoted as Component 2) under compression.

For the Component 2 tests, the specimens were simply supported while the load was applied through an actuator which bolted to the top of the column tube. The instrumentation setup for this type of test consisted of wire position transducers to measure load-point displacements, DCDT's for measuring support displacements and a number of axial and biaxial strain gages which were attached to the through-plates (see Figure 107a) and column tube (see Figure 107b).

The specimens with the 120x10-, 120x12- and 100x12-mm through-plates under monotonic loading failed due to buckling of the through-plate inside the column tube (see Figure 108a). The flexural capacity of the three (3) specimens was similar at load point deflections values close enough. It seems that for the considered differences in plate height and thickness, the flexural response is very similar. The specimen with the thickest and shortest 100x15-mm through-plate failed due to lateral buckling of the plate outside the column tube (see Figure 108b) and exhibited about 17% higher flexural capacity than the other three specimens.

(a) 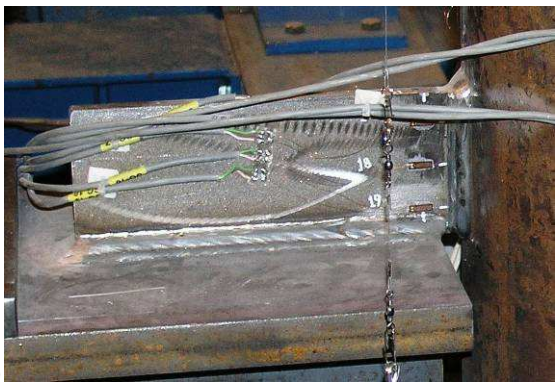 (b) 

Figure 107. Strain measurements for Component 2: (a) the through-plate and (b) the column tube.

(a) 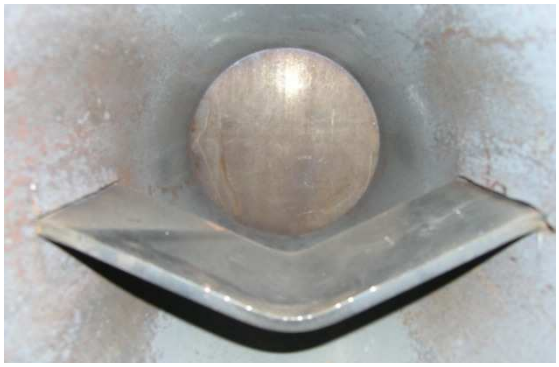 (b) 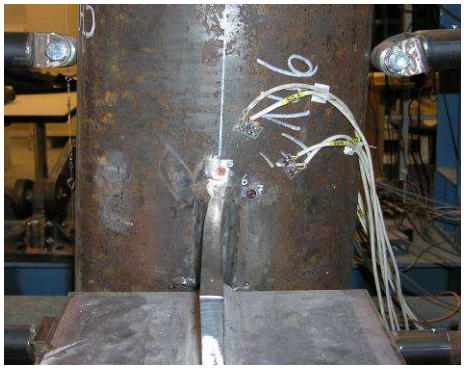

Figure 108. Failure of the through-plate: (a) buckling inside the column tube, (b) lateral buckling outside the tube.

XIII.3. Appendix of WP4 – Fire tests

XIII.3.1. Introduction

This appendix presents some main results within WP4-Fire tests:

- Results of the coupon tests;
- Fire resistances, displacement –time curves and failure modes of the fire tests on the structural elements.

More details of the results can be found in Deliverable D4.

XIII.3.2. Results of the coupon tests

The main results on the coupon tests (as yield and ultimate strength for steel, compression strength and humidity for concrete) are presented in Table 29 and Table 30 below. The names of the structural elements are given in Table 15. The coupon test results for the test on HSS at elevated temperatures are reported in Deliverable D4.

Table 29. Results of coupon tests on steel materials at normal temperature

N^0	**Structural elements**	**Specimen**	**Yield strength** (N/mm^2)	**Ultimate strength** (N/mm^2)
1	End plate of column base CB1 (25mm thickness)	1	353	509
2		2	352	505
3		3	353	514
4		4	356	507
5		5	333	505
6	Vertical plate of joint J1.1 or J1.2 (30mm thickness)	1	306	505
7		2	301	504
8		3	332	505
9		4	328	504
10	Horizontal plate of joint J1.1 or J1.2 (16 mm thickness)	1	408	550
11		2	415	563
12		3	404	560
13		4	402	553
14		5	413	564
15		6	405	557
16	Beam IPE 600 of joint J1.1 or J1.2	1	426	537
17		2	466	541
18		3	427	537
19		4	499	575
20		5	523	606
21		6	480	563
22	Bolts M36 in joint J1.1 or J1.2	1	1039	1095
23		2	1044	1107

Table 30. Results of tests on concrete materials

N°	**Structural elements**	**Specimen**	**Strength** (N/mm2)	**Humidity** (%)
1	Filled concrete of C4	1	68,4	5,16
2		2	64,4	
3	Slap of J1.1	1	56,2	4,21
4		2	53,8	
5	Slap of J1.2	1	65,3	-
6		2	64,0	
7	Slap of J2.1	1	72,2	4,09
8		2	74,8	
9	Slap of J2.2	1	70,2	4,37
10		2	77,0	
11	Foundation block of CB1	1	76,7	2,73
12		2	72,7	
13	Foundation block of CB2	1	78,0	4,23
14		2	76,9	
15	Foundation block of CB3	1	72,4	-
16		2	76,7	

XIII.3.3. Results of structural element tests

Table 31 summarizes the results of the fire tests on the structural elements: the fire resistances, the displacement-curves and the failure modes.

Table 31. Results of the fire tests on the structural elements

Test name	**Load (P in kN in** Figure 109**)**	**Starting of fire tests**(*) **(minute)**	**Time of fire tests (minute)**	**Location of displacement transducers**	**Dis.-time curves**	**Failure modes**
C1	700	33th	22	Figure 110	From Figure 111 to Figure 125	From Figure 126 to Figure 133
C2	1000	35th	20			
C3	1800	36th	21			
C4	2000	32th	108			
J1.1	220	37th	44			
J1.2	165	33th	52			
J2.1	130	28th	72			
J2.2	205	37th	55			
CB1	130	25th	37			
CB2	450	32th	81			
CB3	450	47th	87			
(*): used to know the moment of the starting of the fire tests on the displacement-time curves.						

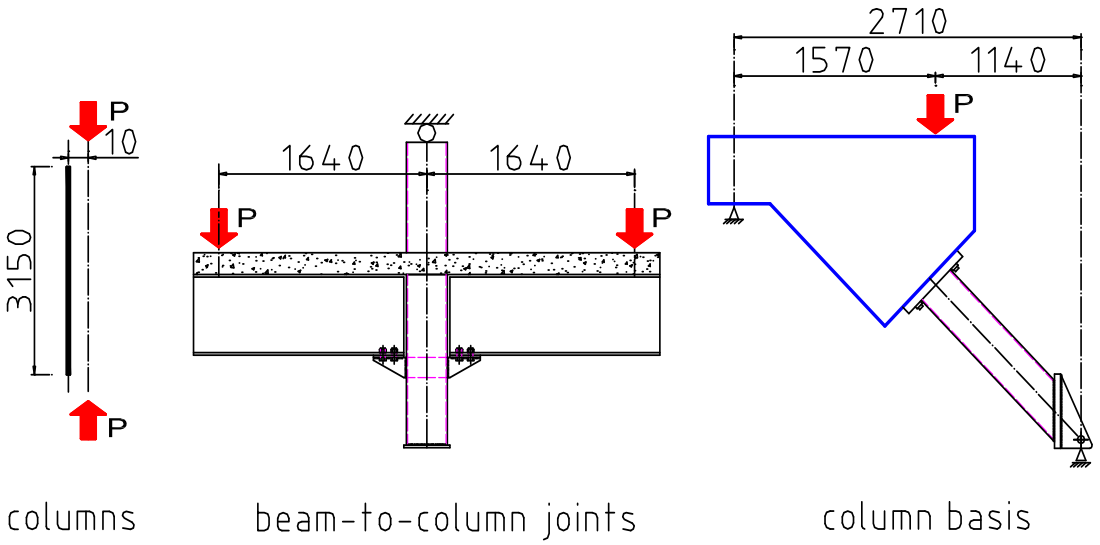

Figure 109. Location and direction of applied loads

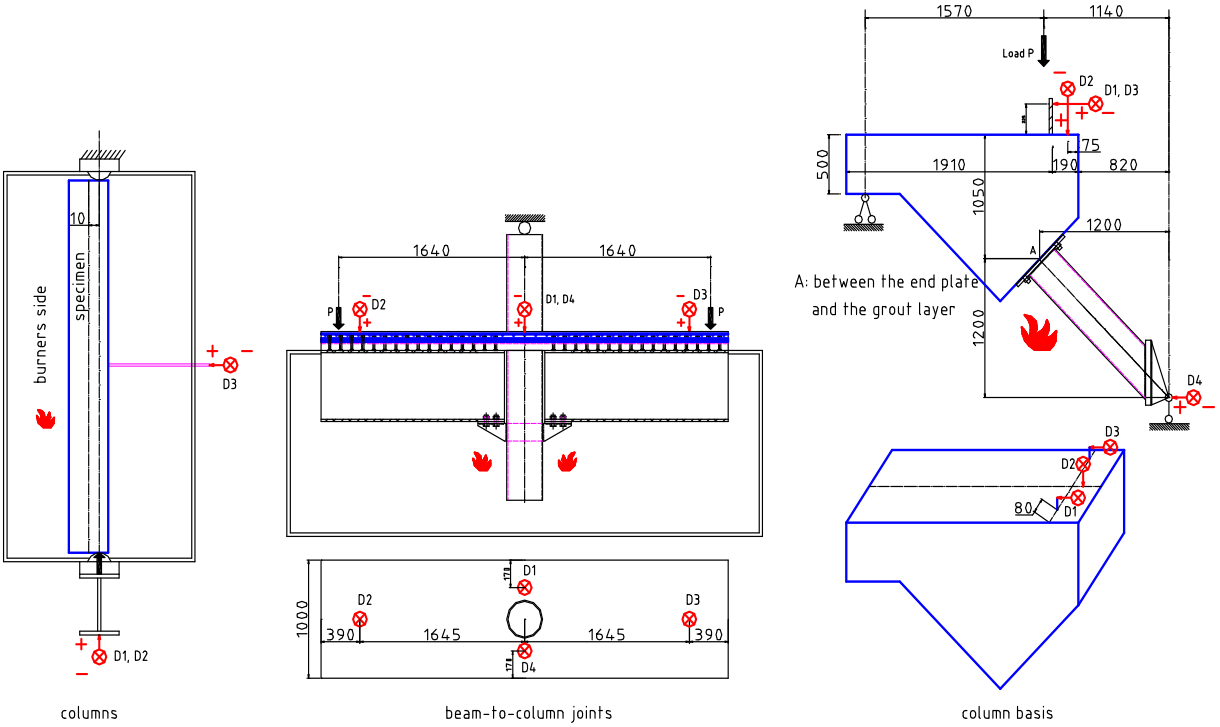

Figure 110. location of displacement transducers on the specimens

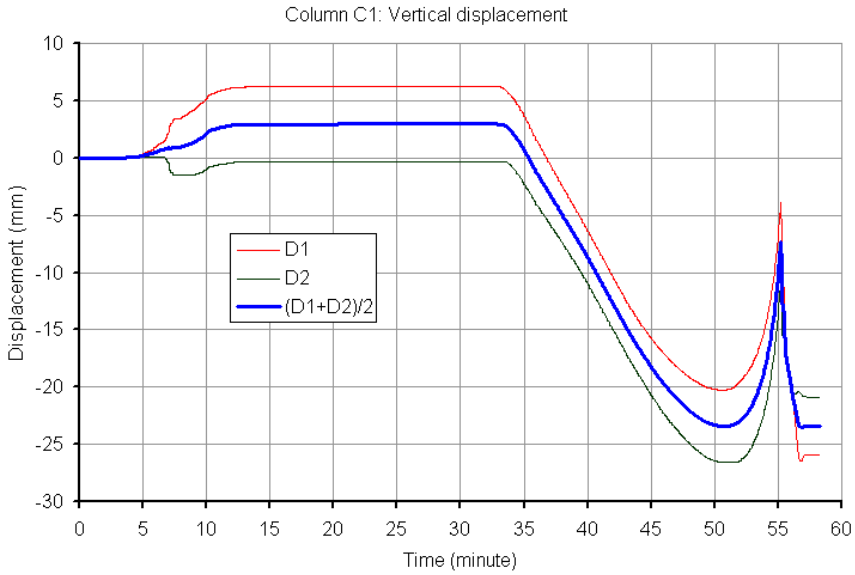

Figure 111. C1displacement-time curves (vertical displacement)

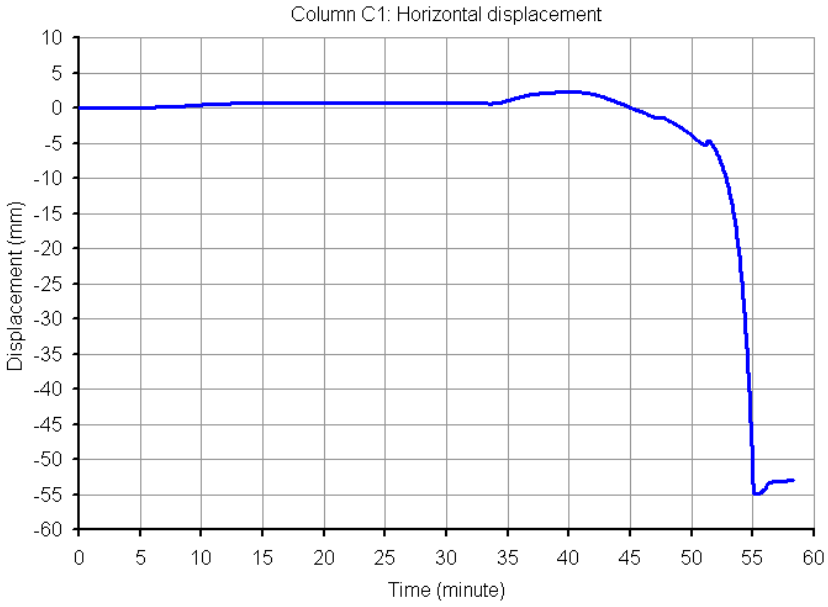

Figure 112. C1displacement-time curve (horizontal displacement)

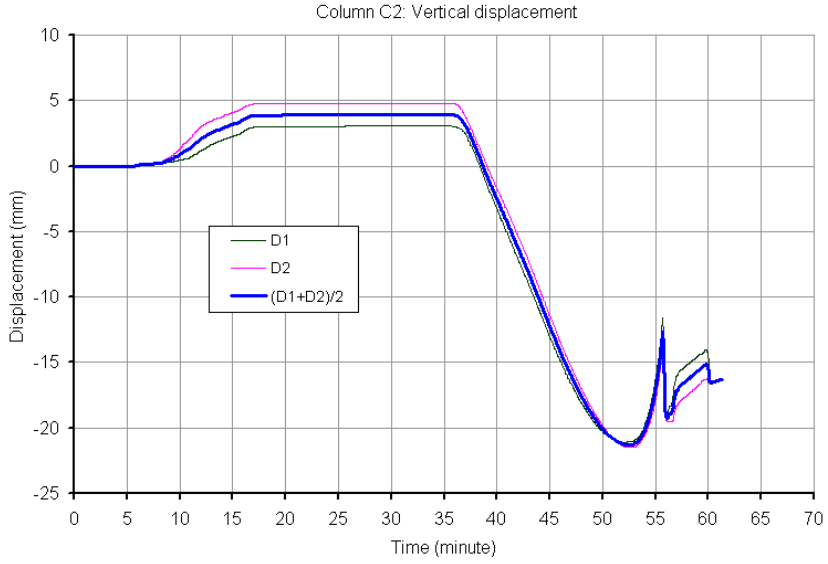

Figure 113. C2 displacement-time curves (vertical displacement)

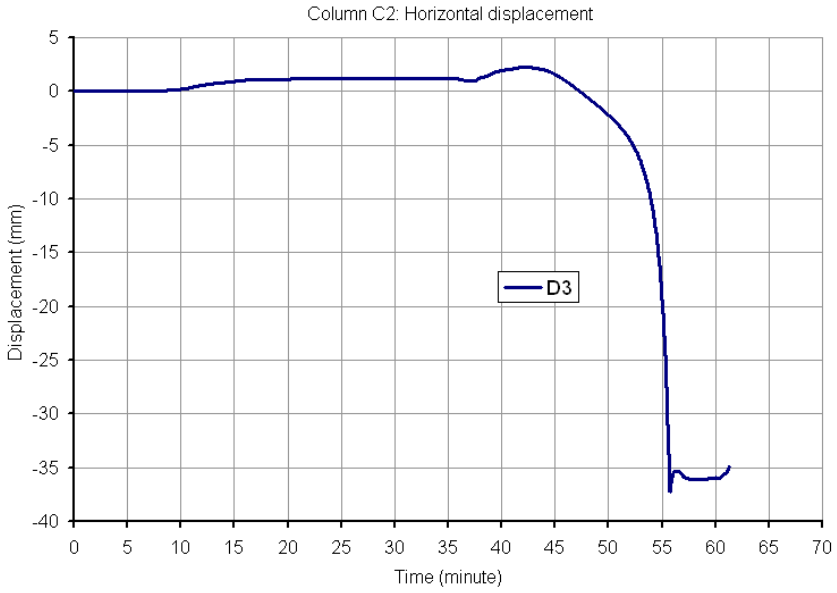

Figure 114. C2 displacement-time curve (horizontal displacement)

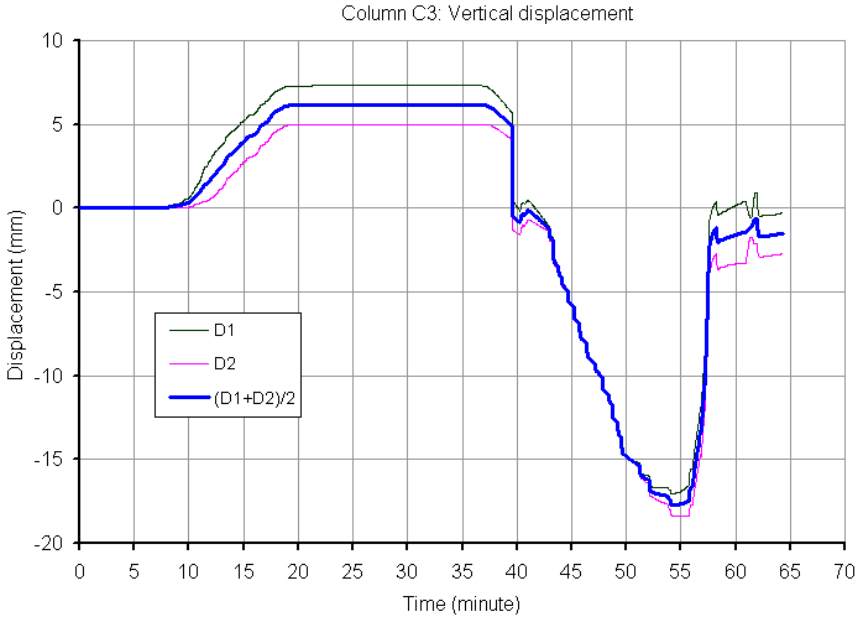

Figure 115. C3 displacement-time curves (vertical displacement)

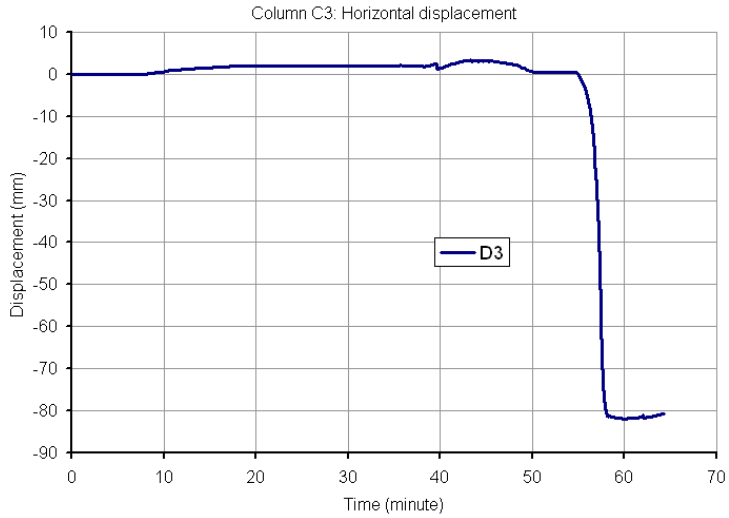

Figure 116. C3 displacement-time curve (horizontal displacement)

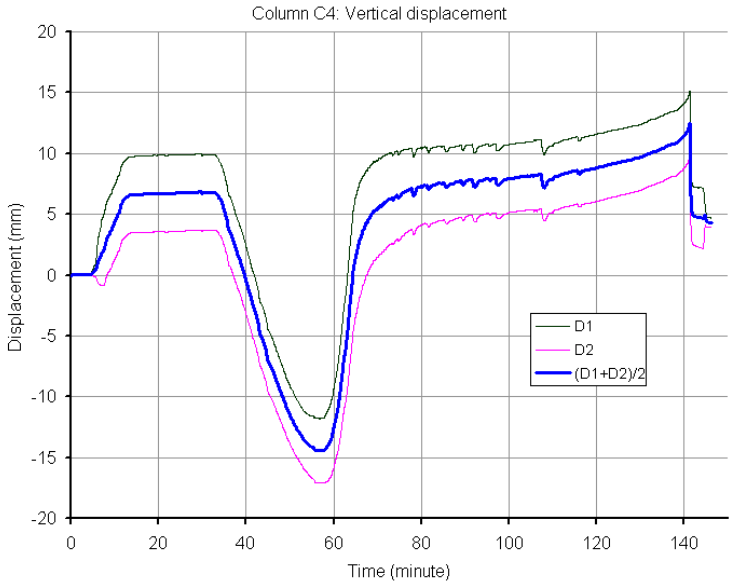

Figure 117. C4 displacement-time curves (vertical displacement)

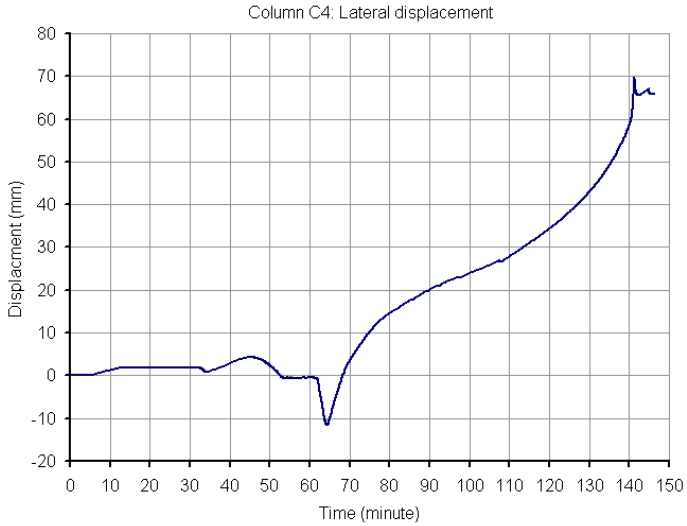

Figure 118. C4 displacement-time curve (horizontal displacement)

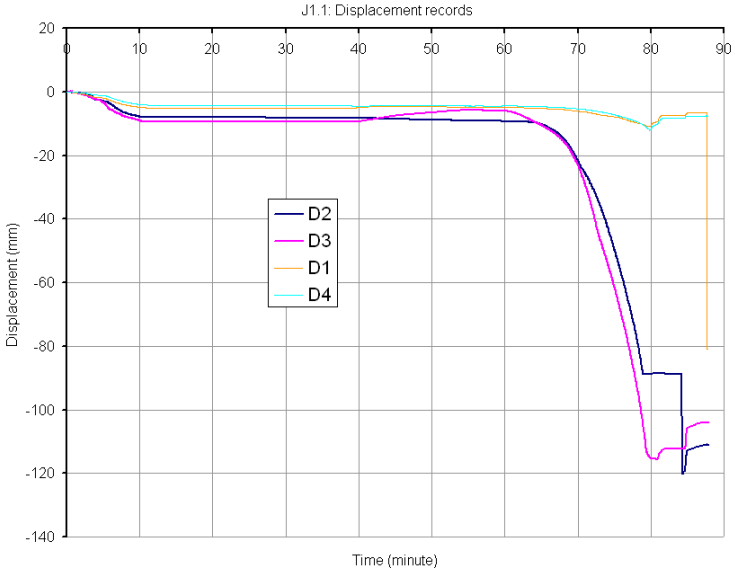

Figure 119. J1.1displacement-time curves

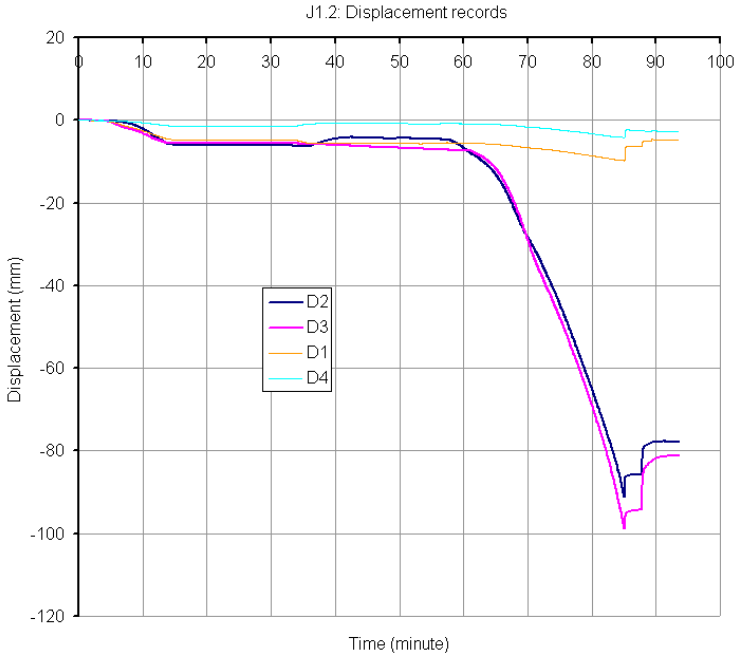

Figure 120. J1.2 displacement-time curves

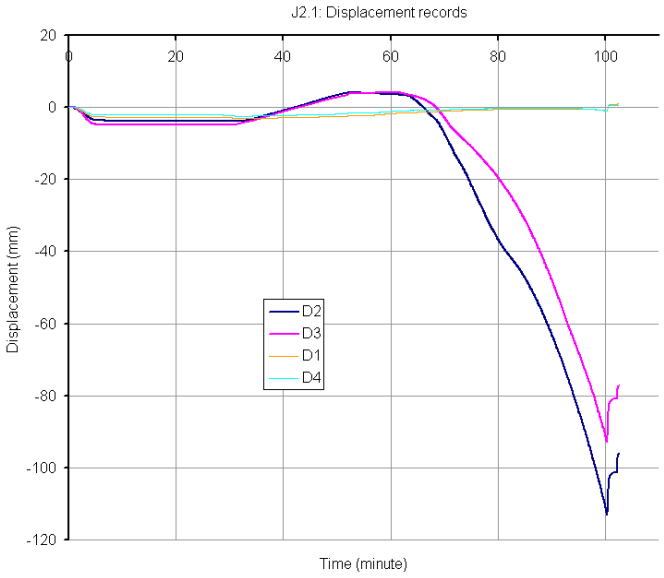

Figure 121. J2.1displacement-time curves

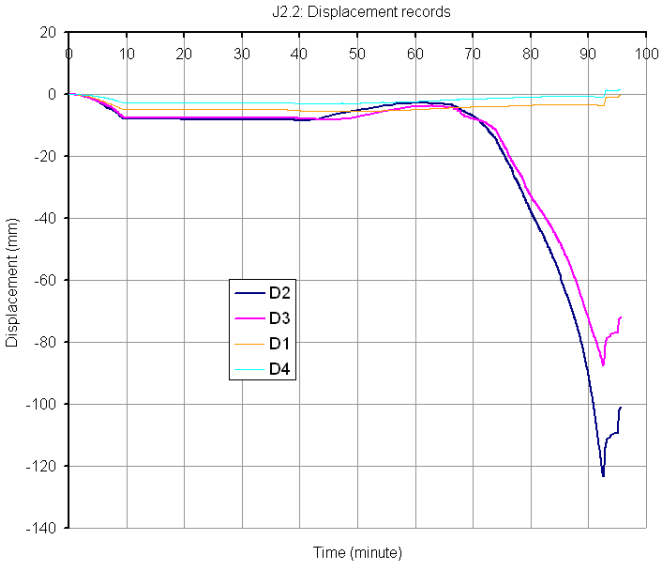

Figure 122. J2.2 displacement-time curves

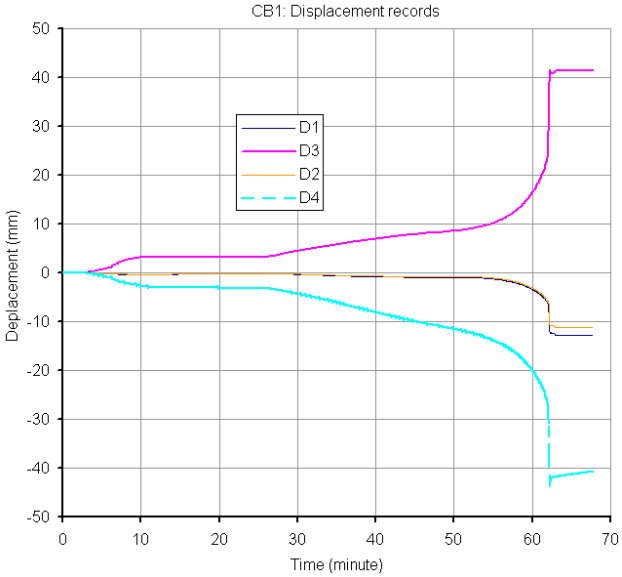

Figure 123. CB1 displacement-time curves

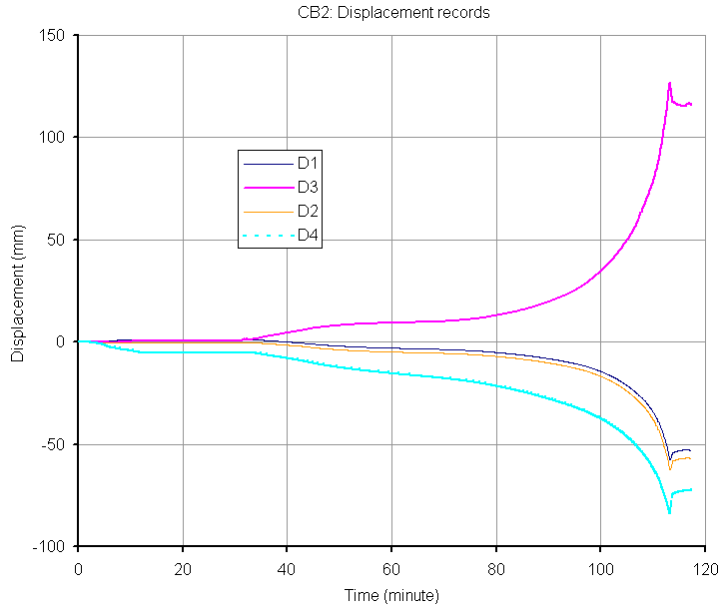

Figure 124. CB2 displacement-time curves

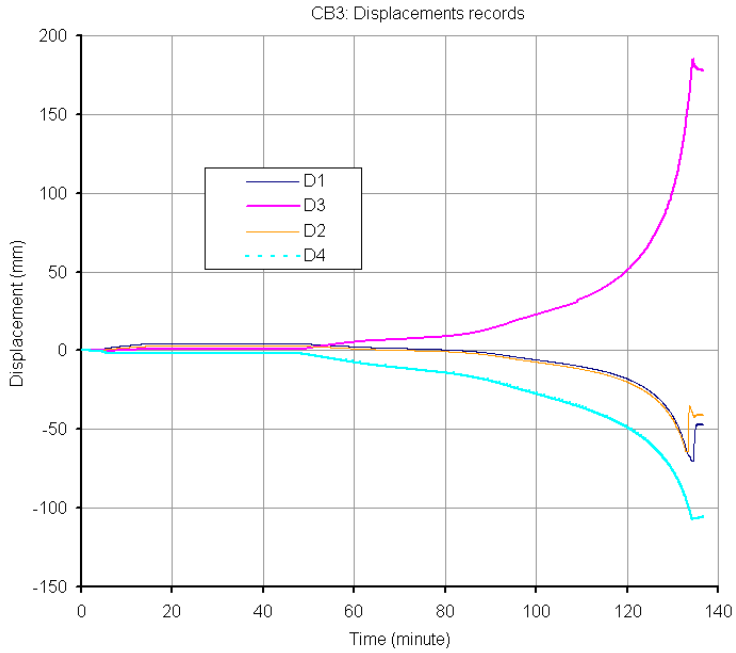

Figure 125. CB3 displacement-time curves

Figure 126. Columns C1, C2, C3 and C4 – failure modes

Figure 127. J1.1 and J1.2 failure mode (steel parts)

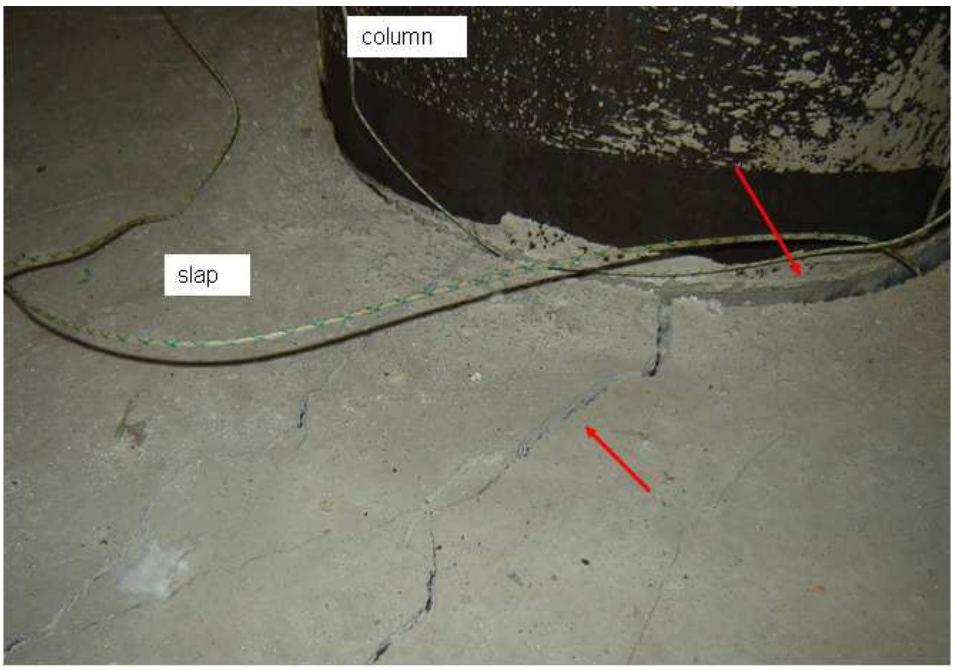

Figure 128. J1.1 and J1.2 failure mode (concrete slap)

Figure 129. J2.1 and J2.2 failure mode (steel parts)

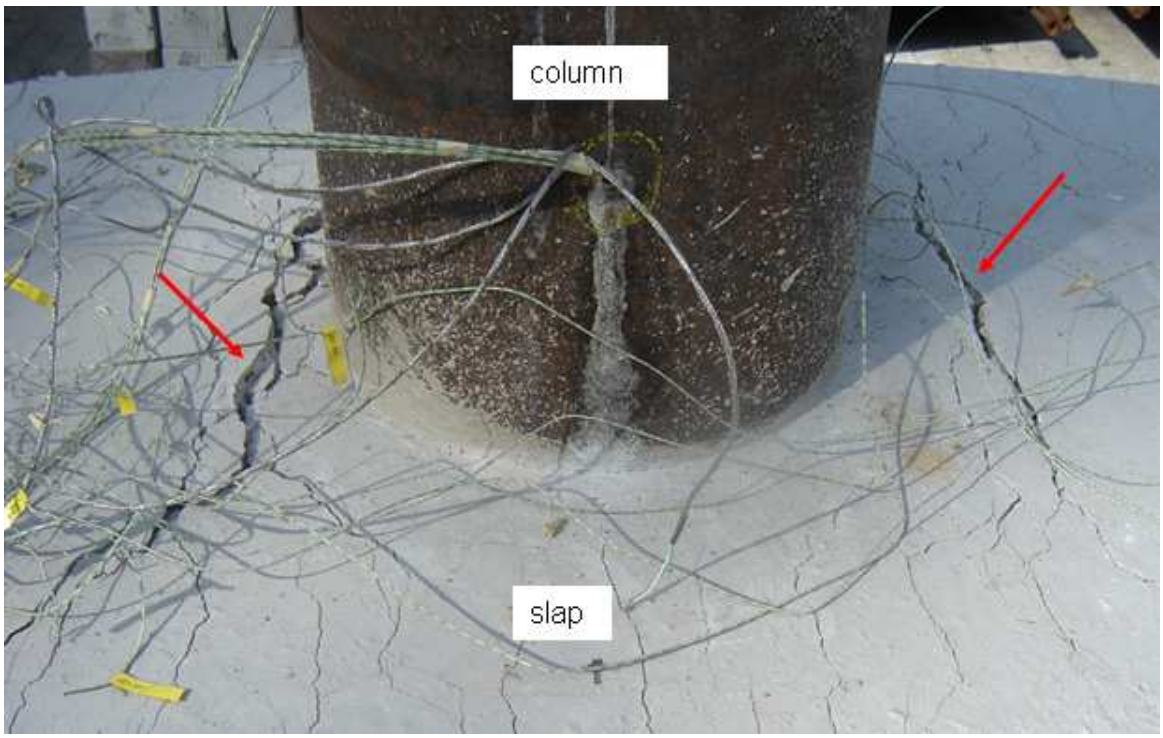

Figure 130. J2.1 and J2.2 failure mode (concrete slap)

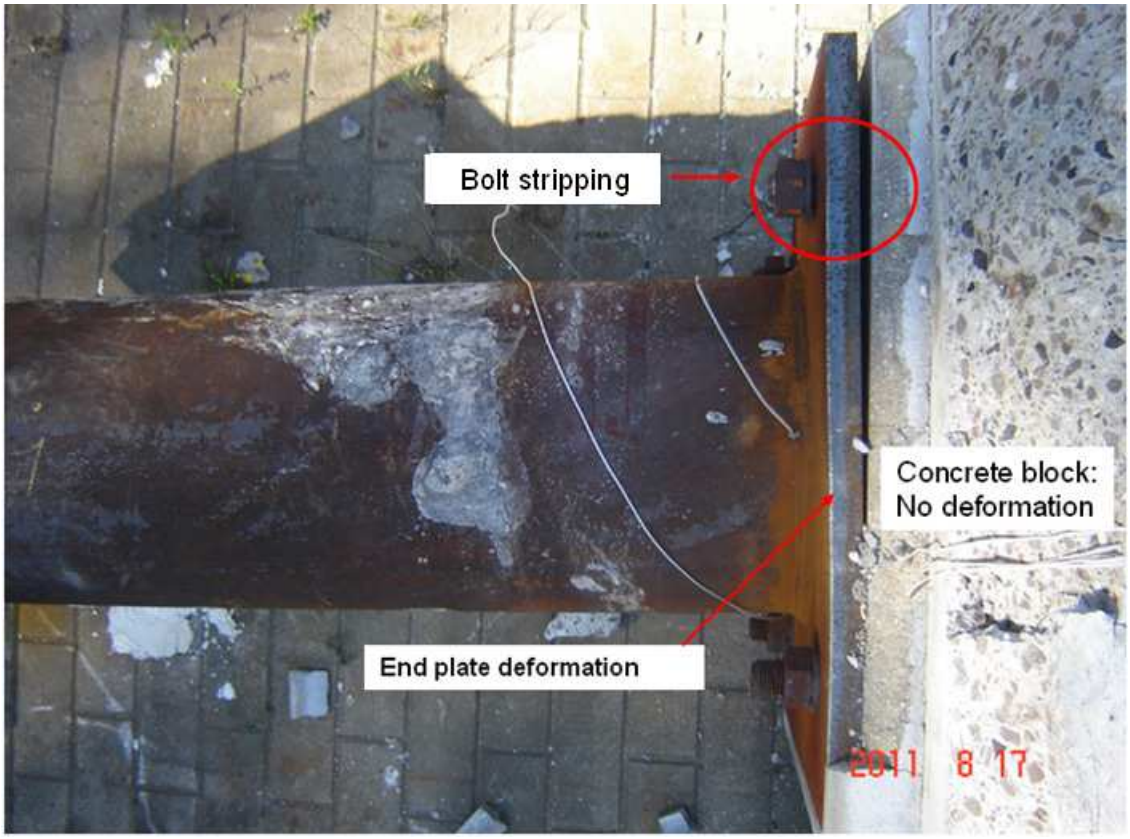

Figure 131. BC1 failure mode

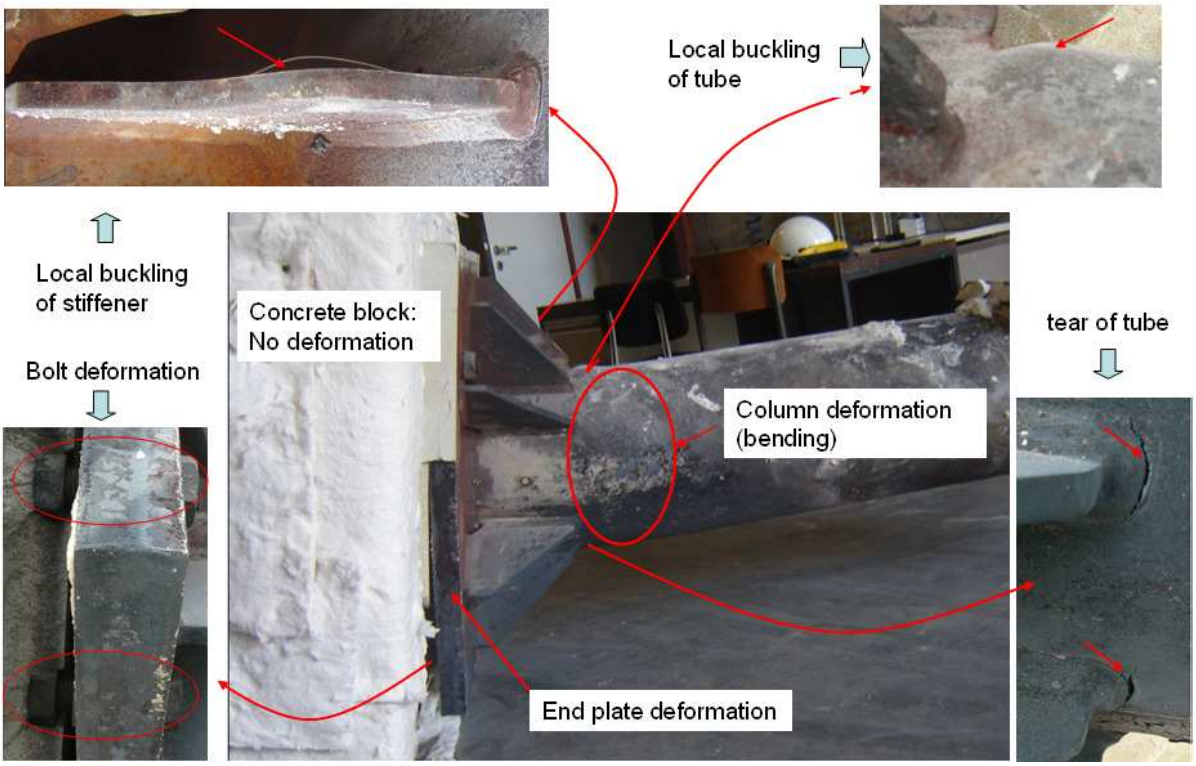

Figure 132. BC2 failure mode

Figure 133. BC3 failure mode

XIII.4. Appendix of WP5 – Model calibration

XIII.4.1. Task 5.2 Calibration of 2D-3D numerical models

The tests conducted both on elements and parts of structure, as beam-to-column and column-base joints, were fundamental to calibrate both 2D and 3D numerical models. In detail, we conducted the modelling and calibration of: i) columns under both axial and bending action; ii) joint's components both under high and room temperature; iii) hysteretic behaviour both of beam-to-column and column base joints; iii) mechanisms in plinth of the innovative seismic joint.

XIII.4.1.1. Columns under axial load and bending moment

Nonlinear finite element tools have been employed to simulate the combined loading experiments described in WP3 conducted by CSM. The main purpose of this numerical simulation is the calibration of the finite element models, to be used in the extensive parametric study, described in Task 5.3.

The experimental investigation consists of sixteen(16) full-scale tests in total; ten (10) on 1.5m and six (6) on 4.5m-long tube specimens of 12-inch and 14-inch nominal diameter. The tubes are seamless, made of TS590 high-strength steel material (nominal yield stress equal to 590 MPa and actual 735MPa). The corresponding cross sectional dimensions are ∅355.6/12 and ∅323.9/10. Two (2) of the 1.5m-long specimens are tested under axial compression and the rest fourteen (14) under combined-loading conditions of thrust and bending.

Simulations were conducted using two different FE programs able to deal with large strain, large displacement, material nonlinearities and instability phenomena typically involved in buckling of CHS members subjected to axial and bending loading. In detail, the FE programs used and the main characteristics of models are reported herein.

- FE program ABAQUS using a J2 (von Mises) flow plasticity model. The tube is simulated with four-node reduced-integration shell elements, involving large inelastic deformations of relatively thick-walled steel cylinders. Based on thickness measurements, the tubes have been assumed with uniform thickness equal to 12.5 mm and 10.26 mm for sections ∅355.6/12 and ∅323.9/10 respectively. The numerical analysis allows for the calculation of the axial load capacity and the bending strength under several levels of axial load (Nu), in accordance with the experimental procedure; axial load is applied first up to a certain prescribed level and, subsequently, keeping the axial load constant, bending is applied through an arc-length continuation algorithm (Riks) until a maximum bending moment is reached. Upon buckling formation, bending load is continued in the post-buckling range to obtain the buckled shape and compare with the experiments. The end sections of the tubular specimens are bolted with the tubular member. Therefore, a “kinematic coupling” technique is adopted, relating the degrees of freedom of the shell nodes around a specific section with the degrees of freedom of a fictitious node, referred to as the “reference node,” located at the centroid of the section under consideration. The entire finite element configuration is simply supported at both ends of the rigid segments;
- FE commercial software MSC.MARC®. Bilinear 4-noded shell elements with 7 integration points through thickness were employed in order to properly simulate the local buckling phenomenon occurring both in bending than in axial load testing. This type of element is particularly suitable to describe curved surfaces subjected to large strains into plastic range. Solid element could also be employed for this purpose, but shell elements were preferred due to their lower consumption of computational resource, without affecting the results. An overview of the model employed for the simulations of tests on short specimens is reported in the Figure 134. Loads have been introduced in the model at end nodes (connecting the testing machine beams frame) by application of axial forces followed by an increasing rotation up to post buckling regime. An equivalent model has been employed to simulate the tests performed on long specimen. A dedicated sensitivity analysis on mesh size in order to obtain the optimal balance in terms of accuracy and computation resource requirements was performed before the simulation of full scale tests. It was thus decided to employ 120 elements along circumference with an axial length of 10mm.

In order to obtain an accurate analysis, we took into account:

- actual properties of the material in terms of true stress – true stain curves. Steel material has been characterized via tensile tests on cylindrical samples in longitudinal direction (task 3.1). The resultant curve used in finite element analysis (FEA) is reported in Figure 135. An isotropic hardening rule in combination with the Von Mises yield criterion have been adopted to describe the elastic-plastic behaviour of the CHS member deformation process;
- initial wrinkling imperfections considered in the form of buckling mode obtained through an eigenvalue analysis of the specimen under bending conditions. The amplitude of initial wrinkling is assumed equal to 2.6% of the tube wall thickness, as a representative value in accordance with the wrinkling measurements performed prior testing (Pappa et al., 2012 and Pournara et al., 2012);
- residual stresses in hoop direction have been considered as initial stresses of the model in the form of a linear anti-symmetric distribution through the tube thickness with a maximum value of 122 MPa;
- residual stresses in the longitudinal direction, but they were quite small and then they were neglected in the numerical model.

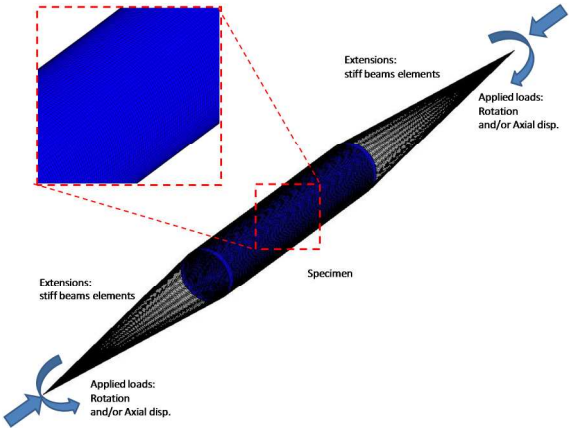

Figure 134. Overview of the FE model employed in the simulation of short column specimen

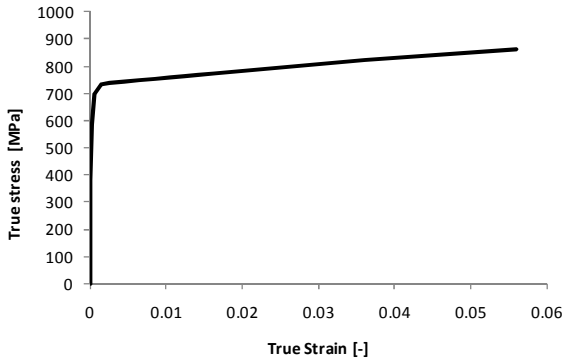

Figure 135. True stress true strain curve adopted in the FE model

The finite element load-displacement curves are compared with the experimental axial compression tests as shown in Figure 136, while the moment-end rotation (M-φ) curves are compared as shown in Figure 138. The failure mode of axial and combined loading case is indicatively shown in Figure 137 and Figure 139 for ∅355.6/12 and ∅323.9/10 sections, respectively

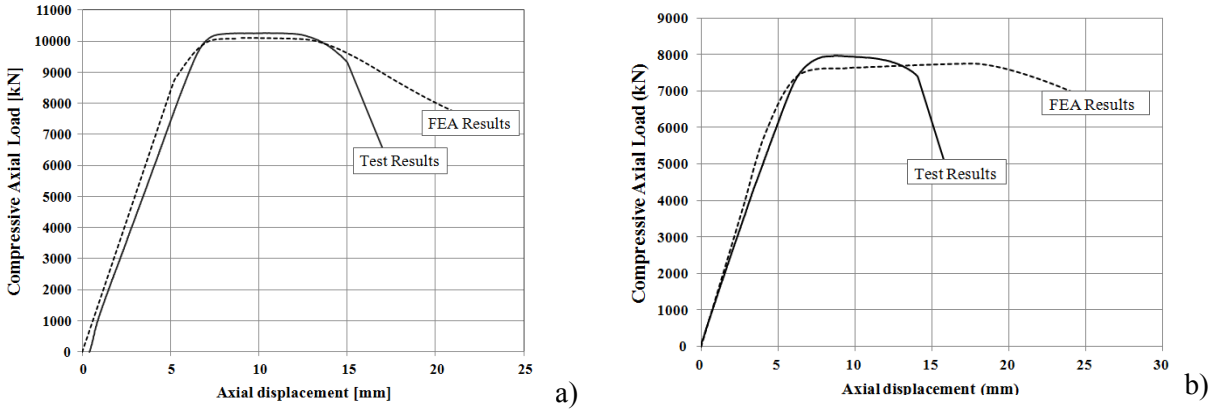

Figure 136. Finite element load-displacement curves in comparison with the axial test results for a) ∅355.6/12.5 and b) ∅323.9/10 1.5m-long specimens

Figure 137. Buckled shape for the ∅355.6/12.5 1.5m-long specimen under axial compression in comparison with the FE model

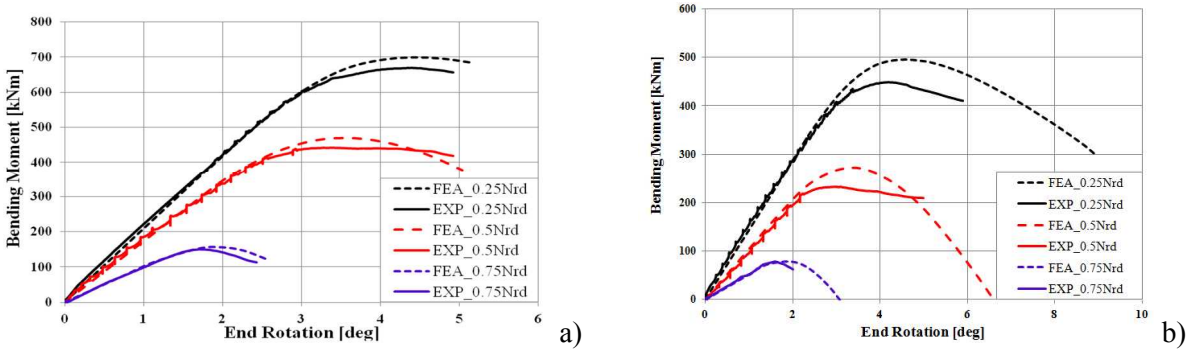

Figure 138. Numerical and experimental M-φ curves for 4.5m-long specimens of a) ∅355.6/12 and b) ∅323.9/10 sections subjected to combined loading

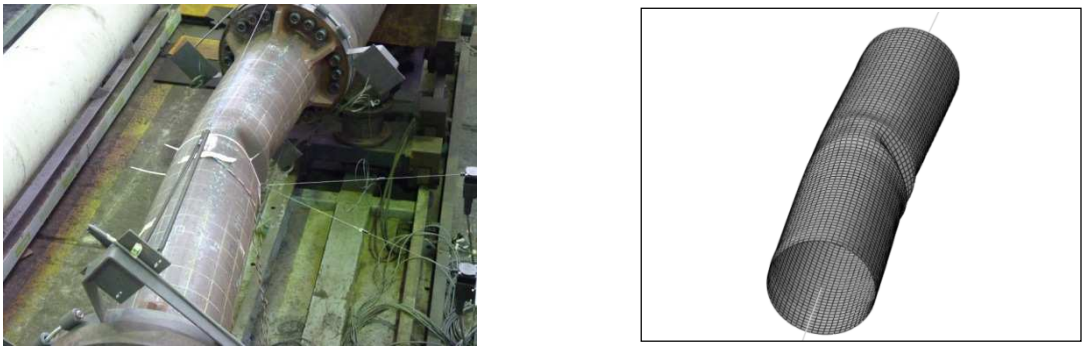

Figure 139. Buckled shape for a 1.5m-long specimen of ∅323.9/10 section under combined loading in comparison with the FE model

Typical deformed shapes and the equivalent plastic strain distribution are reported in Figure 140 for a short specimen. The plastic strain developed at compression side is influenced by the member imperfections and, as a result, buckling is driven in a position which is slightly away from the central section.

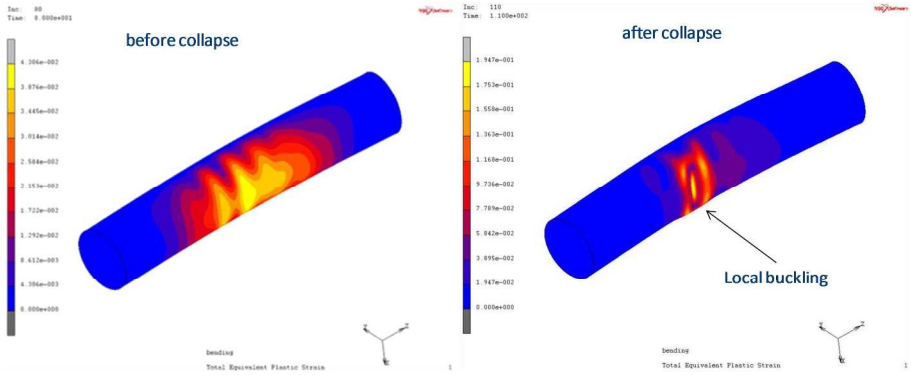

Figure 140. Deformed shape and plastic strain distribution during bending process

It is interesting to notice that the maximum value of the bending moment and the corresponding rotation angle are not significantly influenced by columns imperfections like those measured on the tested products. This is shown in Figure 141 by comparing a perfect model (constant thickness, perfect cylinder) with one where measured imperfections are introduced (thickness variation, dimples and ovality).

The measured residual stresses were found of negligible magnitude too (10% of yield stress) so they were not introduced in the model.

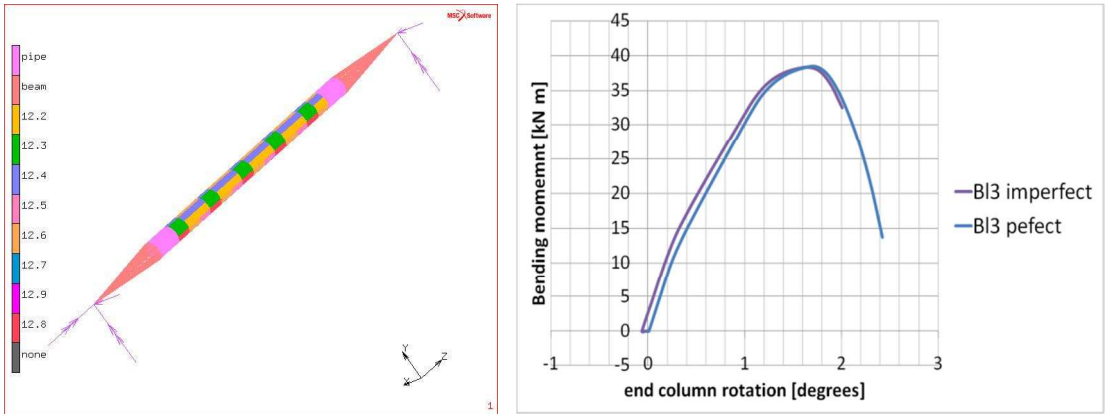

Figure 141. Geometrical imperfections: thickness variations introduced in the model (left) and comparison of moment vs. rotation diagrams obtained for geometrically "perfect" and "imperfect" models of long specimens (right).

The following figures and tables show the agreement between experimental and numerical results of M-N interaction diagrams for short and long A (355x12 mm) and B (323,9 x10mm) specimens. Those are graphically reported in Figure 142 and in Table 32 and Table 33 where both experimental and numerical results are reported.

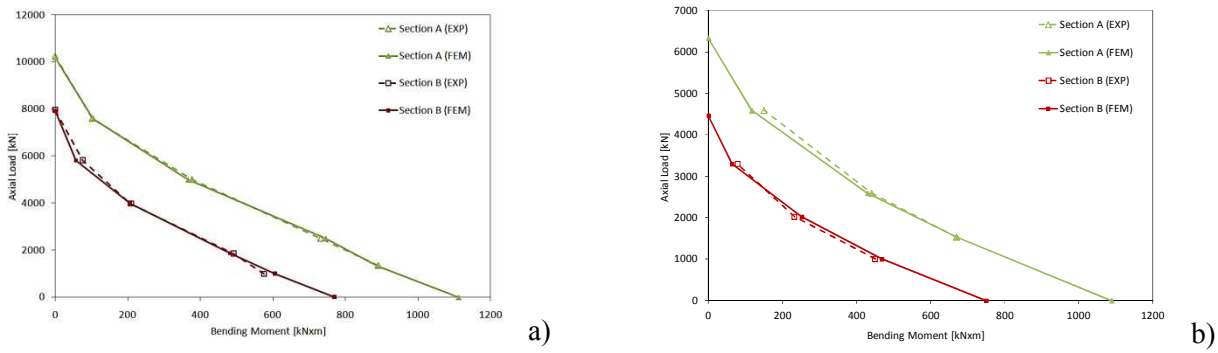

Figure 142. Experimental and numerical interaction diagram both for section A and B respectively for: a) short specimens; b) long specimens

Table 32. Summary of Experimental and numerical results for tests performed on long specimens

Case Id	Axial load		Moment		Limit angle	
	kN		kN m		deg	
	Experim.	FEA	Experim.	FEA	Experim.	FEA
As3	-	0	-	1112	-	6
As3-13	1340	1340	891	888	2.6	2.3
As3-25	2500	2500	732	746	1.92	1.9
As3-50	5000	5000	377	366	1.1	1.2
As3-75	7600	7600	102	104	0.42	0.48
As1	10254	10194	-	-	-	-

Case Id	Axial load		Moment		Limit angle	
	kN		kN m		deg	
	Experim.	FEA	Experim.	FEA	Experim.	FEA
Bs3	-	0	-	770	-	6
Bs3-13	1000	1000	575	606	2.4	2.4
Bs3-25	1865	1865	492	482	1.81	2.1
Bs3-50	3980	3980	209	206	0.98	1.1
Bs3-75	5822	5822	76	57	0.45	0.47
Bs1	7964	7934	-	0	-	0

Table 33. Summary of Experimental and numerical results for tests performed on long specimens

Case Id	Axial load		Moment		Limit angle	
	kN		kN m		deg	
	Experim.	FEA	Experim.	FEA	Experim.	FEA
Al3_25	1530	1530	670	672	4.4	4.2
Al3_50	2590	2590	441	430	3.3	3.2
Al3_75	4588	4588	150	117	1.7	1.8

Case Id	Axial load		Moment		Limit angle	
	kN		kN m		deg	
	Experim.	FEA	Experim.	FEA	Experim.	FEA
Bl3_25	1000	1000	450	468	4.2	4.5
Bl3_50	2020	2020	232	252	3.0	3.2
Bl3_75	3298	3298	79	64	1.5	1.9

XIII.4.1.2. Hysteretic behaviour of both beam-to-column and column-base joints

The modelling of the hysteretic behaviour both of beam-to-column joints and of column-base joints considering lumped plasticity it is adequate because: i) the behaviour recorded during the test which showed the presence of plastic hinge in defined sections; ii) it does not require a large computational cost. The accuracy of models was evaluated considering the whole structure tested and comparing the energy dissipated by the plastic hinges during the test with the energy dissipated in the numerical analysis. The maximum difference of energy was evaluated equal to about 20%.

The calibration of model parameters was obtained applying at the column head of the model the same displacement applied during the test by the actuator. The outputs read by non-linear analysis with the FE program OpenSees were: i) the force at the head of the specimens; ii) the rotations and the moments in the plastic hinges. These values were compared respectively with the actuator forces recorded and the moment-rotation relationship estimated by the inclinometers and the load cells located on the specimens, as showed in WP5.

The model of plastic hinge is one for all tests conducted on the same typology of joint. It required elevated computational cost in order to obtain a better solution that minimizes the energy error on all the test considered. The following figures show the comparison between numerical and experimental results of moment-rotation both of the beam-to-column joint and of seismic joints.

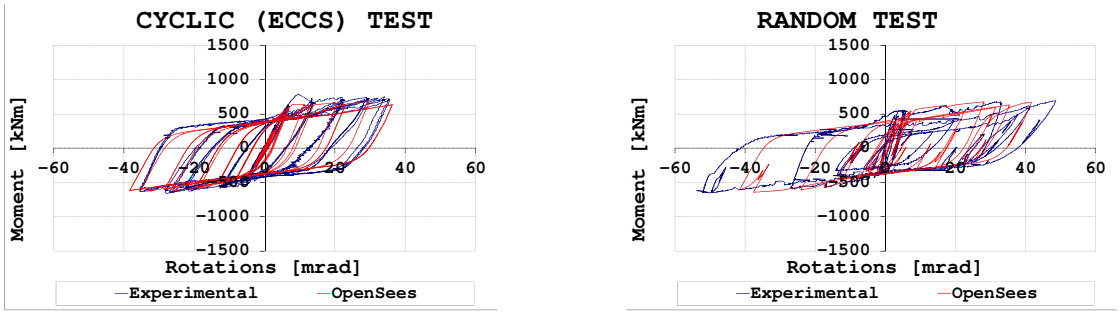

Figure 143. Beam-to-column joint: comparison of moment-rotation relationships of plastic hinges

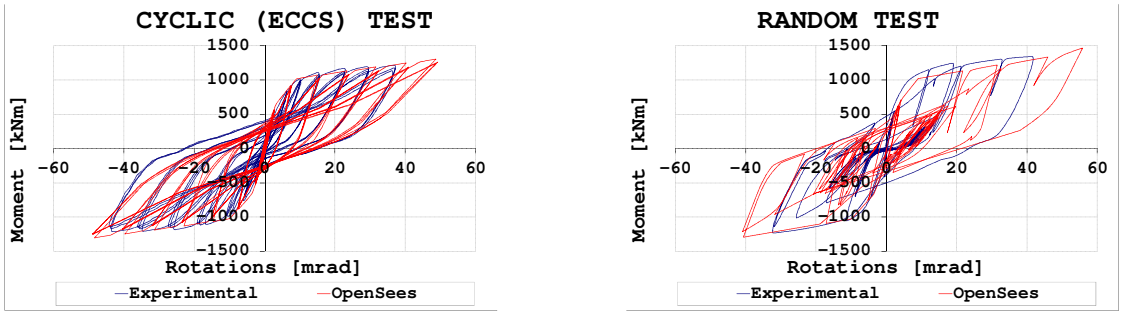

Figure 144. Standard seismic column-base joint: comparison of moment-rotation relationships of plastic hinges

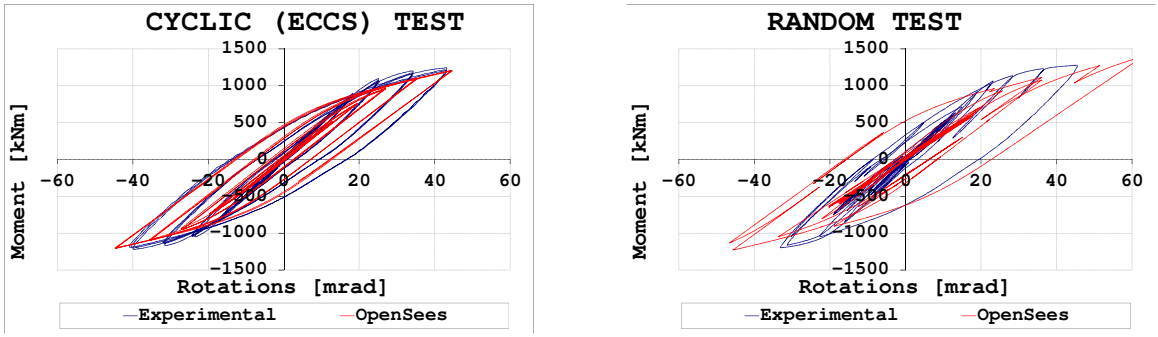

Figure 145. Innovative seismic column-base joint: comparison of moment-rotation relationships of plastic hinges

The hysteretic behaviour of plastic hinges of beam-to-column joints and column-base joints was modelled by Bouc-Wen and Pinching hysteretic models. The two models were considered to operate in parallel way, with exception of the innovative column-base joints where it was possible to model the hysteretic behaviour considering only a Bouc-Wen model. In the beam-to column joint and in the standard column-base seismic joint the Bouc-Wen model provides the main part of actual behaviour, while the pinching model gives the slip due to damaged concrete and consequent hardening.

XIII.4.1.3. Mechanical behaviour of a plinth relevant to an innovative seismic joint

The calibration of the 3D numerical model proposed for the innovative solution realised by a circular column required elevated computational costs due to : i) non-linearity of the problem consequent to damage of the concrete in tension; ii) presence of constrains among the different parts of joint as column surface and concrete of block or the base plate and the grout. The analysis were conducted with FE program Abaqus by a Standard analysis. On the column-base were conducted only cyclic test, then to reduce the computational cost the envelope of force-displacement relationship was considered. The model was calibrate applying monotonic displacement and comparing the force of numerical analysis with force applied by the actuator. The results were in agreement with experimental data till the onset of yielding. After the yielding the numerical response showed higher stiffness respect actual response, probably it was due to impossibility to take account in the model of the damage of the grout, between the base plate of column and block of the foundation, due cyclic action.

XIII.4.2. Task 5.3 Parametric numerical analysis

On the basis of the calibration of 2D-3D numerical models, parametric numerical analyses were conducted in order to investigate the response both of columns and of joints and of the prototype structure. The analysis took into account different input and/or different bond conditions in order to evaluate the effects on the response.

XIII.4.2.1. Analysis of the behaviour of columns at room temperature

Further numerical parametric study has been conducted in order to estimate the influence of the initial imperfections on stability curves and interaction diagrams developed for HSS tubular members.

Stability curves have been developed considering tube lengths between 1m to 14m, various cross sections and imperfection types. The influence of the out-of-straightness imperfection (e0=L/300, L/500 & L/1000) on the buckling strength of tubular models of various lengths and cross sections is shown in Figure 146 and in Figure 147, compared with the proposed equations by current Standards (EN 1993-1-

1, 2005; EN 1993-1-6, 2005; AISC-LRFD, 2000; American Petroleum Institute, 1993). Finally, stability curves have been developed considering a combination of initial imperfections (Pappa et al., 2012), according to the measurements reported in WP3; wrinkling amplitude (w_0=2.6% of the tube thickness), residual stresses (±122 MPa, linearly distributed through the thickness) and initial out-of-straightness of e_0=L/750 (EN-1090-2, 2008) and as shown in Figure 148. The above buckling curves are compared with the proposed equations of the current standards. It should be noted that the axial load and bending moment values are normalized with the values $N_y = A\sigma_y$ and $M_y = W_{el}\,\sigma_y$, where σ_y is the nominal yield stress (590Mpa) and W_{el} is the elastic modulus of the cross-section.

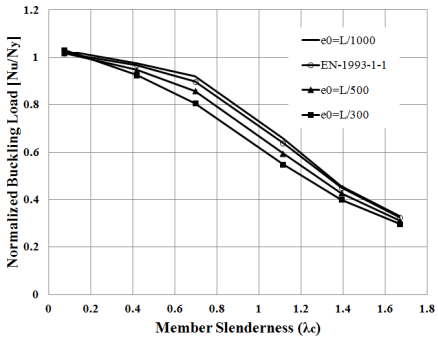

Figure 146. Finite element results for section ∅355.6/12.5 of various amplitudes of out-of-straightness (e_0) in comparison with EN1993-1-1.

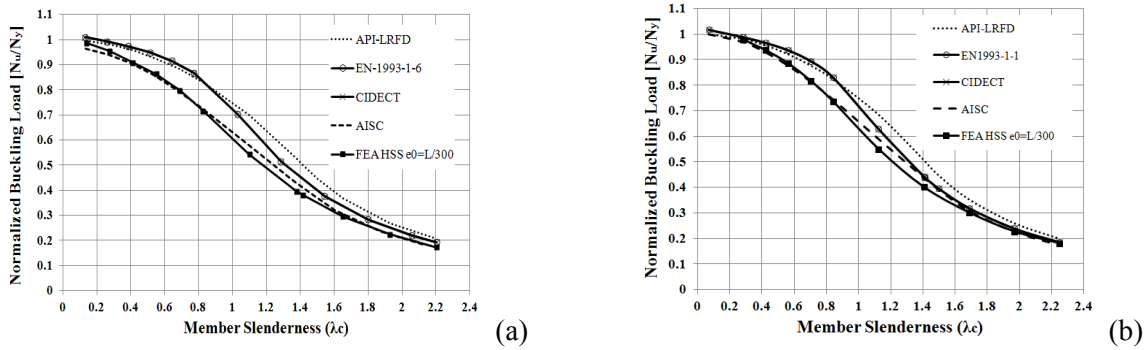

Figure 147. Finite element Results for (a) ∅355.6/8 and (b) ∅355.6/16 sections with out-of-straightness e_0=L/300 in comparison with European and American standards.

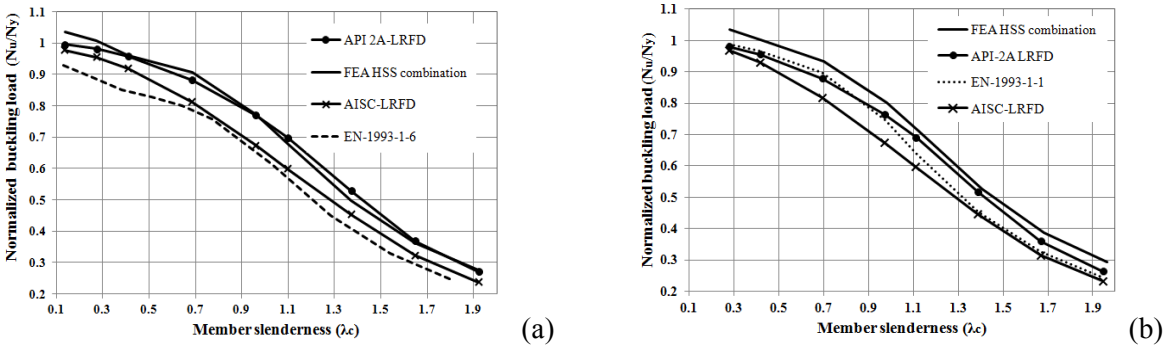

Figure 148. Finite element stability curves for sections (a) ∅355.6/8 and (b) ∅355.6/16 with a combination of imperfections in comparison with European and American provisions.

Interaction diagrams have been developed considering various types of imperfections for HSS 3, 5 and 8m-long beam-columns of various cross sections. The finite element results are compared with the ones proposed by current European standards as shown in Figure 149, for different amplitudes of out-of-straightness imperfection (e_0=L/300 & L/1000). Moreover, the influence of initial wrinkling imperfection in the strength of the HSS beam-columns is shown in Figure 150. Finally, finite element interaction curves were developed considering a combination of imperfection types such as out-of-straightness (L/750), wrinkling amplitude (2.6% of the tube thickness) and residual stresses (±122 MPa,

linearly distributed through the thickness). These curves have been compared with current provisions as shown in Figure 151. It should be noted that the axial load and bending moment values are normalized with the values $N_y = A\sigma_y$ and $M_y = W_{el}\sigma_y$, where σ_y is the nominal yield stress (590Mpa) and W_{el} is the elastic modulus of the cross-section.

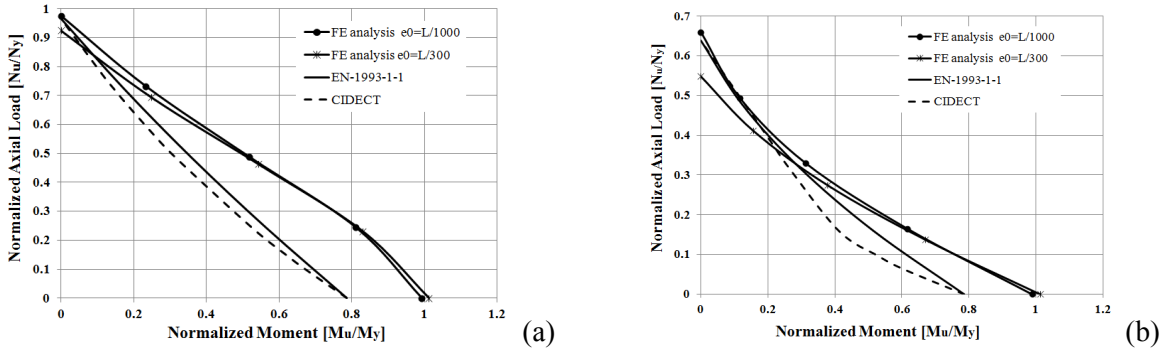

Figure 149. Finite element results for (a) 3m-long and (b) 8m-long tubular member of section ∅355.6/12 with out-of-straightness amplitudes L/300 & L/1000 in comparison with European and American standards.

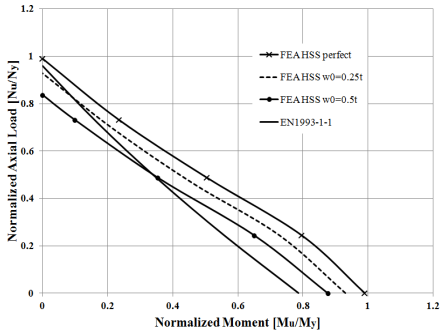

Figure 150. Finite element results for 5m-long tubular member of section ∅323.9/10 with various wrinkling amplitudes in comparison with EN1993-1-1.

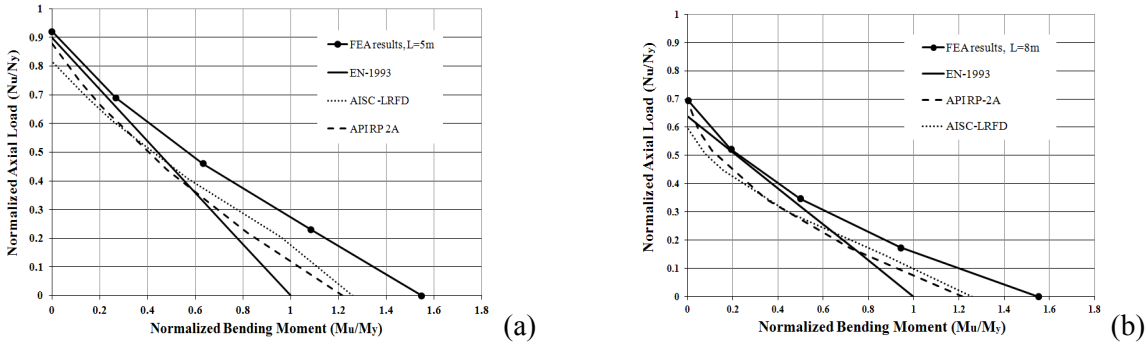

Figure 151. Interaction diagrams for (a) 5m-long and (b) 8m-long tubular members of ∅355.6/8 in comparison with current provisions

It can be concluded that the current standards appear to be rather conservative, especially the EN 1993 Part 1 predictions mainly due to the "penalizing" classification of CHS cross sections in EN 1993-1-1, 2005. More specifically, the axial load-bending interaction curves obtained by the finite element analyses indicate significantly higher ultimate capacity with respect to the design rules of the above specifications. In particular, EN 1993 Part 1 rules penalize by a substantial amount the pure bending strength mainly due to the conservative classification limits when applied to high-strength steel CHS. Finally, the results show that actual geometrical imperfections influence the plastic strain distribution during loading process but their very small magnitude has a negligible effect on the performance of CHS members in terms of load-carrying and rotational capacity up to failure.

XIII.4.3. References (WP5 appendix)

AISC-LRFD (2000). Load Resistance Factor Design Specification for steel hollow structural sections. American Institute of Steel Construction, Chicago, Illinois.

American Petroleum Institute (1993). Recommended Practice, Designing and Constructing Fixed Offshore Platforms-Load and Resistance Factor Design. Recommended practice 2A-LRFD, 1st Edition. Washington.

CIDECT (1992). "Structural Stability with Hollow Sections," CIDECT design guide No. 2, Springer-Verlag.

EN1993-1-1 (2005). "Eurocode 3: Design of steel structures - Part 1-1: General rules and rules for buildings", CEN, Bruxelles.

EN 1993-1-6 (2007). "Eurocode 3: Design of steel structures. Part 1-6: Strength and Stability of Shell Structures." CEN, Bruxelles.

EN-1090-2 (2008). "Execution of steel structures and aluminium structures - Part 2: Technical requirements for steel structures" CEN, Bruxelles.

Pappa, P., and Karamanos, S. A. (2012). "Buckling of High-Strength Steel CHS Tubular Members under axial compression and bending," 14th International Symposium on Tubular Structures, Paper No. 104, London, UK.

Pournara, A.E., Karamanos, S.A., Ferino, J., Lucci, A. (2012). "Strength and stability of high-strength steel tubular beam-columns under compressive loading," ISTS 2012, London.